The Effects of Methacrylated Glucosamine on the Mechanical Properties of Gelatin Methacryloyl Hydrogels and Gelatin-Methacryloyl/Nanohydroxyapatite Composite Materials.

by

Cullen James Tielemans

A thesis

presented to the University Of Waterloo

in fulfilment of the

thesis requirement for the degree of

Master of Applied Science

in

Systems Design Engineering

Waterloo, Ontario, Canada, 2021

Author's Declaration

I hereby declare that I am the sole author of this thesis. This is a true copy of the thesis, including any required final revisions, as accepted by my examiners.

I understand that my thesis may be made electronically available to the public.

Abstract

Gelatin-methacryloyl (GelMA) has been a material of keen research interest in the past few decades, with diverse potential applications such as drug delivery, tissue engineering, and 3D bioprinting, due to it possessing many desirable properties. However, pure GelMA hydrogel materials in published literature exhibit relatively weak mechanical properties when considering its application as a tissue-engineering material for load-bearing tissues, such as cartilage or bone.

In this study, two new UV-curable additives based off the monosaccharide glucosamine were developed, with one additive being monofunctional and the other polyfunctional. These additives were explored to improve the mechanical properties of a GelMA hydrogel and a GelMA/nanohydroxyapatite composite material. Additionally, the effects of the divalent salt, $CaCl_2$, were explored as previous research on similar materials had shown favourable interactions to lower the viscosity of uncured materials, improving handling and enabling the material to be used as a 3D printer ink.

Cast hydrogel and composite materials were mechanically tested cyclically and compressively and the effects of the additives compared. Rheological properties of all materials were explored using a cup-and-bob rheometer with shear stress controlled between samples. Finally, the materials were tested on a masked stereolithography 3D printer to determine material printability.

It was found that the monofunctional additive was unable to improve the mechanical properties of the hydrogel or composite materials at any tested concentration, but the polyfunctional additive improved the mechanical properties of the materials significantly, with the hydrogel being 125% tougher than the control with a 1 molar concentration. Similar improvements were observed for the composite materials. The inclusion of 100 mM $CaCl_2$ was found to lower the viscosity of all hydrogel inks, as did the inclusion of the polyfunctional additive. The same trends were not observed for the composite material, however, as both additives increased the viscosity of the composites compared to the control, and the salt had minimal effect on the rheology of the control and polyfunctional additive composites. Both the polyfunctional additive-containing hydrogel and composite materials were found to be printable on a masked stereolithography 3D printer.

The development of the polyfunctional glucosamine additive represents a step forward in the development of additives to improve the mechanical properties of biologically-derived hydrogel and composite materials, and provides insight into potential mechanisms that could be exploited in the design of future additives to drive the properties of these materials closer to the properties of load-bearing tissues while maintaining manufacturability.

Acknowledgements

First, I would like to thank my supervisor, Professor Thomas Willett, for his extensive and continuous support, supervision, expertise, guidance and advice along with thoughtful questions and discussions, all of which were extremely important in the success of this work. I would also like to give special thanks Dr. Patricia Comeau for her invaluable, on-the-ground guidance, training, advice, supervision, and sharing her expertise on the materials and processes in this work. I would also like to thank my committee members, Professor Maud Gorbet and Professor Evelyn Yim for committing their time to review this work and offering their feedback and comments. I'd also like to thank the other members of the Waterloo Composite Biomaterial System Systems lab, past and present, for their ever-present support, advice and encouragement through my time in the lab. Finally, I would like to extend gratitude to my friends and family for their ongoing support.

Table of Contents

Author's Declaration ii
Abstract iii
Acknowledgements iv
List of Figures viii
List of Tables x
List of Abbreviations xi
1. Introduction 1
1.1 Limitations in Current Materials for Tissue Engineering 1
1.2 Hydrogel Materials and Their Modifications 1
1.3 Methods to Further Improve Hydrogel-Based Material Mechanical Properties 4
1.4 Three-Dimensional Printing 6
1.5 Objectives and Hypotheses 6
2. Experimental Outline 8
3. Materials and Methods 10
3.1 Materials 10
3.2 Gelatin Methacrylation 10
3.3 Glucosamine Methacrylation 10
3.4 Proton Nuclear Magnetic Resonance Spectroscopy 12
3.5 Hydrogel Ink Fabrication 12
3.6 Composite Ink Fabrication 13
3.7 Dynamic and Quasi-Static Compressive Mechanical Testing 14
3.8 Cure Depth 15
3.9 Swelling 16
3.10 Rheology 16
3.11 Settling Experiments 17
3.12 mSLA 3D Printing of Hydrogel and Composite Materials 18
3.13 Data Analysis 18
4. Glucosamine Methacrylation and Hydrogel Characterization 19
4.1 Results 19
4.1.1 ^{1}H NMR 19
4.1.2 Salt Negative Hydrogel Rheology 21
4.1.3 Salt Negative Hydrogel Cure Depth 22

4.1.4 Salt Negative Hydrogel Mechanical Testing 23
4.1.5 Salt Negative Hydrogel Swelling 25
4.1.6 Salt Effect on Rheology 26
4.1.7 Salt Effect on Cure Depth 28
4.1.8 Effects of Salt on Mechanical Properties 29
4.1.9 Salt Effect on Swelling 32
4.1.10 mSLA Printing Proof of Concept 32
4.2 Discussion 33
4.2.1 The Methacrylation of Glucosamine 33
4.2.2 Salt Negative Hydrogel Rheology 34
4.2.3 Curing Kinetics of Salt Negative GelMA/GlcN-MA Solutions 36
4.2.4 Salt Negative Hydrogel Compressive and Dynamic Mechanical Properties 36
4.2.5 Salt Negative Hydrogel Swelling Profiles 39
4.2.6 Salt Effect on Hydrogel Rheology 40
4.2.7 Effect of Salts on Curing Kinetics of GelMA/GlcN-MA Hydrogel Materials 41
4.2.8 Salt Effect on Hydrogel Mechanical Properties 42
4.2.9 Salt Effect on Cured Hydrogel Swelling 44
4.2.10 mSLA Printing of GelMA/GlcN-MA Hydrogel Materials 44
5. The Effects of Compositing GelMA/GlcN-MA Hydrogels with nHA 46
5.1 Results 46
5.1.1 Particle Settling Experiment 46
5.1.2 Composite Material Rheology 46
5.1.3 Composite Material Cure Depth 48
5.1.4 Composite Mechanical Testing 49
5.1.5 Composite Swelling 53
5.1.6 mSLA Printing of Composite Inks 55
5.2 Discussion 55
5.2.1 Particle Settling 55
5.2.2 Composite Rheology 56
5.2.3 Cure Depth and Kinetics of GelMA/GlcN-MA/nHA Composite Materials 57
5.2.4 Mechanical Properties of GelMA/GlcN-MA/nHA Composite Materials 58
5.2.5 Swelling Profiles for Composite Materials 59
5.2.6 mSLA Printing of GelMA/GlcN-MA/nHA Composite Materials 60

6. Limitations 61
7. Conclusion 63
8. Future Work 65
Bibliography 68

List of Figures

FIGURE 1 CHEMICAL STRUCTURE OF GLUCOSAMINE AND ALDEHYDE RING-OPENING REACTION. 6
FIGURE 2 HIGH-LEVEL OVERVIEW OF THESIS EXPERIMENTAL PLAN. 8
FIGURE 3 FLOWCHART OF THE METHACRYLATION OF GLUCOSAMINE. 11
FIGURE 4 UNIVERT CELLSCALE MECHANICAL TESTING APPARATUS WITH COMPRESSION TESTING ATTACHMENTS AND 200N LOADCELL. 15
FIGURE 5 BOHLIN CS RHEOMETER WITH C25 CUP-AND-BOB GEOMETRY MEASURING THE VISCOSITY OF A COMPOSITE GELMA/NHA MATERIAL. 17
FIGURE 6 ^{1}H NMR SPECTRA FOR GELATIN AND GELMA 19
FIGURE 7: A) ^{1}H NMR SPECTRA FOR D-GLCN, 1.2X GLCN-MA, AND 5X GLCN-MA B) ANTICIPATED CHEMICAL STRUCTURES OF GLCN-BASED ADDITIVES. 20
FIGURE 8 RHEOLOGICAL PROFILES OF SALT-NEGATIVE GELMA/GLCN-MA HYDROGEL INKS OF VARYING GLCN-MA TYPE AND CONCENTRATION COMPARED TO A GELMA-ONLY CONTROL. 21
FIGURE 9 CURE DEPTH PROFILES FOR 1.2X (A) AND 5X (B) GLCN-MA/GELMA INKS COMPARED TO A GELMA-ONLY CONTROL FOR 385 NM UV LIGHT 23
FIGURE 10 REPRESENTATIVE (OF AN N OF AT LEAST 5) COMPRESSIVE ENGINEERING STRESS-STRAIN PROFILES OF SALT-NEGATIVE HYDROGEL INKS. 23
FIGURE 11 COMPARISON OF COMPRESSIVE AND DYNAMIC MECHANICAL PROPERTIES OF SALT-NEGATIVE GELMA/GLCN-MA HYDROGEL INKS WITH VARYING TYPES AND CONCENTRATIONS OF GLCN-MA 24
FIGURE 12 SWELLING IN TERMS OF MASS GAIN FOR SALT-NEGATIVE GELMA/GLCN-MA HYDROGEL INKS, COMPARED TO A GELMA-ONLY CONTROL, IN ROOM TEMPERATURE MQ WATER 26
FIGURE 13 RHEOLOGICAL MEASUREMENTS OF GELMA/GLCN-MA HYDROGELS MADE WITH 100 MM $CACL_2$ SOLUTION (POSITIVE) OR MQ WATER (NEGATIVE) COMPARED TO GELMA-ONLY CONTROLS 27
FIGURE 14 CURE DEPTH PROFILES FOR GELMA/GLCN-MA HYDROGEL MATERIALS, COMPARED TO GELMA-ONLY CONTROLS, WITH AND WITHOUT SALT, CURED WITH 385 NM LIGHT 29
FIGURE 15 COMPARISON BETWEEN COMPRESSIVE AND DYNAMIC MECHANICAL TESTING PROPERTIES OF SALT-POSITIVE AND SALT-NEGATIVE GLCN-MA/GELMA HYDROGELS, COMPARED TO GELMA-ONLY CONTROLS 30
FIGURE 16 COMPRESSIVE AND DYNAMIC MECHANICAL PROPERTIES SALT-EFFECT COMPARISON OF GELMA-ONLY HYDROGELS TESTED DURING THE SUMMER SEASON OF 2020 31
FIGURE 17 SWELLING CHARACTERISTICS BY MASS COMPARING FRESHLY CURED SALT-NEGATIVE AND SALT-POSITIVE GLCN-MA/GELMA HYDROGELS, WITH GELMA-ONLY CONTROLS, IN ROOM-TEMPERATURE MQ WATER 32
FIGURE 18 A DOGBONE OF CURED 1M 5X GLCN-MA/GELMA/CACL2 HYDROGEL MATERIAL PRINTED ON A PHROZEN MSLA PRINTER. 33
FIGURE 19 EXPECTED CHEMICAL STRUCTURES OF METHACRYLATED GLCN 35
FIGURE 20 CARTOON OF EXPECTED CROSSLINKING STRUCTURE FOR RANGES OF GLCN-MA 37
FIGURE 21 CARTOON REPRESENTATION OF ANTICIPATED GELMA STRUCTURE IN MQ WATER AND GELMA IN A SALT SOLUTION. 43
FIGURE 22 GRAVIMETRIC SETTLING RESULTS OF NHA NANOPARTICLES DISPERSED IN SOLUTIONS OF THE DEVELOPED ADDITIVES OVER 24 HOURS. 46
FIGURE 23 RHEOLOGICAL PROFILES OF 10 VOL% NHA, GELMA/GLCN-MA COMPOSITE INKS WITH AND WITHOUT CACL2 SALT, COMPARED TO NHA/GELMA-ONLY COMPOSITE INKS. 47
FIGURE 24 CURE DEPTH PROFILES OF GELMA/GLCN-MA/NHA COMPOSITE MATERIALS, COMPARED TO NHA/GELMA-ONLY COMPOSITES, WITH AND WITHOUT SALT, CURED WITH 385 NM LIGHT 49
FIGURE 25 COMPARISON OF COMPRESSIVE AND DYNAMIC MECHANICAL PROPERTIES OF SALT-NEGATIVE AND SALT-POSITIVE GELMA/GLCN-MA/NHA COMPOSITE INKS WITH NHA/GELMA-ONLY CONTROLS 50

FIGURE 26 MECHANICAL PROPERTY COMPARISON BETWEEN SALT POSITIVE HYDROGELS AND THEIR RESPECTIVE COMPOSITES 52
FIGURE 27 SUMMARY OF SWELLING EFFECTS OF: (A) COMPOSITING SALT-FREE HYDROGEL WITH 10% VF NHA, (B) COMPOSITING SALT-CONTAINING HYDROGEL WITH 10% VF NHA AND (C) SALT EFFECT ON COMPOSITE MATERIALS. N=3. 54
FIGURE 28 A DOGBONE OF CURED 1M 5X GLCN-MA/GELMA/NHA/CACL2 COMPOSITE MATERIAL PRINTED ON A PHROZEN MSLA 3D PRINTER. 55

List of Tables

TABLE 1 COMPARATIVE TABLE OF THE COMPRESSIVE STRENGTH AND MODULUS OF LOAD-BEARING TISSUE VS RECENT GELMA-BASED MATERIALS 3
TABLE 2 MATERIAL CONTENTS IN %W/W FOR TESTED HYDROGEL INKS 13
TABLE 3 DEPTH OF UV LIGHT PENETRATION AND CRITICAL ENERGY FOR GELMA/GLCN-MA SOLUTIONS CURED WITH 385 NM LIGHT. 22
TABLE 4 EXPERIMENTAL RESULTS COMPARING THE EFFECTS DIVALENT SALT HAS ON THE HYDROGEL'S CURING KINETICS WITH 385 NM LIGHT. 28
TABLE 5 CURING KINETICS AND COEFFICIENT OF DETERMINATION OF THE FIT FOR COMPOSITE MATERIALS. 48
TABLE 6 SIGNIFICANCE OF SALT AND ADDITIVE FACTORS FOR VARIOUS MECHANICAL PROPERTIES OF GELMA/GLCN-MA/NHA COMPOSITE MATERIALS AS DETERMINED BY TWO-WAY ANOVA AND A HOLM-SIDAK POST-HOC TEST. 51

List of Abbreviations

- 3D – three-dimensional
- DIW – Direct ink writing
- DPBS – Dulbecco's phosphate buffer solution
- GelMA – Gelatin Methacrylate
- GlcN – Glucosamine
- GlcN-MA – Glucosamine Methacrylate
- LAP – Lithium phenyl-2,4,6-trimethylbenzoylphosphinate
- LCD – Liquid Crystal Display
- mSLA – Masked stereolithography
- mQ – MilliQ
- nHA – nanohydroxyapatite
- NMR – Nuclear Magnetic Resonance
- PEEK – polyether ether ketone
- PS – polystyrene
- SBF – simulated body fluid
- TGA – Thermal gravimetric analysis
- UCS – Ultimate compressive strength
- UV – ultraviolet
- VF – Volume fraction

1. Introduction

1.1 Limitations in Current Materials for Tissue Engineering

Significant advances in manufacturing processes, stem cell research, materials science, foreign body response and other related disciplines has pushed the prospect of clinical use for tissue engineering closer to reality. However, much work still needs to be done. An ideal material for tissue engineering requires matching mechanical properties to the tissue being replaced, notable bioactivity, good biocompatibility, biodegradability, tunable degradation rate, and non-toxic degradation products, with some tissues having further requirements, such as bone needing osteoconductivity and osteoinductivity[1] [1, 2, 3, 4]. Unfortunately, current materials rarely meet all requirements for an optimum tissue engineering material. Synthetic materials, such as poly(vinyl) alcohol, poly(ethylene glycol) are typically non-toxic, have tunable mechanical properties and batchwise homogeneity [1]. However, many of these materials often lack bioactive sites for cell adhesion and have unfavourable acidic degradation products, with large implants risking high local acid concentrations that can lead to inflammation or necrosis of adjacent tissues [1, 2, 5, 6]. Natural materials, such as collagen, alginate, chitin and gelatin, on the other hand, often show good degradability, biocompatibility and often have bioactive sites [1, 7]. However, natural materials are also often mechanically inferior with poor control over their properties, thermally unstable, difficult to process and exhibit significant batch variance [7, 1].

1.2 Hydrogel Materials and Their Modifications

As polymeric materials with high water contents, hydrogels are a material class of keen research interest as potential tissue engineering materials due to their resemblance to natural extracellular matrix [8, 9]. To form a hydrogel, polymer macromolecules must be able to bind to one another in some way in order to prevent solubilization. One way to classify hydrogels is through their binding methods, namely physical hydrogels and chemical hydrogels. Physical hydrogels use molecular interactions, such as physical entanglement, hydrogen bonding, Van der Waals interactions and/or ionic interactions, to bind polymer molecules together [8, 10]. An advantage of physical hydrogels is the ability to cause gelation without the use of potentially toxic additives through environmental changes, such as changes in pH or temperature [8, 10, 11, 9]. However, physical hydrogels are often weaker than chemical hydrogels, and gelation is often reversible if the gelling stimulus is removed [12, 13]. Chemical hydrogels use covalent bonds and chemical crosslinks to bind the hydrogel

[1] Osteoconductivity meaning bone will grow across the surface, osteoinductivity meaning the recruitment of pre-osteoblast stem cells into/onto the material/implant

matrix together [8]. Chemical hydrogels must be cured, often through free-radical polymerization, in order to form solid materials through permanent crosslinks, preventing the hydrogel from dissolving into the aqueous phase [8, 14]. Additionally, chemical hydrogels tend to be stronger and more thermally stable than their physically bound counterparts [4]. However, chemical hydrogels often require the introduction of chemicals with known detrimental effects to the biological response of the hydrogel if the additives aren't reacted or removed before use [4, 14].

A number of approaches to crosslinking naturally derived polymers have been explored, including condensation reactions, reacting hydroxyl groups with aldehydes, and free-radical polymerization [14]. A common set of condensation reaction crosslinking agents are N,N-(3-dimethylaminopropyl)-N-ethyl carbodiimide (EDC) with N-hydroxysuccinimide (NHS) acting as a side-reaction suppressor [15, 16, 17, 18, 19]. These agents allow for native amine and hydroxyl groups to be crosslinked with carboxylic acids. Glutaraldehyde was once an extremely prominent crosslinking agent used to react with natively available hydroxyl groups, but cytotoxic effects of free glutaraldehyde have raised concerns for the use of glutaraldehyde and other aldehyde crosslinkers [20, 21, 22, 23, 24]. A very popular method to make a naturally derived polymer capable of crosslinking via free-radical polymerization is by grafting it with methacryloyl groups. Often, naturally occurring functional groups, such as amines, carboxyls and hydroxyls, are reacted with molecules such as glycidyl methacrylate [25, 26, 27], methacrylic anhydride [28, 29, 30] or methacryloyl chloride [31] to graft methacryloyl groups to the polymer chain. By adding vinyl groups via methacryloyls, chemical crosslinking can be achieved via free radical polymerization in the presence of an initiator and energy source. Optical or ultraviolet (UV) irradiation is typically used to cure, though thermal crosslinking can also be used [31, 32, 33, 34, 35].

One of the most important structural proteins is collagen, a protein with a notable triple-helix structure, noted for giving extracellular matrix its strength [4]. Unfortunately, collagen is quite challenging to extract and has limited solubility in water. Gelatin, which is denatured collagen, is readily water-soluble and inexpensive due to not requiring careful extraction processes. Gelatin loses much of the collagen's original triple-helix structure, though it retains the protein's bioactive motifs as the amino acid sequence is mostly unaffected, and additionally gelatin often shows good biodegradation and biocompatibility [12, 36]. Gelatin can also form physical gels in water. However, these gels tend to be mechanically weak and thermally unstable, and most gelatin gels will dissolve at 37^0C, limiting its biomedical applications [12, 37]. As gelatin has plentiful reactive functional groups and some attractive material properties, modifications of gelatin have been extensively explored in recent years [37, 17, 38, 39, 40, 29, 41]. Van Den Bulke first published a method for

grafting vinyl groups to gelatin, forming a photocrosslinkable "gelatin-methacryloyl" (GelMA), which when cured can overcome gelatin's poor thermal stability [28, 12]. Many applications for GelMA have been explored in the decades following, including as potential materials for wound healing [34, 42], drug release [43, 44], tissue engineering [45] and bioprinting [32]. The cured GelMA material shows good biodegradability, bioactivity, and biocompatibility, and through varying the protein concentration, the extent of curing and the degree of functionalization, the hydrogel material has tunable mechanical properties [12, 46, 47, 41]. Unfortunately, GelMA hydrogel materials found in the literature still lack the mechanical properties required for use in tissue engineering scaffolds intended for robust, load-bearing applications such as that of replacing bone or articular cartilage (see Table 1)

Table 1 Comparative Table of the Compressive Strength and Modulus of Load-Bearing Tissue vs Recent GelMA-Based Materials

Material	Compressive Strength	Compressive Modulus
Articular Cartilage	14-59 (mean 35.7) MPa [48]	0.41-0.45 MPa [49]
Human Femoral Cortical Bone	153-205 MPa (longitudinal) [50, 51]	11.7-18.97 GPa (longitudinal) [50, 51]
57% amine-functionalized GelMA, 10% concentration	-	10 kPa [41]
15% w/v GelMA, loaded with halloysite nanotubes and nanosilver	0.5-0.12 MPa [52]	0.2-0.5 MPa [52]
GelMA-hydroxyapatite "hybrid hydrogel", HA formed *in situ*	-	13-25 kPa [53]
GelMA-PEGDA hydrogel (30% w/w GelMA, 5% w/w PEGDA)	~320 kPa [37]	-
GelMA-nHA composite		6 MPa (Dynamic Modulus) [45]

It is well established that the presence of salt and other ions has a significant effect on the properties of proteins and their solutions, such as their solubility, viscosity and swelling characteristics [45, 54, 55]. The species and concentration of ion play a significant role in the effect observed on protein solutions, such as illustrated by the Hofmeister series ranking the effectiveness of ions for salting-out globular proteins [56, 57]. At low concentrations of salt, protein solubility can

be increased with the addition of salt, which may shield surface charges on the protein and stabilize its structure, leading to a salting-in effect [58, 59]. However, at high salt concentrations, salt-induced protein-protein interactions can lead to the protein precipitating, potentially due to salts interacting with the water such that water cannot hydrate the proteins as effectively, making protein-protein interactions more favourable [57, 58]. Inorganic salts have also been used as additives to lower the viscosity of highly concentrated protein solutions, thought to be due to the anions interacting with the protein in such a way as to help break protein-protein interactions and reduce the formation of protein networks [60, 61]. Work done previously in the lab has shown some of these effects as well as the addition of the divalent salt, $CaCl_2$, lowered the viscosity of a high-concentration GelMA solution [45]. It was also shown that highly-modified GelMA is negatively charged, as the majority of the amines become capped with methacrylamide groups, and it is thought that the addition of the Ca^{2+} effectively masked some of the charges on the GelMA, allowing for less electrostatic repulsion between GelMA molecules and thus enabling the GelMA strands to take on a less rigid, more free-flowing conformation, leading to the observed decreases in viscosity [45].

1.3 Methods to Further Improve Hydrogel-Based Material Mechanical Properties

Further methods have been explored to improve the mechanical properties of hydrogel materials, including the fabrication of double network hydrogels [62, 1, 63], small-molecule additives [64, 65, 37], and compositing with a stiffening phase, such as ceramic or clay micro- or nano-particles [66, 29, 67]. Double network hydrogels, a subset of interpenetrating networks, involve two intermeshed polymer networks, often one a densely-crosslinked, brittle network, and the other a lightly-crosslinked, ductile network [68, 69]. Internal fracture of the brittle network while the ductile network remains unbroken allows for energy dissipation and increased material toughness [69]. Small molecule additives can be used to affect many material properties, such as changing the uncured material's viscosity and the cured material's mechanical properties [64, 38]. Additionally, small molecule additives can be free-floating or copolymerized into the hydrogel network as crosslinking bridges [70, 64, 38]. Finally, when compositing a compliant hydrogel with a stiff ceramic phase, the matrix helps distribute applied stresses across the stiff phase more evenly through the material, reducing stress concentration effects on the stiff phase and increasing strength by applying stress to the stronger phase [71].

Polymer science provides clues on how to improve the mechanical properties of hydrogel networks further. Due to its pendant aromatic ring, styrene is used to tune the mechanical properties in a number of materials, such as acrylonitrile butadiene styrene rubber and unsaturated polyesters,

through steric hinderance and phase separation, and polyether ether ketone (PEEK) and other aromatic polymers are known to have extremely high mechanical properties due to having an aromatic ring structure in the polymer backbone [72]. Unfortunately, many benzene-containing molecules are toxic, and these polymers are typically not biodegradable.

Monosaccharides, such as glucose, ribose, and glucosamine (GlcN) are small, naturally occurring ring-structured molecules. Monosaccharides contain many reactive functional groups per molecule, mostly hydroxyls and sometimes amines, but lack the double-bond resonance structure of benzene. Additionally, most monosaccharides are capable of opening to a linear, aldehyde or ketone form, as shown in Figure 1. If the hydroxyl on a monosaccharide's carbon 1 is modified, the cyclic structure is essentially locked in place as the ring-opening reaction is no longer possible. GlcN, a monosaccharide resembling glucose with the hydroxyl on carbon 2 replaced with an amine, is an abundant monosaccharide and a prominent building block of chitin and chitosan [73]. Given GlcN has two different functional groups with different reactivities, it is an interesting case material for testing methacryloyl functionalization of monosaccharides. The differing reactivities of the amine and hydroxyls might be exploited to consistently make a material with only the amine grafted with vinyl groups to make a monofunctional UV-curable material [64]. A polyfunctional UV-curable material could possibly be fabricated by reacting all the amine and hydroxyl groups. A monofunctional glucosamine-methacryloyl (GlcN-MA) would likely resemble polystyrene when cured, with a linear backbone and pendant ring groups, where a polyfunctional GlcN-MA would be anticipated to form a complex polymer somewhat resembling PEEK, with the ring structure incorporated into the backbone, though the potential for pendant ring groups would still be present.

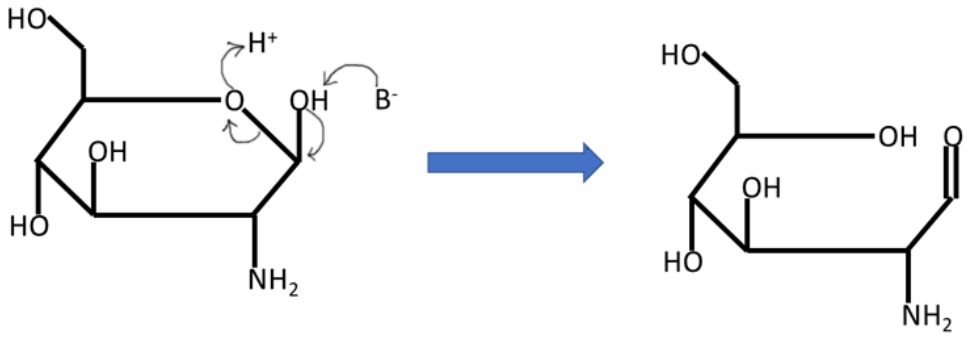

Figure 1 Chemical structure of glucosamine and aldehyde ring-opening reaction. B^- represents a base and H^+ represents a proton.

1.4 Three-Dimensional Printing

The field of three-dimensional (3D) printing has been rapidly growing in the recent past, and has seen research and success in many fields, such as aerospace engineering and bioprinting [74]. Two common 3D printer types used with polymeric materials are the direct ink writing (DIW) 3D printer, and the mask stereolithography (mSLA) 3D printer. One of the main properties that determines what type of printer an ink is suitable for is the ink's rheological properties, such as its viscosity over different shear stresses, if it has a shear-yield strength, or if the ink is a Newtonian fluid or shear-thinning [75, 29]. With DIW printers, ink is deposited layer-wise onto a print bed via a nozzle following a preprogrammed pattern, and the ink is cured almost immediately upon laydown. DIW printers typically make use of UV-curable, viscoelastic inks that exhibit a notable shear yield (>50 Pa) and some degree of shape-holding, as there is a brief period of time between laydown and curing where the ink may slump and reduce print shape fidelity [76, 75]. mSLA printers work by dipping the print bed into a pool of photo-curable ink to a defined distance above a liquid crystal display (LCD) screen which emits the curing light in the pattern of each layer. Once the layer is cured, the print bed is lifted and dipped back into the ink to replenish the available uncured ink between print bed and LCD screen. Since mSLA printers require inks to be free-flowing, low-viscosity (<5 Pa·s) inks without shear yield strength and shape holding properties are ideal [77].

1.5 Objectives and Hypotheses

The main objective of this work is to develop a new, monosaccharide-based UV-curable additive for hydrogels to increase the mechanical properties closer to that of load-bearing tissues. As such, a number of hypothesis have been posited:

1) It is thought that the reactive functional groups on glucosamine, namely hydroxyls and amines, can be reacted with vinyl-containing molecules to form glucosamine-methacryloyl (GlcN-MA).
2) Given the inherent ring structure of monosaccharides, it is hypothesized that these additives will form rigid crosslinking bridges between GelMA molecules when cured and improve the mechanical properties of the hydrogel material.
3) The anticipated improvement in hydrogel mechanical properties is also hypothesized to translate to improved mechanical properties of a composite material using the developed hydrogels as the polymer matrix.
4) Due to masking charges, the addition of $CaCl_2$ will reduce the viscosity of the GelMA/GlcN-MA based materials.
5) With tunable rheology, the hydrogel and composite materials are expected to be able to print on 3D printers.

2. Experimental Outline

With the end-goal of developing a composite material based on nHA, GelMA and the GlcN-based additives, a strong experimental plan was necessary to ensure success. The broad overview of this experimental plan is given in Figure 2.

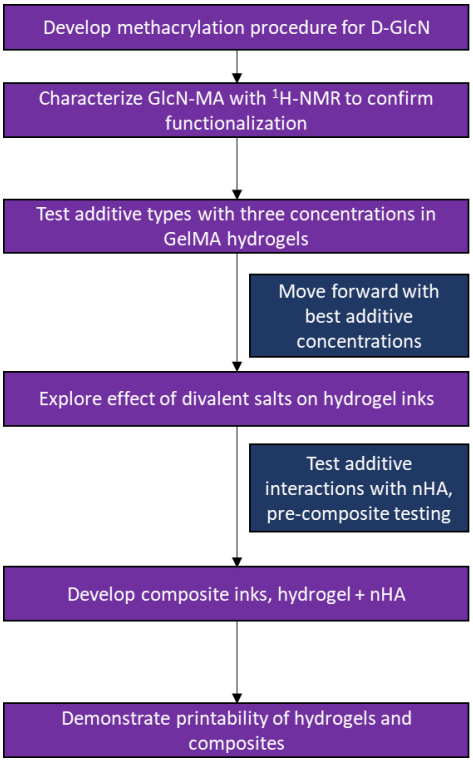

Figure 2 High-level overview of thesis experimental plan.

The first step in this thesis was to develop the procedure necessary to fabricate the additives tested throughout the thesis. This step included literature review of similar procedures, testing and optimization of the procedure to provide the most practical and effective functionalization method [36, 64, 78]. Successful functionalization and batch consistency during the methodology development was confirmed using proton nuclear magnetic resonance (NMR) spectroscopy.

Once the GlcN-MA fabrication procedure was finalized, the additives were tested at three different concentrations to explore the effects of each additive on the GelMA hydrogel. Throughout the work, the material's rheology, curing kinetics, compressive and dynamic mechanical properties, and water-uptake in aqueous environments was explored. Once the most promising concentration for both additives is determined, those materials were chosen for continued exploration.

Understanding that the presence of ions can significantly affect the properties of proteins and their solutions, and previously performed research in the lab on similar materials showed improved rheological properties with the inclusion of salts [45], hydrogels with the chosen additive concentrations were fabricated using a salt solution. The same characterizations previously performed were performed on salt-containing materials, and the effects of the presence of salt were determined by comparing to the previously obtained salt-free materials. Additionally, the hydrogel materials were printed using an mSLA printer as a proof of concept to show that the developed materials could effectively be used as 3D printer inks.

Before fabricating composite inks with the chosen hydrogels, nHA-additive interactions were tested through gravimetric settling. As the polarity, charge and hydrogen-bonding capability of each additive is expected to be different, it is possible that nHA particles, with surface phosphates and calcium ions, may interact favourably with one or more of the additives. Favourable nHA-additive interaction may allow for improved dispersion and/or longer suspension times, but could also affect the composite ink's rheological characteristics. This may provide preliminary insight into the performance of the composite materials with the developed additives.

Finally, composite materials of the hydrogel materials and 10% volume fraction (VF) nHA, with and without salt, were fabricated. The same characterization techniques performed on the hydrogel materials were performed on the composite materials. Results from the composites were compared to their respective hydrogel materials, and the effects of salt on the composite material compared. Finally, a composite material containing the developed additives was printed on an mSLA printer to confirm its potential as a 3D printer ink.

3. Materials and Methods

3.1 Materials

All materials were sourced from Millipore-Sigma and used as received, unless otherwise stated. Type-B, 255-bloom gelatin from bovine skin and D-(+)-Glucosamine HCl were the base materials used for methacrylation. Methacrylic anhydride was used as the methacrylating agent. Sodium hydroxide (NaOH) pellets and hydrochloric acid were used to maintain pH throughout the study. $CaCl_2 \cdot 2H_2O$ was used to make 100 mM $CaCl_2$ solutions in MilliQ (mQ) water. Lithium phenyl-2-4-6 trimethylbenzoylphosphinate (LAP) was used as the photoinitiator for the UV curing inks. 120 nm long, 20-30 nm diameter rod-like calcium-deficient, carbonated nHA with 66% crystallinity and Ca/P molar ratio of 1.52 was obtained from MKNano, Mississauga, Canada and used as received [79].

3.2 Gelatin Methacrylation

Highly functionalized (>90% amine conversion) GelMA was fabricated following an already published procedure with minor modification [36]. 100 g of Type-B Gelatin was dissolved in 800 mL of mQ H_2O heated to 40°C under constant stirring. The solution's pH was adjusted to pH 7.4 using 4 M NaOH, measured using a pH meter (Thermo Fisher Scientific Accumet AB150). 52 mL of methacrylic anhydride (10:1 methacrylic anhydride molecules to free gelatin amines) was added dropwise, and then reacted for 2 hours while protected from excess light, with the pH maintained between 7.0 and 7.4. The solution was then brought to pH 8.0 and placed into cellulose dialysis tubing (MWCO ~13 kDa) to dialyze against room-temperature mQ water over one week while protected from light, and with the solution rebuffered and water replaced at the halfway timepoint. The GelMA was then frozen at -4°C, and lyophilized (using a Labconco Freezone) for 3 days to obtain the dry, spongy GelMA material. Dry GelMA was powdered using a mechanical grinder to allow for easy dissolution, stored sealed at room temperature, and protected from light until use.

3.3 Glucosamine Methacrylation

As no other published methodology for methacrylating D-GlcN was known at the time of writing, a procedure was developed following procedures on similar materials as guidelines [36, 78]. It is important to note, however, that there has been precedent in developing an acrylated GlcN with the use of acryloyl chloride, lending support that functionalizing GlcN is possible [64]. However, the equivalent chemical to that used for the acrylated GlcN for methacrylating, methacryloyl chloride, is noted for being very dangerous, with the SDS from ThermoFisher Scientific citing "fatal if inhaled" as one of its hazard statements [80]. As such, a method for functionalizing GlcN with a significantly

less dangerous methacrylating agent, such as methacrylic anhydride was desired [81]. A pictographic representation of the methacrylation procedure using methacrylic anhydride is given in Figure 3.

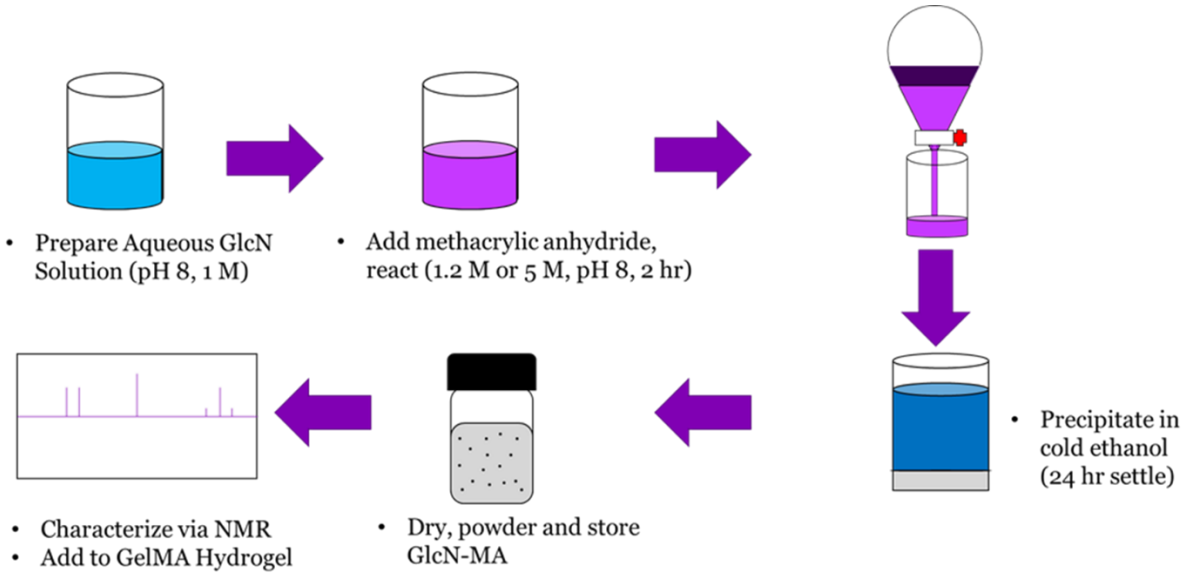

Figure 3 Flowchart of the methacrylation of glucosamine.

A 1 M solution of D-GlcN HCl was prepared by dissolving 10.749 g of D-GlcN HCl in 60 mL of room temperature mQ water under constant stirring. The pH of the solution was measured and brought to pH 8.0 using 4 M NaOH, and the sides of the beaker covered to prevent excessive light exposure. Two anticipated levels of functionalization were tested throughout this work, achieved by adjusting the amount of methacrylic anhydride used for the reaction. Either 10.8 mL (~1.2 molar equivalent) or 45 mL (~5 molar equivalent) of methacrylic anhydride was added dropwise to the GlcN solution over approximately 5 minutes. The solution was allowed to react over 2 hours, with the pH maintained between 7.7 and 8.3 using 4 M NaOH. This produced what is referred to throughout this work as "1.2X GlcN-MA" (from 1.2X molar equiv.) or "5X GlcN-MA" (from 5X molar equiv.). The pH was then adjusted to 6.0 using 4 M HCl, quenching the reaction. Using toluene as the organic phase, excess methacrylic anhydride and by-products (methacrylic acid), which enter the organic phase, was removed using liquid-liquid extraction. The aqueous solution containing the GlcN-MA was then concentrated using heated convection until signs of precipitation appear. The concentrated solution was then precipitated into ~200 mL of cold (-4°C) ethanol, which was covered and kept at -4°C overnight to allow for the precipitation to finish and products to settle to the bottom of the vessel. The eluent was then poured off and dried, and when liquid was no longer visible, the remaining material was dried at 50°C until the sugar was no longer tacky. The dried GlcN-MA was then

collected, powdered with a mortar and pestle to allow easier dissolution, sieved and stored in a sealed glass jar in a refrigerator until use.

3.4 Proton Nuclear Magnetic Resonance Spectroscopy

Proton (^{1}H) NMR spectroscopy was performed to confirm successful functionalization of GlcN-MA, and to ensure batch consistency of GelMA functionalization. NMR samples were prepared by dissolving 20 mg of material into 1.4 mL of deuterium oxide, which was then placed into liquid-state NMR tubes. GelMA functionalization was analyzed by monitoring the existence of lysine amino acid peaks, centred around 3.0 ppm, and the appearance of methacrylate vinyl group peaks from approximately 5.25-5.75 ppm [47]. GlcN methacrylation was monitored by observing the loss of spectral peaks from 2.8-3.3 ppm and 3.4-4.0 ppm (amine and hydroxyl protons, respectively), and the gain of peaks from 1-2 ppm and 5.2-5.8 ppm (methyl and vinyl protons, respectively), along with comparisons to literature proton NMR spectra for GlcN [82, 83, 84]. ^{1}H NMR was performed on a Bruker 500 MHz NMR, and data was analyzed using Topspin 1.3.

3.5 Hydrogel Ink Fabrication

Hydrogel inks consisting of 62% w/v GelMA, and varying concentrations of 1.2X- or 5X GlcN-MA, were fabricated with the recipes shown in Table 2. Concentrations of GlcN-MA were chosen to maintain a consistent ratio of anticipated GelMA methacryloyl groups (assuming full amine conversion) and GlcN-MA molecules. Three concentrations of GlcN-MA were chosen, 50 mM, 250 mM and 1 M, which correspond to GlcN-MA: GelMA amine ratios of 0.25, 1.25, and 5, respectively.

Inks were fabricated by heating the water to ~40^{o}C while mixing at 60 RPM, then dissolving the ingredients roughly in order of increasing molecular weight; LAP, then GlcN-MA (if applicable), and finally, dissolving the GelMA scoopwise. Once all solids were dissolved, 1-Octanol was added dropwise as an anti-foaming agent [85]. The beaker was then fully covered with aluminum foil to protect the ink from excessive light exposure and allowed to mix at heat for 20 minutes. The heat was removed, and the ink allowed to mix and slowly cool towards room temperature over 15 minutes. The ink was then poured through a fine-meshed sieve into a 50 mL conical tube, which was sealed, fully covered in aluminum foil, and stored overnight to allow any remained bubbles to dissipate before use.

Table 2 Material contents in %w/w for tested hydrogel inks

Ink Name	Solvent (mQ H_2O or 100 mM $CaCl_2$)	Lithium phenyl-2-4-6 trimethylbenzoylphosphinate photoinitiator	1.2X GlcN-MA	5X GlcN-MA	GelMA	1-Octanol
Control	60.23	0.06	0.00	0.00	39.21	0.50
50 mM 1.2X	59.78	0.06	0.74	0.00	38.92	0.50
250 mM 1.2X	58.08	0.06	3.58	0.00	37.81	0.48
1M 1.2X	52.45	0.05[2]	12.91	0.00	34.15	0.44
50 mM 5X	59.30	0.06	0.00	1.54	38.61	0.49
250 mM 5X	55.86	0.06	0.00	7.25	36.37	0.46
1M 5X	45.89	0.05[1]	0.00	23.81	29.87	0.38

[1] the values given in the table are weight %, and the large mass of additive shifts the overall mass of the ink enough to cause the %w/w to appear low, but the ratio of GelMA to LAP remains the same

3.6 Composite Ink Fabrication

To see if improvements seen in the hydrogel inks translate to a composite ink, 10% VF nHA composite inks were fabricated with previously developed hydrogel inks as the matrix. The ratio of GelMA methacryloyl groups to GlcN-MA molecules was maintained between the hydrogel and composite inks. Hydrogel materials were first fabricated as reported above. Then, 5 mL of hydrogel was then added to 15 mL conical tubes, and 1.637 g of nHA (ρ=2.92 g/mL) was added scoop-wise to achieve the 10% VF nHA content. A probe ultrasonicator (Branson Sonifier 450) was used at 50% duty cycle for 1 min to disperse and mix each scoop of nHA into the hydrogel. Inks were covered and allowed to cool between sonication to ensure ink did not get too hot and gel pre-emptively. As sonication is known to introduce air bubbles into the inks, the composite inks were allowed to sit

overnight sealed and protected from light. Inks were sonicated for 30 seconds before use to disperse the particles with minimal air bubble introduction.

3.7 Dynamic and Quasi-Static Compressive Mechanical Testing

Mechanical testing for hydrogel inks was performed on cast cylinders with dimensions ~4 mm tall, ~4.5 mm diameter. To ensure the samples would not overload the loadcell, composite materials were tested using cylindrical samples ~ 4 mm tall, 3.1 mm in diameter. Cylinders were cast in polyethylene molds with glass slides bookending the mold. Inks were cured for 30 seconds using a Dymax PrimeCure 385 nm LED wand at 100% intensity and no lens. Curing parameters were chosen based on previously performed work in the lab, and confirmed later in this work through Cure Depth [45, 86]. Of note is that the molds are not completely opaque, and the diameter of the mechanical testing samples is significantly smaller than the Dymax wand, leading to additional curing from indirect UV light. Cylinder dimensions were measured using a micrometer, loaded onto a petri dish and fully covered with mQ water droplets to prevent the sample drying out during mechanical testing. Samples were tested on a Univert tester with a 200 N loadcell (CellScale, Waterloo, Ontario) shown in Figure 4. Samples were preloaded to ~0.5 N to ensure contact, and then cyclically loaded to ~10% strain at a frequency of 0.1 Hz for three cycles, then compressed to failure at a rate of 1 mm/min. The resulting engineering stress-strain curves were analyzed using MATLAB code. The complex modulus was determined using a Fourier Transform of the cyclic portion of the test. Toughness was defined as the area under the quasi-static portion of the stress-strain curve. The elastic modulus was taken as the slope of the initial linear portion (0.75-7.5% strain) of the stress-strain curve. At least 5 samples were obtained for each material.

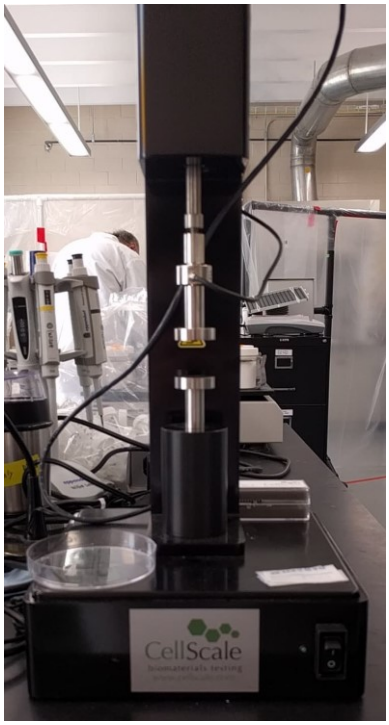

Figure 4 UniVert CellScale mechanical testing apparatus with compression testing attachments and 200N loadcell.

3.8 Cure Depth

As one of the main thrusts of the work is to see if the developed materials are capable of functioning as 3D printer inks, it is important to assess the curing kinetics, primarily the cure depth, of the materials. This will allow early insight into potential issues for sufficient curing on a printer if it is found that the materials require too large a dosage to cure sufficiently, or give assurance that curing would not be an issue. For sufficient curing, the materials should be able to easily cure on the order of hundreds of microns, a typical length scale for 3D printer layers. To determine the curing kinetics of the UV curing inks, samples in ~1 cm deep polyethylene molds were cured with a single Dymax Primecure 385 nm wand with no lens. Lenses were not used for cure depth to ensure even curing, as a lens would focus the light to its focal point. Intensity was maintained at 100%, and exposure time was changed to vary the total dosage of energy to the sample, 3 samples were made per dosage. Energy dose was measured 3 times before curing the samples. Cured samples had side-profile photos taken next to an object of known height (Canadian nickel, height = 1.76 mm). Images were analyzed using ImageJ (National Institutes of Health, University of Wisconsin) to obtain the height of the cured samples. Cure depth was then plotted against the natural log of normalized energy dosage, and fitted using the equation:

$$C_d = D_p \ln\left(\frac{E}{E_c}\right)$$

where C_d represents cure depth, D_p is the depth of penetration, E is the applied energy dosage, and E_C is the critical energy of the material. As previously noted, the main focus of this study for each material is to determine if there are likely to be curing issues for a given printer, and as such, while the curing kinetic parameters of D_p and E_c will be analyzed, the thrust of the experiment is for sufficient cure depth at low dosages.

3.9 Swelling

Often hydrogels swell and increase in both size and mass when submerged in water, which could lead to issues for implants made of these materials. Therefore, given that the anticipated applications for the developed materials involve being used in aqueous environments, understanding how much water the developed materials absorb when submerged in water is important for predicting potential future issues for implants.

Samples for swelling were prepared using the same method and molds as used for mechanical testing. Freshly cured samples were weighed initially (M_o), and then placed in 5 mL of room temperature mQ water in 15 mL conical tubes. mQ water was chosen as the swelling medium to prevent any potential salt-induced interactions from ions not intentionally added to the system. Samples were allowed to swell for 24 hours and were then had their surface carefully dried with a Kimwipe and then reweighed (M_{24}). The water was then replenished, and the samples swelled for a further 6 days before being dried and weighed again, for a total swelling time of 1 week. Mass gain as a fraction of initial mass was determined by dividing a swelled time-point by the initial mass of the sample, as calculated with the example equation for the 24-hour time point given below. Three specimens were tested per material.

$$\%swell = 100 * \left(\frac{M_{24}}{M_0} - 1\right)$$

3.10 Rheology

To understand which 3D printer types the developed hydrogel inks would be best suited for, and gain insight into molecular interactions of the uncured inks, rheological measurements were taken over a range of shear stresses (0.1-250 Pa). First, the effects of adding the three concentrations of GlcN-MA additive were explored to gain insight on the potential interactions of the two additives and GelMA. Then, as it was expected that adding nHA to the tested hydrogels would significantly

increase the viscosity of the uncured materials, the hydrogel materials were tested with the inclusion of 100 mM $CaCl_2$, as recently published research from the lab on a similar GelMA material has shown the addition of salt significantly lowers the viscosity of the tested materials [45]. Given the interaction of salts with GlcN-MA is unknown, characterizing the effects salt has on the hydrogel material would prove useful before fabricating the composites.

Inks intended for rheology were fabricated using the same methods used to make hydrogel inks intended for mechanical testing or compositing. Viscosity was measured using a Bohlin CS Rheometer and a C25 cup-and-bob geometry at room temperature, as shown in Figure 5. Three rheology measurements were made per ink.

Figure 5 Bohlin CS Rheometer with C25 cup-and-bob geometry measuring the viscosity of a composite GelMA/nHA material.

3.11 Settling Experiments

It is known that nHA has multiple charged sites, with negative phosphates and positive calcium ions, which may allow the particles to interact with liquid-state molecules, lowering the amount of particle aggregation and settling. Given the varying levels of polarity and hydrogen bonding capabilities of the developed additives, gathering evidence of favourable interactions may give additional insight on how stable suspensions of the pre-cured composite materials will be with the differing types of additives.

In preparation for the compositing of the hydrogels, getting a preliminary understanding of the interactions between the two functionalized GlcN-MA, water and nHA was desired. 20 mL of

solution (mQ water, 50 mM 1.2X GlcN-MA and 50 mM 5X GlcN-MA) was prepared and placed in a 20 mL scintillation vial with 0.1 g of nHA, or ~0.5 wt% particle concentration, near the reported upper limit for use in light scattering techniques for settling [87, 88]. Samples were then sonicated for 1 minute, and photos taken against a dark background at timepoints 0s, 1 min, 2 min, 5 min, 10 min, 20min, 30 min, 24 hr, and then visually compared. Solutions that can suspend the nHA particles for longer periods of time are thought to have more favourable interactions with the nHA, which keep the nHA particles dispersed [87].

3.12 mSLA 3D Printing of Hydrogel and Composite Materials

To test if the developed materials can function as 3D printer inks, a hydrogel and composite material were chosen for test prints on a Phrozen Sonic Resin 3D Printer, an mSLA printer. Materials are fabricated as previously discussed.

The Phrozen printer makes use of 405 nm light to cure, and a layer thickness of 100 μm was chosen to reduce overall print time. Hydrogel materials were printed with 30 seconds of curing per layer, and composite materials were cured for 45 seconds per layer, as preliminary tests indicated these cure times should be sufficient to cure the layer height with the Phrozen printer.

3.13 Data Analysis

Data is graphically presented as the mean value with error bars representing one standard deviation. Statistical significance compared to a control was determined using a one-way analysis of variance with a Holm-Sidak post hoc test, and tests comparing two variables were analyzed using a two-way analysis of variance with a Holm-Sidak post hoc test. Results are considered significant for $P < 0.05$.

4. Glucosamine Methacrylation and Hydrogel Characterization

4.1 Results

4.1.1 ^{1}H NMR

As the GelMA used in this study was fabricated in house, regular consistency checks to ensure the anticipated degree of functionalization is achieved are important. Checks were performed using proton NMR, with a sample spectra of gelatin and the fabricated GelMA provided in Figure 6.

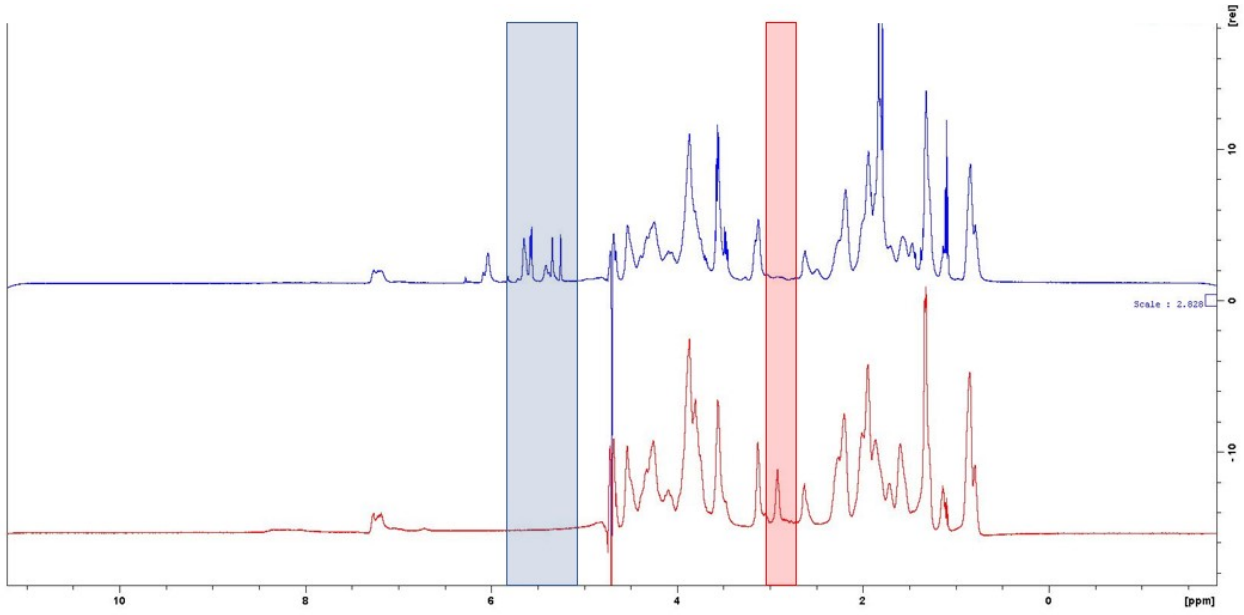

Figure 6 ^{1}H NMR spectra for Gelatin (red, bottom) and GelMA (blue, top)

As can be observed in the red shaded box, the gelatin peak at 3.0 ppm, representing the lysine residue, is not observed in the spectra of the fabricated GelMA. Additionally, significant peaks not observed for the gelatin spectra appear between 5 and 6 ppm for the GelMA spectra, which are related to the addition of vinyl groups to the gelatin structure. These combined results suggest the successful fabrication of a highly-modified GelMA.

Given that the procedure used for fabricating the GlcN-MA is new, it is of critical importance to characterize the material and ensure that functionalization proceeded as expected. As with GelMA, the functionalization of GlcN can be examined using proton NMR, as shown in Figure 7.

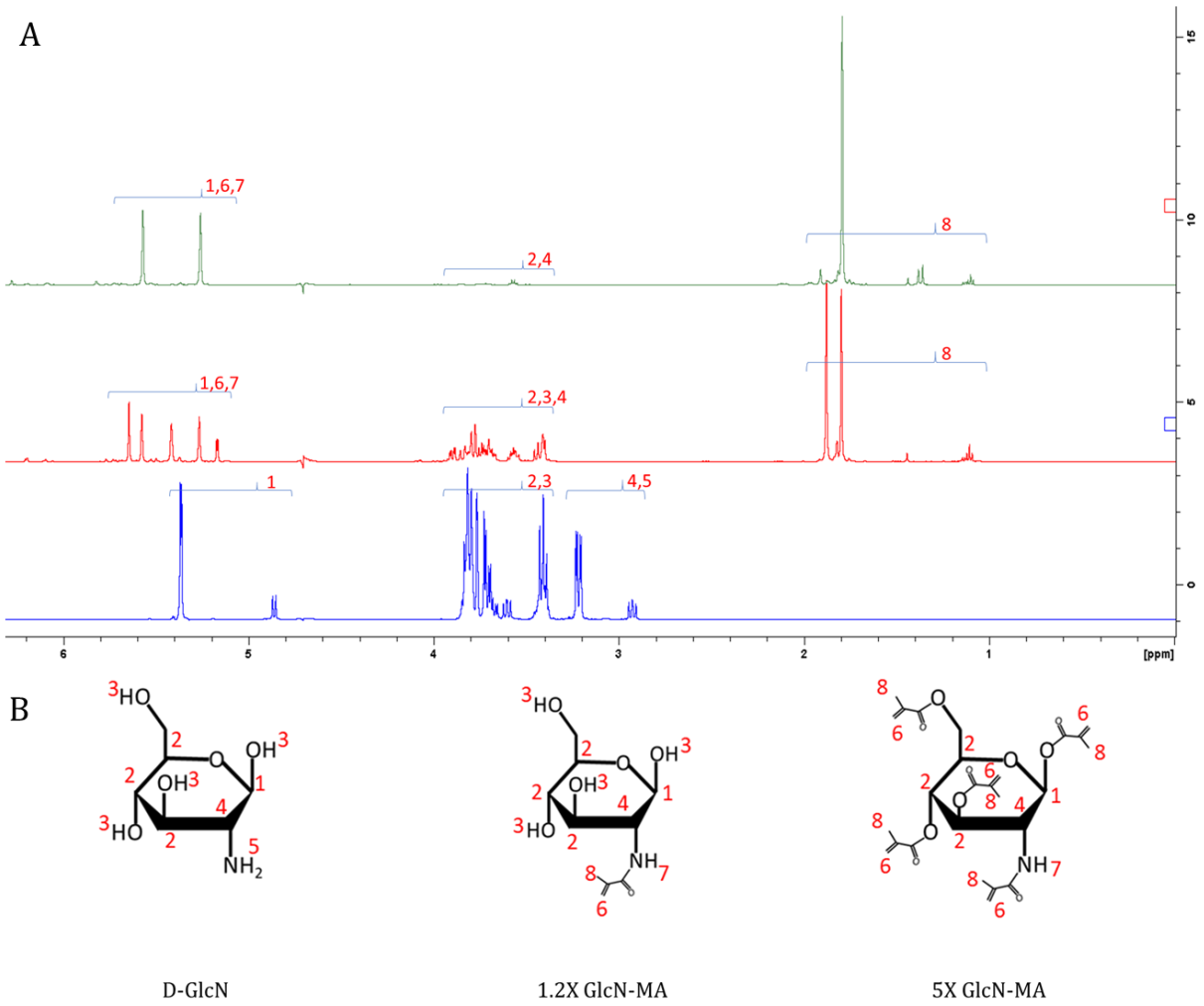

Figure 7: A) ^{1}H NMR spectra for D-GlcN (Blue, bottom), 1.2X GlcN-MA (Red, middle), and 5X GlcN-MA (Green, top) B) Anticipated chemical structures of GlcN-based additives with red numbers indicating which group of NMR peaks the hydrogens are thought associated with.

Examining the gains and losses of peaks between the bottom, blue spectra of unreacted D-GlcN and the other two spectra representing GlcN-MA gives insight into the state of GlcN's functionalization. Looking at the middle, red spectra of the 1.2X GlcN-MA, peaks from 2.8-3.3 ppm are no longer present when compared to the bottom spectra of D-GlcN. However, peaks appeared over the ranges of 1-2 ppm and 5-6 ppm. Examining the top, green spectra of the anticipated 5X GlcN-MA, it is immediately apparent that the majority of the peaks originally between 2.8 and 4 ppm in D-GlcN are no longer present, but peaks at 1-2 and 5-6 ppm are also present. This gives evidence of successful modification of amines and hydroxyls on the original GlcN structure.

4.1.2 Salt Negative Hydrogel Rheology

The rheological characteristics of the uncured hydrogel materials with varying concentrations of GlcN-MA additive without salt are displayed in Figure 8 below.

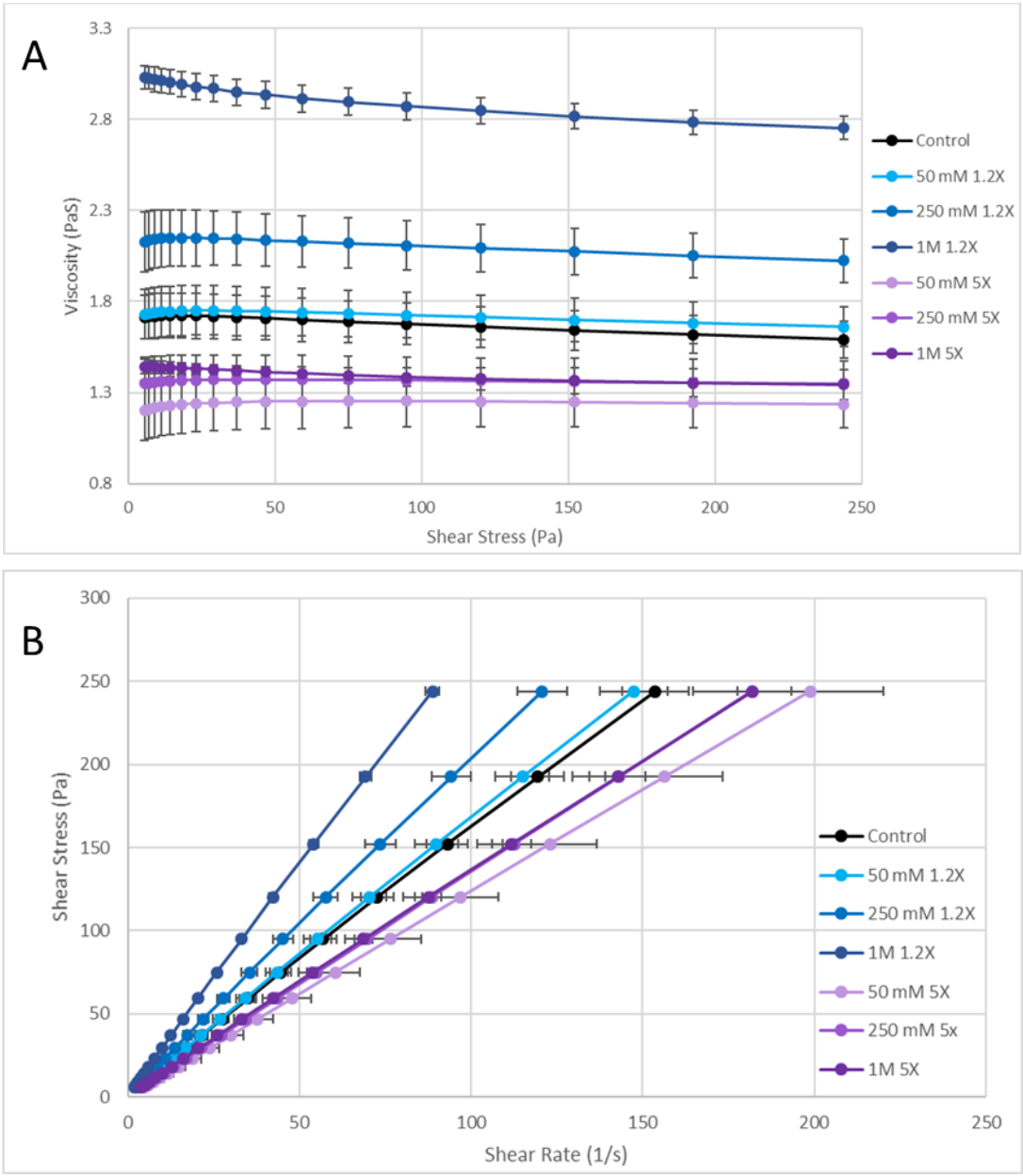

Figure 8 Rheological profiles of salt-negative GelMA/GlcN-MA hydrogel inks of varying GlcN-MA type and concentration compared to a GelMA-only control, N=3.

To begin, all of the inks tested in this experiment appear to be Newtonian, as there is a linear relation between shear rate and shear stress. Additionally, as the curves all appear to pass through the origin in the shear stress vs shear rate graph, there is no observed shear yield point for the tested inks [89].

The viscosity of the inks was dependent on the type and concentration of additive used. The viscosity of the inks increased compared to the control when the 1.2X GlcN-MA is used as the additive, with higher viscosities observed with higher concentrations of additive. At the 50 mM concentration, the difference in high-shear viscosity is not significant compared to the control (P= 0.691). However, the high-shear viscosity increases by ~ 27% at 250 mM (P=0.002), and nearly doubles with the 1 M concentration of 1.2X GlcN-MA (P<0.001). In contrast to the 1.2X GlcN-MA, however, the viscosity of the inks decreases with the addition of 5X GlcN-MA. Interestingly, 50 mM, the lowest concentration tested, showed the largest effect by having the lowest viscosity of all the tested inks at ~1.2 Pa·s, an ~22 % drop compared to the control (P=0.010). The viscosity appears to rise slightly with the higher concentrations of 5X and are not statistically different from the control at high shear (P=0.071 and 0.076 for 250 mM and 1 M concentrations, respectively).

4.1.3 Salt Negative Hydrogel Cure Depth

Representative curves and key properties for hydrogels cured with 385 nm light are given in Table 3 and Figure 9 below.

Table 3 Depth of UV light penetration and critical energy for GelMA/GlcN-MA solutions cured with 385 nm light.

Sample	Depth of Penetration (mm)	Critical Energy (mJ)	R^2
Control	2.14	23.0	0.94
50 mM 1.2X	2.04	21.1	0.98
250 mM 1.2X	1.93	25.6	0.98
1M 1.2X	1.81	42.2	0.94
50 mM 5X	2.48	43.7	0.96
250 mM 5X	1.95	17.2	0.95
1M 5X	2.17	39.7	0.95

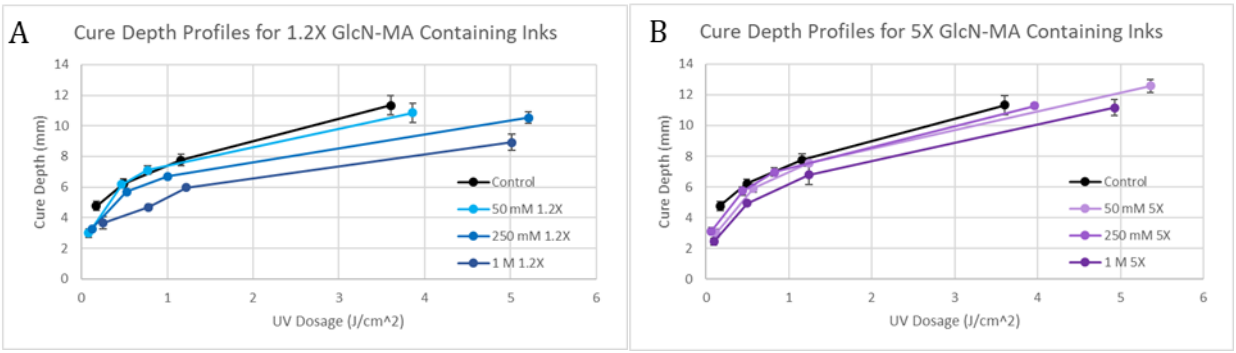

Figure 9 Cure Depth Profiles for 1.2X (A) and 5X (B) GlcN-MA/GelMA inks compared to a GelMA-only control for 385 nm UV light, N=3.

The most immediate take away regarding fabricating with these inks is that all of the inks cure quickly. For all materials, the lowest dosage of UV light, which is measured on the order of 0.2 J/cm^2 and relates to only ~0.2 seconds of curing time, was sufficient to cure more than 2 mm of material. Regardless of additive type, the critical energy for initiating curing is less than 50 mJ, and the depth of UV penetration is above 1.8 mm. The addition of GlcN-MA does appear to lower the overall curing of the hydrogel materials, especially for larger cure depths, as most readily observed in Figure 9. However, drawing further trends from the obtained data set becomes difficult.

4.1.4 Salt Negative Hydrogel Mechanical Testing

Representative engineering stress-strain curves, and average mechanical properties shown in Figures 10 and 11 below.

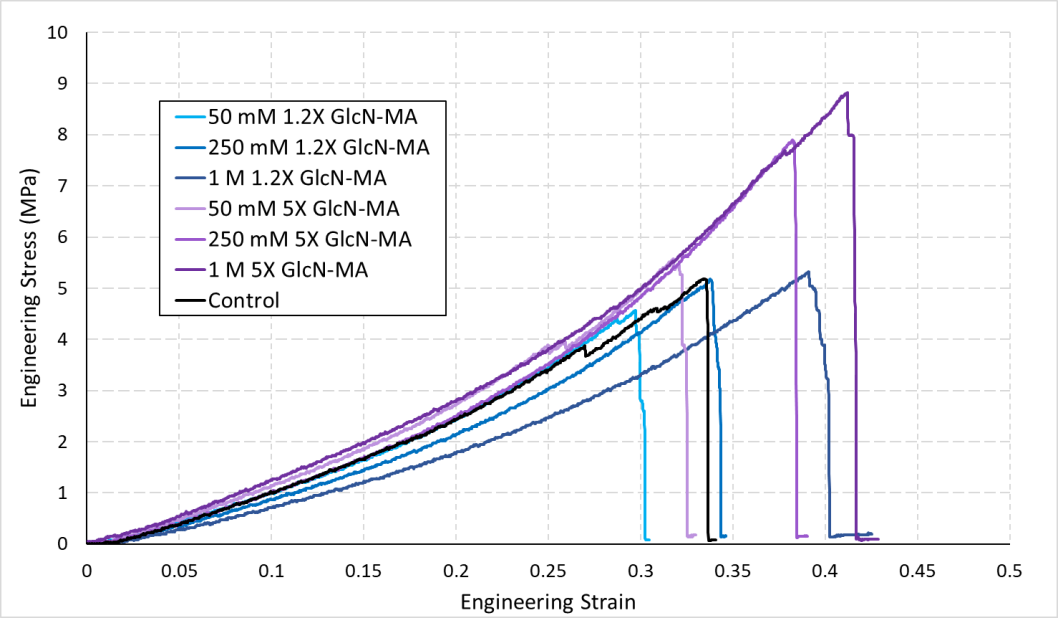

Figure 10 Representative (of an N of at least 5) compressive engineering stress-strain profiles of salt-negative hydrogel inks.

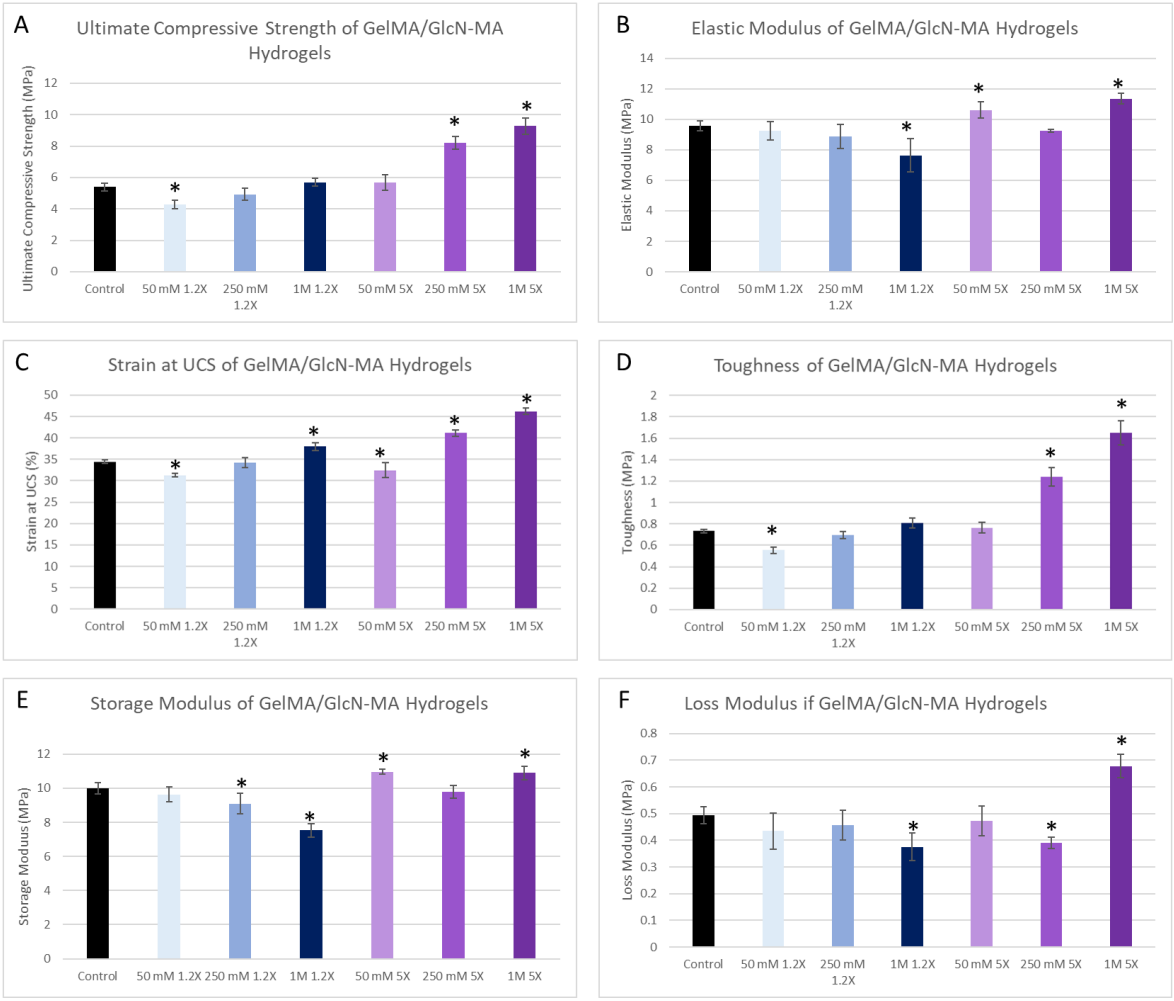

Figure 11 Comparison of compressive and dynamic mechanical properties of salt-negative GelMA/GlcN-MA hydrogel inks with varying types and concentrations of GlcN-MA. '" represents values statistically different from the GelMA-only control. N≥5*

The average ultimate compressive strength (UCS) of the GelMA-only control ink was approximately 5.4 MPa. Overall, the 1.2X GlcN-MA additive did not significantly improve the UCS of the hydrogel at any concentration. At 50 mM, the additive appears to be slightly detrimental to the material's UCS, lowering the UCS ~21% to 4.3 MPa ($P<0.001$). The UCS recovers with higher concentrations but does not significantly improve the UCS at any concentration. For 5X GlcN-MA, the low, 50 mM concentration does not significantly change the UCS from the control ($P=0.445$). However, the UCS improves with the higher concentrations of additive, with the 250 mM ink at about 8.2 MPa (+52%) and the 1 M ink nearly doubling the UCS at 9.3 MPa (both $P<0.001$).

The elastic modulus of the control material was approximately 9.6 MPa. At the 50 mM and 250 mM concentrations, the 1.2x GlcN-MA does not detectably effect the hydrogel's elastic modulus ($P=0.476$ and 0.259, respectively). However, at the 1 M concentration, the 1.2X GlcN-MA had a

detrimental effect on the material's elastic modulus, lowering to about 7.6 MPa (-21%, P<0.001). The trend for 5X is quite interesting, as the 50 mM and 1M concentration inks show significantly improved elastic moduli, at 10.6 (+10%, P=0.040) and 11.4 MPa (+19%, P<0.001), respectively, but the middle, 250 mM concentration showed no detectable improvement over the control (P=0.736).

On average, the control ink reaches UCS at approximately 34.4% strain. Comparing between the 1.2X GlcN-MA inks, the strain at UCS increases with concentration. However, when comparing these results to the control, the 50 mM has a lower strain at UCS than the control at about 31.3% (-9%, P<0.001)), and at the 250 mM concentration, there is no significant difference between it and the control (P=0.796). Only at the 1 M concentration of 1.2X GlcN-MA is the strain at UCS higher than the control at about 38.0% (+10%, P<0.001). Like the 1.2X GlcN-MA, the 5X GlcN-MA also demonstrated increasing strain at UCS with concentration when comparing within the group, and when comparing with the control, the 50 mM ink also has lower strain at UCS than the control. However, 5X GlcN-MA exhibits significant improvements for both the 250 mM and 1 M concentrations, at 41.1% (+19%) and 46.2% (34%), respectively (both P<0.001).

The toughness of the control hydrogel was found to be about 0.73 MPa. For 1.2X GlcN-MA, the 50 mM ink was less tough than the control at ~0.55 MPa (-25%, P<0.001), and did not significantly increase at any tested concentration of additive. For the 5X GlcN-MA, on the other hand, the toughness was either maintained, as with the 50 mM ink, or improved when compared to the control. The 250 mM concentration was found to be ~69% tougher than the control, and the 1M concentration more than twice as tough, with a 125% increase (both P<0.001).

For all inks, the storage modulus follows a similar trend to the elastic modulus discussed previously. The 1.2X GlcN-MA appears to lower storage modulus with increasing concentration, with the 250 mM concentration lowering by ~9% (P=0.003) and 1 M concentration lowering by 25% (P<0.001). The 5X GlcN-MA increases the storage modulus at the 50 mM and 1 M concentrations 10% (P=0.004) and 9% (P=0.005), respectively. The loss modulus also generally shows the same trend, with the 1 M 1.2X GlcN-MA lowering the loss modulus by ~24% (P=0.002). Interestingly, the 50 mM 5X GlcN-MA concentration doesn't improve the loss modulus, and the 250 mM concentration lowers the modulus significantly (-21%, P=0.011). Only the 1M 5X GlcN-MA concentration increases the loss modulus over the control, with a 37% increase (P<0.001).

4.1.5 Salt Negative Hydrogel Swelling

The amount of mass gain compared to freshly cured samples when submerged in room temperature mQ water for given periods of time is reported in Figure 12.

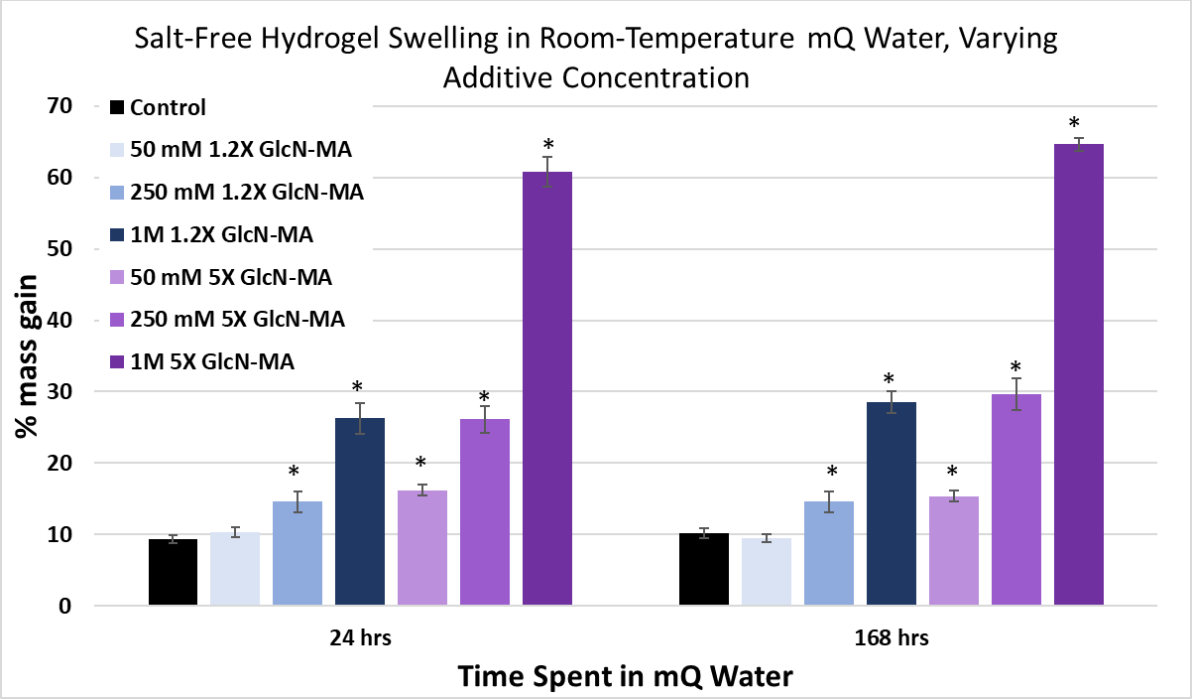

Figure 12 Swelling in terms of mass gain for salt-negative GelMA/GlcN-MA hydrogel inks, compared to a GelMA-only control, in room temperature mQ water. "" indicates statistical significance (P<0.05) when compared to the control for a given swelling time point. N=3.*

All inks, with the exception of 50 mM 1.2X GlcN-MA, gained significantly more mass than the control, which gains ~10% more water over 1 week in water. There also appears to be a positive correlation between the amount of swelling and the concentration of additive used. Another observation across all inks is that the bulk of the water uptake occurs within the first 24 hours, minimal mass gain if any occurs between 24 hours and 1 week in water.

Comparing between the two additives, 1.2X GlcN-MA appears to be less sensitive to swelling than the 5X GlcN-MA for the same concentration. The 1 M 1.2X GlcN-MA ink, which swelled most of the set of 1.2X GlcN-MA inks, swelled to approximately the same degree as the 250 mM 5x GlcN-MA ink at 30% mass gain. The most concerning result, however, is for the 1 M 5X GlcN-MA ink, exhibiting more than a 60% mass gain over a week submerged in water. Notable increases in sample dimensions were noted, but only mass change was measured.

4.1.6 Salt Effect on Rheology

Given that the 1 M concentrations showed the most promising mechanical results for each of the developed GlcN-MA materials, only the control, 1M 1.2X GlcN-MA and 1M 5X GlcN-MA hydrogel formulations are carried forward for the rest of the study.

The rheological characteristics of the hydrogel materials made with 100 mM $CaCl_2$ and compared to those made with mQ water are given in Figure 13.

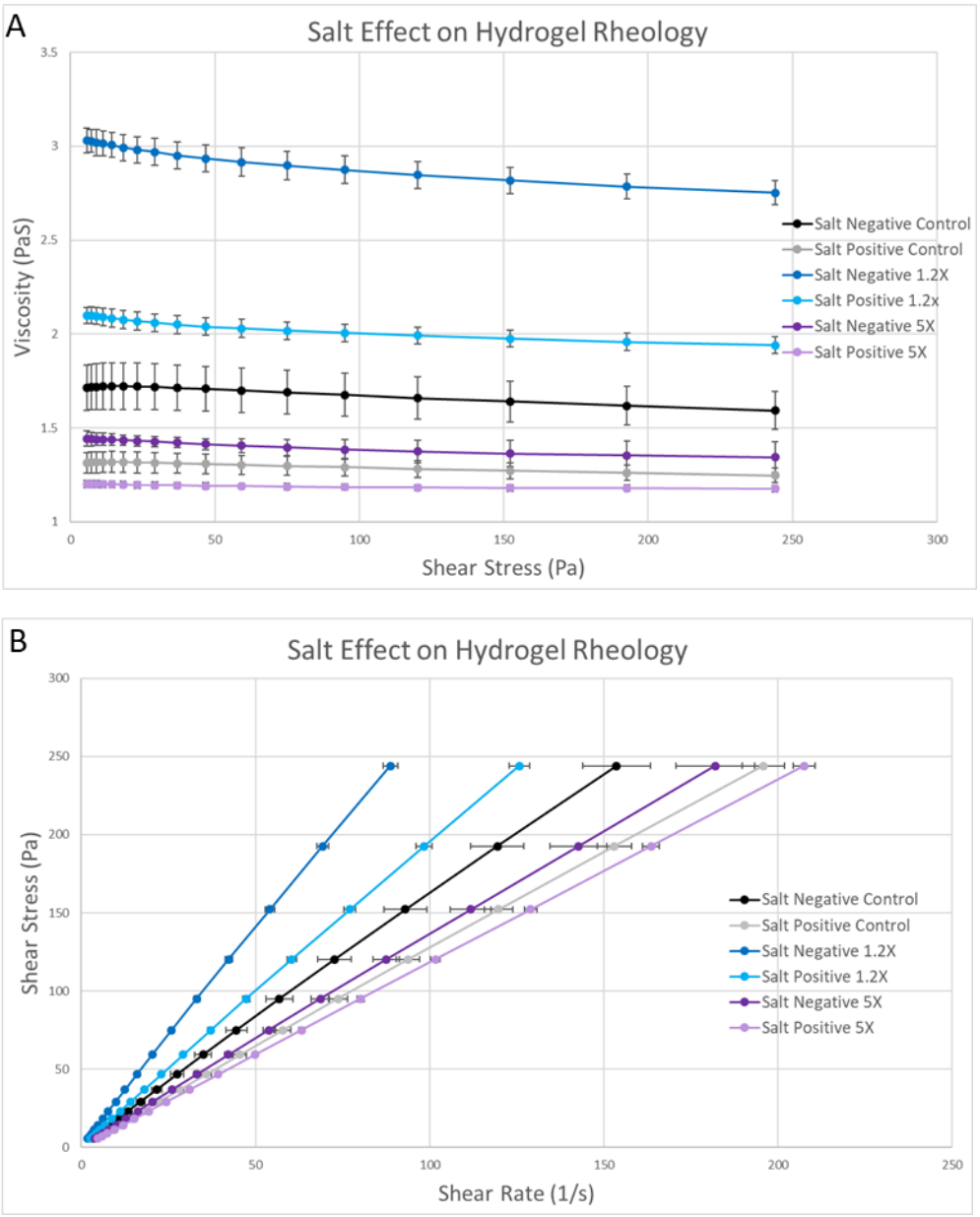

Figure 13 Rheological measurements of GelMA/GlcN-MA hydrogels made with 100 mM $CaCl_2$ solution (positive) or mQ water (negative) compared to GelMA-only controls, N=3.

Upon first look at the rheological results, the trend between additive types appears maintained with the inclusion of salt. The 5X GlcN-MA additive lowers the viscosity of the hydrogel material compared to the control, and the 1.2X GlcN-MA increases the viscosity.

The addition of divalent salts lowered the viscosity for all tested inks when compared to the same formulation without salts. The effect is more pronounced for the control than the 5X GlcN-MA ink. The control's high shear viscosity lowers ~17% from ~1.6 Pa·s without salt to ~1.2 Pa·s with $CaCl_2$ ($P<0.001$), where as the 5X GlcN-MA ink lowers ~8% from ~1.3 Pa·s to ~1.2 Pa·s when salt is incorporated ($P=0.022$). The effect is even more pronounced for the 1.2X GlcN-MA material, which had its viscosity dropped by nearly 30%, from ~2.75 Pa·s to ~1.94 Pa·s with the incorporation of divalent salts ($P<0.001$).

4.1.7 Salt Effect on Cure Depth

The cure depth and curing kinetics results for the salt positive hydrogel cure depths are given in Table 4 and Figure 14

Table 4 Experimental results comparing the effects divalent salt has on the hydrogel's curing kinetics with 385 nm light.

Sample	Depth of Penetration (mm)	Critical Energy (mJ)	R^2
Salt-Negative Control	2.14	23.0	0.94
Salt-Negative 1M 1.2X	1.81	42.2	0.94
Salt-Negative 1M 5X	2.17	39.7	0.95
Salt-Positive Control	2.70	48.8	0.96
Salt-Positive 1M 1.2X	1.60	16.0	0.94
Salt-Positive 1M 5X	2.24	17.5	0.92

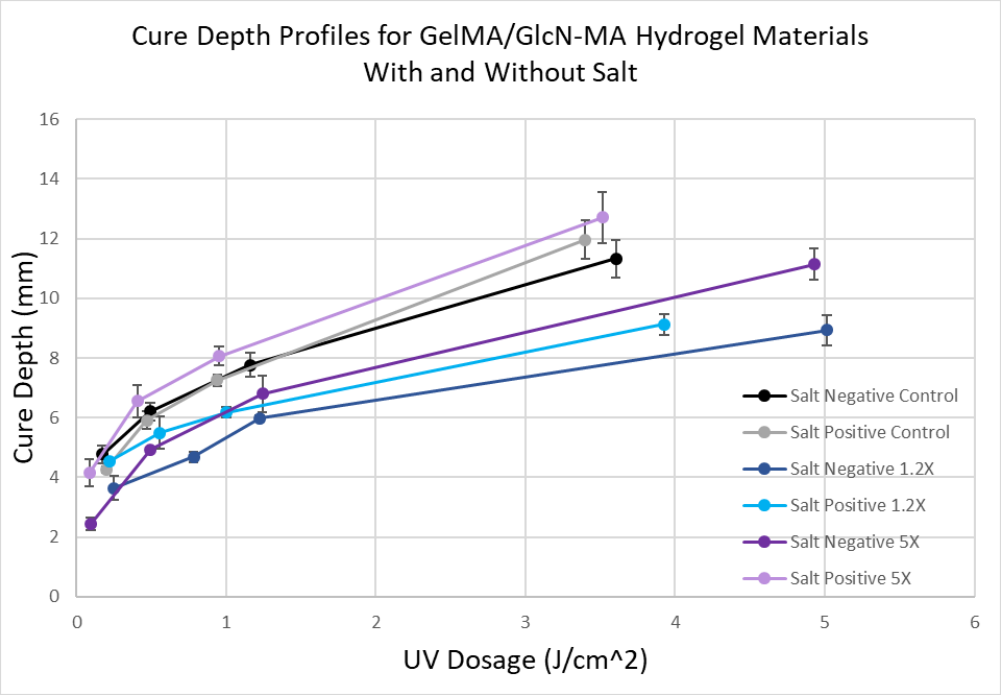

Figure 14 Cure Depth Profiles for GelMA/GlCN-MA hydrogel materials, compared to GelMA-only controls, with and without salt, cured with 385 nm light. N=3

Regarding Figure 14, it is noted that with the lowest measured dosage, approximately 0.2 J/cm^2, which relates to 0.2s of cure time, all of the tested materials cured over 2 mm deep. Additionally, at larger dosages, the incorporation of salts appears to lead to the materials curing slightly deeper for similar UV dosages, regardless of GlcN-MA additive. There may be some differences for curing kinetics between hydrogels with and without salt present, as seen in Table 4. However, both with and without salt present, the depth of penetration of the UV light is above 1.6 mm and the critical energy required to begin curing is below 50 mJ.

4.1.8 Effects of Salt on Mechanical Properties

The comparison between the salt-positive hydrogels and their corresponding salt-negative counterparts is given in Figure 15.

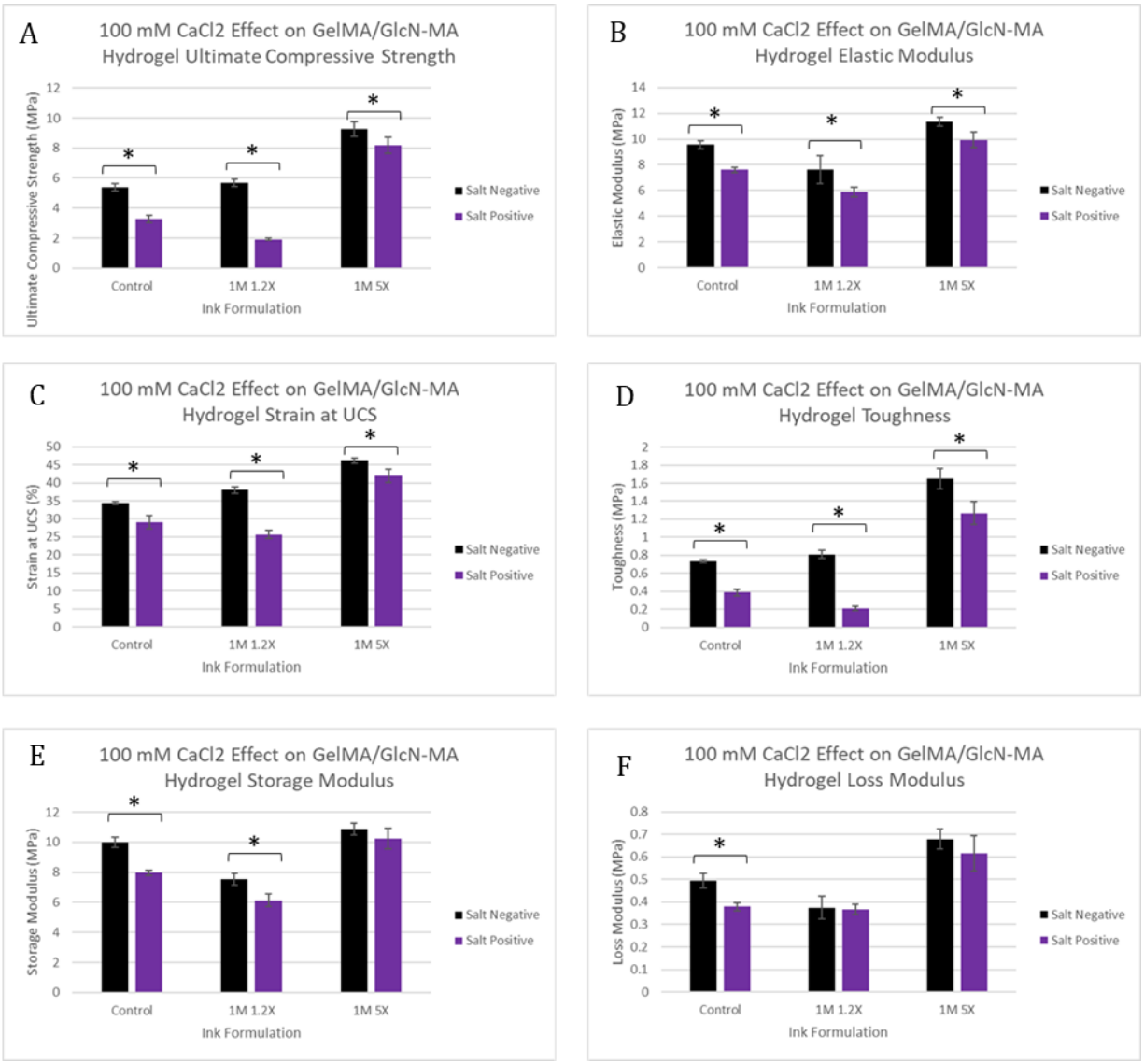

Figure 15 Comparison between compressive and dynamic mechanical testing properties of salt-positive and salt-negative GlcN-MA/GelMA hydrogels, compared to GelMA-only controls. N≥5.

As a whole, the same trends observed for the hydrogels made without salt are observed for the hydrogels made with salt; the 1.2X GlcN-MA-containing hydrogels show equal or lower mechanical properties than the control, while the 5X GlcN-MA-containing hydrogels show improved mechanical properties over the control across the board.

Notably, pair-wise comparison between salt-negative and salt-positive hydrogels of otherwise equal formulations shows a significant drop in the complex modulus (storage and loss) for the control formulation, among other notable decreases in mechanical properties. This loss in complex modulus was not expected given previously reported data from the laboratory [45]. A potential source of error is the difference in season for testing, due to the CoViD-19 pandemic, the salt

negative results were obtained in the relatively drier winter season, while the salt positive results were obtained during the summer months. To parse if the observed effects are due to environmental changes between seasons, the control formulation was fabricated with and without salt at the same time and compared, as shown in Figure 16.

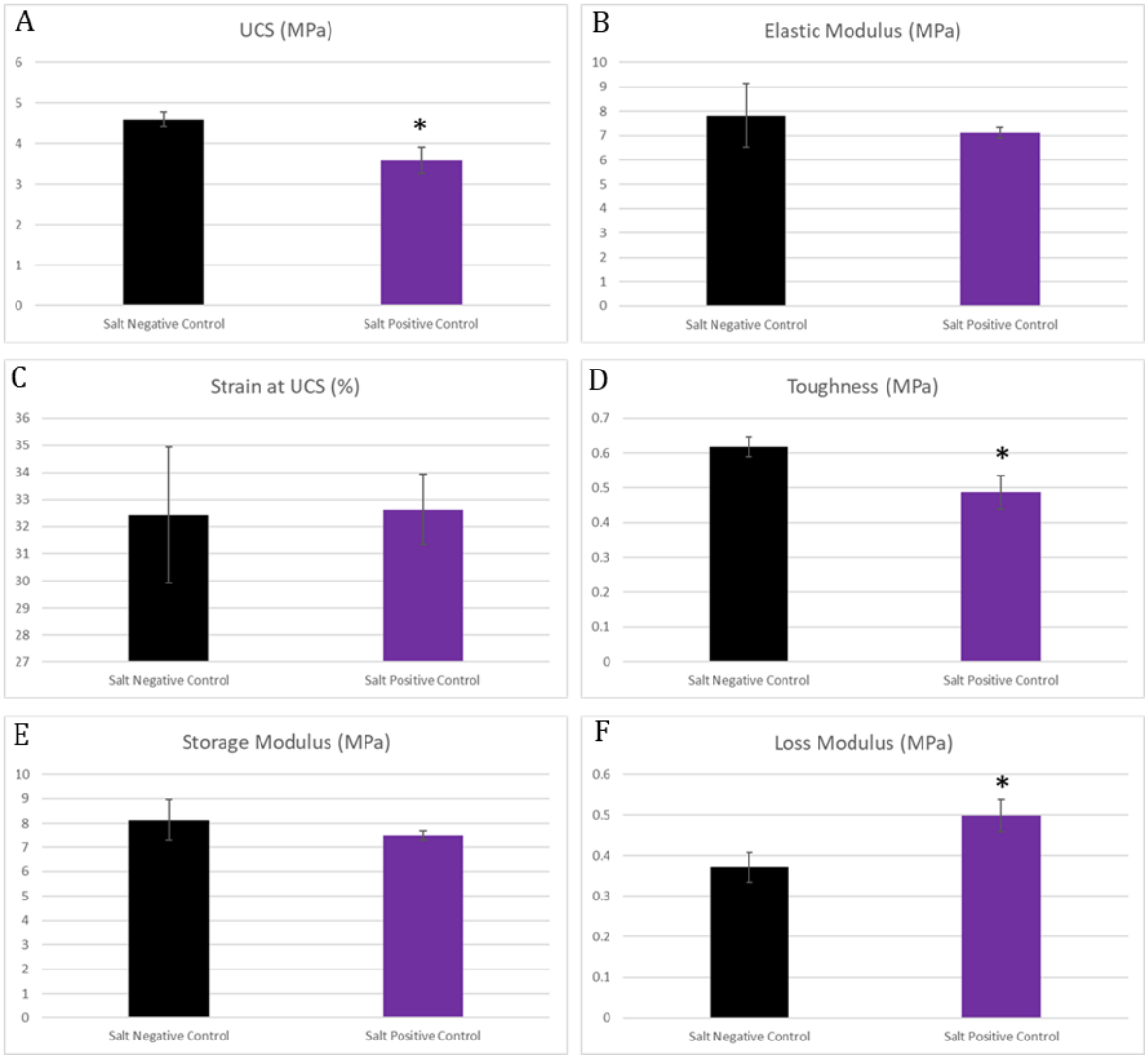

Figure 16 Compressive and dynamic mechanical properties salt-effect comparison of GelMA-only hydrogels tested during the summer season of 2020, "" indicates results statistically significant from one another.*

The first observation noted from Figure 16 is that the storage modulus is approximately the same regardless of salt content when the hydrogels are tested at the same time, which is in line with the previous results from the lab. However, the loss modulus appears to increase ~26% with the inclusion of salt ($P<0.001$). Additionally, the elastic modulus and strain at UCS converged to be not detectably different regardless of the addition of salt once tested at the same time. However, the

toughness and UCS of the salt-positive hydrogels appears to be significantly lower even when tested at the same time as the salt-negative hydrogel, lowering ~28% (P<0.001) and ~27% (P<0.001), respectively.

4.1.9 Salt Effect on Swelling

The swelling results for salt-containing hydrogels submerged in mQ water is given in Figure 17.

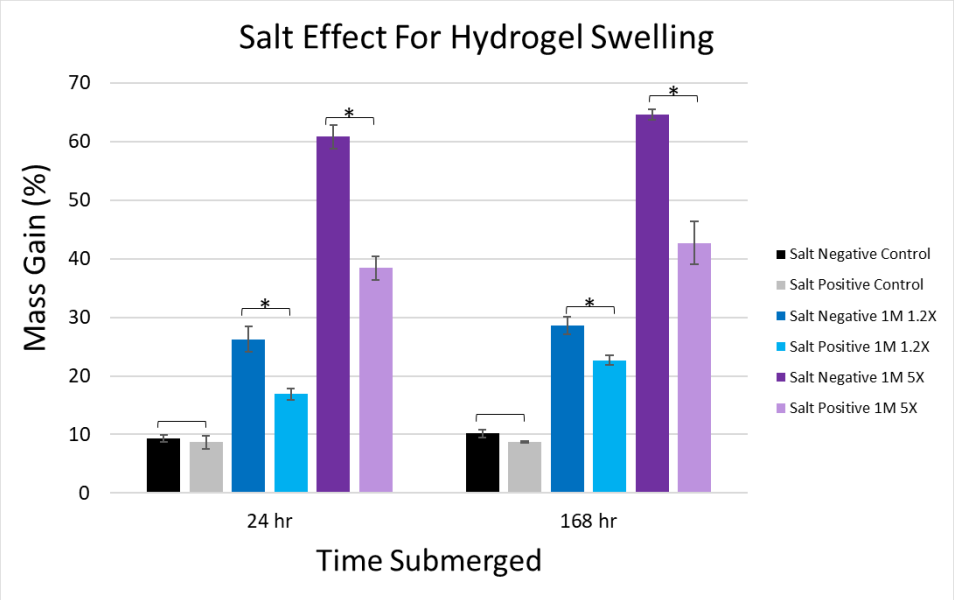

Figure 17 Swelling characteristics by mass comparing freshly cured salt-negative and salt-positive GlcN-MA/GelMA hydrogels, with GelMA-only controls, in room-temperature mQ water. "" represents significance with the pairwise comparison for salt within an additive group. N=3*

No significant change in swelling was noted for the control hydrogel with salt (P=0.634). For the 5X GlcN-MA hydrogel, the inclusion of salt lowered the swelling mass gain by about a third, from ~60% gain without salt to ~38% with (P<0.001). The 1.2X GlcN-MA hydrogel also exhibited a drop in water uptake of about a third with the inclusion of salt, lowering from ~26% mass gain without salt to ~17% mass gain with salt (P<0.001).

4.1.10 mSLA Printing Proof of Concept

The result of printing the 1M 5X GlcN-MA hydrogel with $CaCl_2$ is shown in Figure 18.

Figure 18 A dogbone of cured 1M 5X GlcN-MA/GelMA/CaCl2 hydrogel material printed on a Phrozen mSLA printer.

The print shown in Figure 18 was printed with a layer height of 100 microns, and the print measured 1.1 mm in thickness post-printing. Therefore, the 1M 5X GlcN-MA hydrogel was able to cure 11 consecutive layers on an mSLA printer.

4.2 Discussion

4.2.1 The Methacrylation of Glucosamine

Regarding Figure 7, the peaks that are gained or lost between the various samples can be correlated and assigned to known proton-containing functional groups by the chemical shifts of the peaks. In the unreacted D-GlcN spectra, the peaks ranging from 2.8-3.3 ppm are attributed to primary amine groups [83]. Thus, the observed loss of these peaks in the 1.2X GlcN-MA spectra indicates the loss of amine protons due to the reaction. The two ranges of new peaks are indicative of protons associated with methacrylate groups (methyl protons at 1-2 ppm, vinylic protons 5-6 ppm) [82]. This provides good evidence that the amine is selectively grafted with a methacrylamide group, and that the fabrication of a monofunctional GlcN-MA was successful.

Returning to the unreacted D-GlcN spectra, the group of peaks ranging from 3.3-4.0 ppm can be assigned to the various hydroxyl groups of the sugar [82]. Seeing as these peaks, along with the previously discussed amine peaks, are not present in the NMR spectra of the 5X GlcN-MA, this indicates near full conversion of the amine and hydroxyl functional groups of D-GlcN. Additionally, many of the previously discussed peaks in the methyl and vinylic regions appear in the 5X GlcN-MA spectra, which strongly indicates the successful fabrication of a polyfunctional GlcN-MA additive.

Given the results obtained from ^{1}H NMR, a method for developing monofunctional and polyfunctional GlcN-MA using significantly less dangerous methacrylating agents has successfully been developed.

4.2.2 Salt Negative Hydrogel Rheology

The rheological characteristics of the uncured inks are important to assess since properties such as viscosity and a shear-yield strength affect which handling methods and manufacturing processes are best suited for the materials. For example, a Newtonian material with low viscosity and no shear yield may be ideal for mSLA 3D printing or casting, whereas a pseudoplastic (shear-thinning) ink with an observable shear yield and higher viscosity may be better suited for extrusion processes such as DIW printing.

As noted previously from Figure 8, there is a positive correlation with additive concentration and viscosity, regardless of additive type. However, the 1.2X GlcN-MA increases the viscosity compared to the control for all concentrations, acting as a thickening agent, where the 5X GlcN-MA decreases the viscosity compared to the control, acting as a plasticizer.

While the GelMA used in this study is known to be highly modified, it still has many groups with the potential to act as hydrogen bond donors and acceptors, such as hydroxyls, secondary amines, and carboxylic acids. It is possible that some of the viscosity observed for the GelMA solution is due to hydrogen bonding between GelMA strands. Referring to Figure 19, which reexhibits the proposed structures of the modified GlcN, the 1.2X GlcN-MA has many hydroxyl groups and a secondary amine, all of which are capable of acting as hydrogen bond donors and acceptors. Perhaps, with the addition of 1.2X GlcN-MA, the total amount of potential hydrogen bonding sights increases, and the 1.2X GlcN-MA may even increase the amount of hydrogen bonding between GelMA molecules by acting as a hydrogen bonding bridge, with functional groups on different parts of a 1.2X GlcN-MA molecule interacting with different GelMA strands, or other 1.2X GlcN-MA molecules. Thus, as the concentration of 1.2X GlcN-MA increases, the hydrogen bonding within the system increases, leading to an increase in molecular interaction and an increase in viscosity.

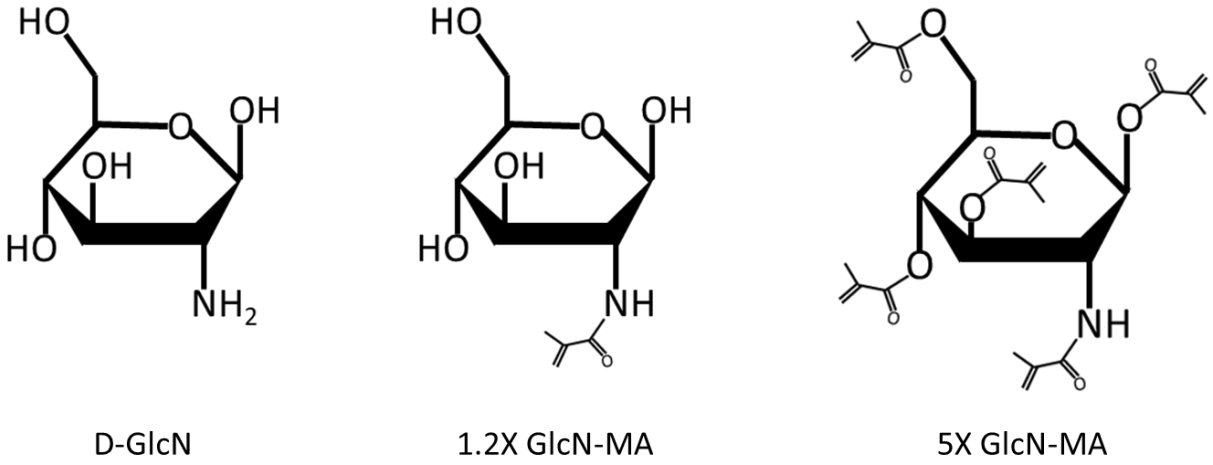

Figure 19 Expected chemical structures of methacrylated GlcN

Following a similar line of thought, the 5X GlcN-MA additive is expected to have all the GlcN's hydroxyls and amines reacted with methacryloyl groups, leaving the molecule, for the most part, incapable of acting as a hydrogen bond donor, with the exception of one secondary amine. Therefore, perhaps the 5X GlcN-MA interacts with the GelMA and other 5X GlcN-MA molecules more weakly than the 1.2X GlcN-MA, as it cannot significantly donate protons for hydrogen bonding. Instead, it may cap some of the hydrogen bonding functional groups natively on GelMA by accepting the GelMA's protons, but not having protons itself to further hydrogen bonding with other GelMA or 5X GlcN-MA molecules. Thus, by adding 5X GlcN-MA, the ability for GelMA to form hydrogen bonding bridges between other GelMA molecules is reduced, and the overall system's interactions reduces, leading to a lowering of viscosity as observed. This effect might be saturated at lower concentrations, however, and perhaps at higher concentrations the lone secondary amine on the 5X GlcN-MA may have a larger effect and start forming further hydrogen bonding bridges, leading to the observed drop in viscosity for the 50 mM concentration, but the viscosity rising again for higher concentrations of 5X GlcN-MA.

Overall, these results suggest that, provided there are no interactions between the additives and nHA, the lower viscosity of the 5X hydrogels may allow for easier fabrication of composite materials. Additionally, being Newtonian fluids with a viscosity range between 1.2 and 3.8 Pa·s and no notable shear yield strength, these inks are suitable for casting, where lower viscosities are easier to handle, and mSLA printing, which ideally prints inks with viscosities between 0.5 and 5.0 Pa·s [77].

4.2.3 Curing Kinetics of Salt Negative GelMA/GlcN-MA Solutions

Since the inks used in this study are cured through UV irradiation, quantifying the curing kinetics by UV exposure is important for ensuring sufficient curing is achieved for various manufacturing processes. For the salt-free hydrogel materials, each cured over 2 mm with the smallest tested amount of UV exposure, ~0.2 J/cm^2, which related to 0.2 s of cure time. Thus, for 3D printing methods often involving layers on the order of hundreds of microns, such as mSLA and DIW, all tested inks should readily cure for these fabrication methods if 385 nm light is used. Regarding the critical energy and depth of UV penetration, there may be a small effect due to additive type and concentration, but no clear trend can be drawn, and none of the results are concerning when in the context of curing the inks layer-wise on a 3D printer.

4.2.4 Salt Negative Hydrogel Compressive and Dynamic Mechanical Properties

The main thrust of this study is to determine if one of the additives improves the mechanical properties of a GelMA/nHA composite ink by improving the mechanical properties of the GelMA hydrogel. Therefore, the first step to showing this was to determine how the developed additives effect the properties of a GelMA hydrogel at varying concentrations.

Referring back to Figure 11, it was noted that the elastic moduli of the two additive types have different trends. Notably, the modulus for 1.2X GlcN-MA containing materials lowered with increasing additive concentration, where the 5X GlcN-MA only saw improvements to the modulus at the lowest and highest tested concentrations. The 1.2X GlcN-MA is expected to polymerize in a way that resembles polystyrene (PS) with the sugar ring acting as a pendant group, as shown in Figure 20 below, so it can be reasoned that as the concentration of the additive increases, the distance between GelMA molecules, and thus the total free volume, increases. Additionally, given the expected structure of the 1.2X GlcN-MA has only the amine functionalized, the sugar ring may still be capable of opening into its aldehyde form. Perhaps having a pendant ring that can take a linear form does not aid the overall stiffness of the material, and the increasing molecular weight of the crosslinks between GelMA molecules lowering the overall density of the matrix (more free volume between molecules) is the cause for lower stiffness in the hydrogel material.

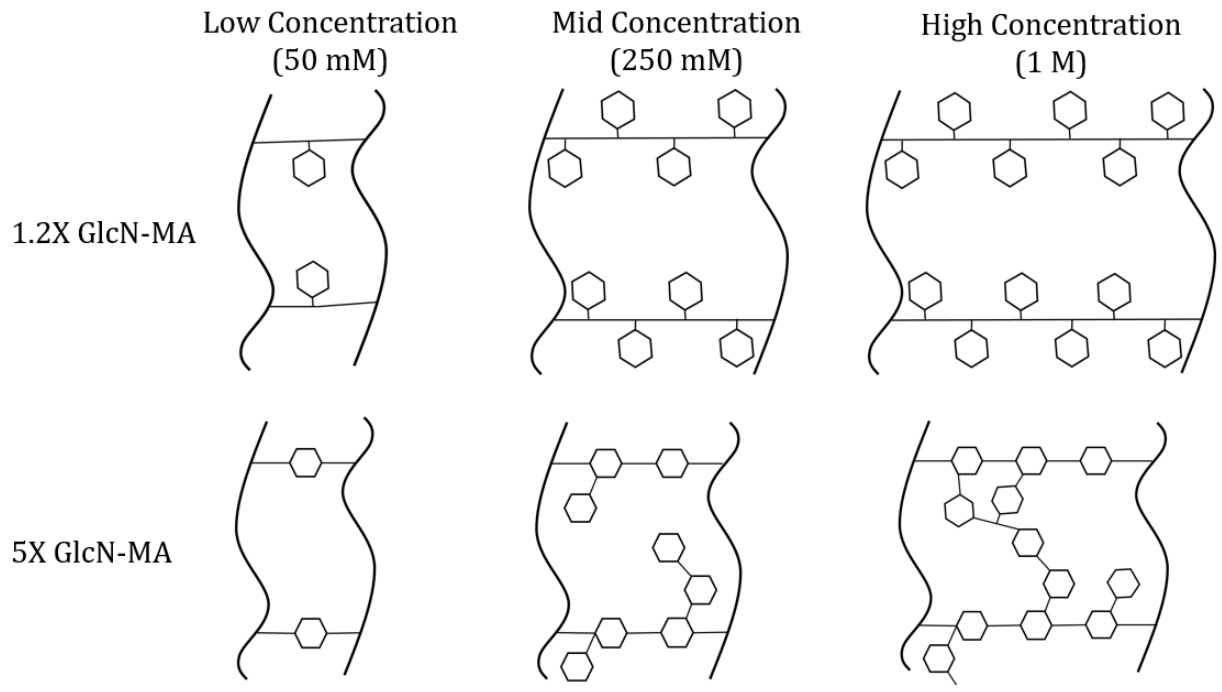

Figure 20 Cartoon of expected crosslinking structure for ranges of GlcN-MA

The 5X GlcN-MA, having up to 5 reactive groups per ring, is expected to polymerize in a complex way. The structure schemed in Figure 20 is likely a simplified version of the reality, as it can be expected that the 5X will react to form branches along the crosslink, with rings in the polymerized backbone like PEEK or other aromatic polymers. However, some sugar rings could also react 3+ times to form a star-polymerization core, or alternatively some additives may still react a single group and form a section resembling PS like the 1.2X GlcN-MA. Additionally, due to the hydroxyl on 5X GlcN-MA's carbon 1 being functionalized, the sugar's ring structure should be locked such that it can't form into the aldehyde structure under non-extreme conditions. This is due to carbon 1 in the ring structure forming the aldehyde/ketone group in the linear form of the sugar, as displayed in Figure 1. At low concentrations, the cured material may have short crosslinking bridges with a backbone-ring structure that gives the stiffening effect of having a ring structure without being too long to significantly increasing the matrix free volume, improving stiffness. However, as shown in Figure 20, perhaps at moderate concentrations, the length and branches of the crosslinking bridges starts to increase enough to start effecting the stiffness, but there hasn't been enough material added yet to have the branches between crosslinking bridges connect into a network, lowering the stiffness compared to the lower concentration. At high concentrations, on the other hand, perhaps the branching becomes significant enough that branches start connecting with one another,

forming a GlcN-MA network between GelMA molecules, and once again increasing the stiffness and strength of the material.

It is noted that for both additive types, the UCS increases with additive concentration. The increase in UCS with concentration may be due to a larger fraction of curable material in the high concentration inks, so there is more solid or "bound" phase in the cured material to spread the applied force over, and less free water phase. The 1.2X GlcN-MA was noted to decrease the UCS at the lowest concentration, which then steadily increased back to the UCS of the control with the 1 M concentration. This suggests that the bonds associated with the 1.2X GlcN-MA may be weaker than the bond formed between GelMA normally, but by increasing the number of these weak bonds by increasing additive concentration, the applied force is spread over more bonds, meaning more force has to be applied to break any of the GlcN-MA's bonds, and thus the material exhibits increasing strength with increasing concentration. The same logic can be applied to the 5X GlcN-MA material. However, the lower concentrations exhibit equal or higher UCS than the control, suggesting that the 5X GlcN-MA crosslink is at least as strong as the original GelMA-GelMA bond. Thus, but increasing the number of bonds and spreading the force out to more groups, the high concentrations of 5X GlcN-MA become stronger than the control.

The trends for toughness make sense when looking at the results of the UCS, modulus and max strain. For example, 50 mM 1.2X has lower UCS and strain at UCS than the control and therefore is less tough, but the 1 M ink is slightly stronger and had higher strain at UCS, but had a slight decrease in elastic modulus, making it about as tough as the control. Similarly, for the 5X GlcN-MA materials, for the 50 mM ink, likely the decrease in strain at UCS was slightly more impactful than the increase in the modulus, resulting in a material slightly less tough than the control. The 250 mM ink, however, had improved max strain and UCS, and thus showed a 69% improvement in toughness. The 1 M ink significantly improved the UCS, elastic modulus and strain at UCS compared to the control, and likewise the toughness for this material is more than double that of the control, at approximately 1.62 MPa (+121%).

The first major observation made on the complex modulus for all tested inks is that the storage modulus dominates, being approximately 20x greater than the loss modulus. This suggests that all the materials are more elastic than viscous. Additionally, for the most part, the observed trends for the elastic modulus translate to the trends for the storage modulus namely the decrease in modulus with increasing 1.2X concentration, and improvement of modulus at the 50 mM and 1 M concentrations of 5X. The loss modulus also follows the same trend as the elastic modulus for the

1.2X GlcN-MA, with 1.2X lowering the loss modulus with increasing concentration, and the 250 mM concentration of 5X showing the lowest loss modulus of the additive type, though only the 1 M concentration of 5X GlcN-MA increases the loss modulus to a significant degree.

Overall, the 5X GlcN-MA showed the most promising mechanical results, with significant improvements over the control for all compressive mechanical properties studied at the highest tested concentration, with notable improvements at lower concentrations as well. Unfortunately, the same cannot be said for the 1.2X, monofunctional GlcN-MA, which proved detrimental to many mechanical properties at lower concentrations, and limited improvements even at the highest tested concentrations. Relating the 1 M 5X GlcN-MA/GelMA hydrogel to the biological tissue articular cartilage, the ultimate compressive strength is just under the lowest-reported value of 14 MPa, and elastic modulus of the hydrogels is approximately an order of magnitude higher than the articular cartilage's reported values [48, 49].

4.2.5 Salt Negative Hydrogel Swelling Profiles

An important observation made from Figure 12 is that most of the swelling occurs within the first 24 hours of submersion. This is good to note for both analysis of the swelling characteristics of the material, as future experiments, such as further swelling tests, mechanical testing of the swelled material, and attempting to add further material by submerging the cured material in a solvent containing other monomers, may be performed sufficiently after 24 hours of swelling instead of a full week.

Referring to Figure 12, it is observed that degree of swelling increases with additive concentration, and that the 5X GlcN-MA increases swelling significantly more than the 1.2X GlcN-MA for similar concentrations. There are a few potential explanations for this, which may not be mutually exclusive.

Firstly, as noted previously, the 5X GlcN-MA is expected to form a branched crosslinking structure at moderate to high concentrations, as shown in Figure 20, while the 1.2X GlcN-MA material is expected to form a linear crosslinking chain. Additionally, the maximum crosslink density of the GelMA material is limited by the number of methacrylates attached to the GelMA polymer chain. It is known that the existence of branching in a crosslink can lead to further separation of primary polymer chains (GelMA), which increases the free volume of the polymer further [90]. Additionally, the swelling of a crosslinked polymer can be described by the Flory-Rehner theory of polymer swelling, which relates an increasing molecular weight of the crosslinks to an increased degree of swelling [91, 92]. Regarding Figure 19 and using the known masses of the constituent atoms, the

molecular weight of the 5X GlcN-MA material should theoretically be much higher than the molecular weight of the 1.2X GlcN-MA due to the additional methacrylate groups (519 g/mol and ~246 g/mol, respectively). Taking this into account, for similar concentrations, the molecular weight of a crosslink made of 5X GlcN-MA should be larger than one made of 1.2X GlcN-MA, and the combined effect of increased molecular weight of the crosslink and existence of branching in the crosslink may contribute to the concentration dependence of swelling for both additives and overall increased swelling observed for the 5X GlcN-MA material when compared to the 1.2X GlcN-MA material.

A second possibility concerns the number of available hydrogen-bonding sites between the materials. As can be gleaned from Figure 19, 1.2X GlcN-MA has 7 groups capable of hydrogen bonding, though two of these sites are only capable of acting as hydrogen bond acceptors. 5X GlcN-MA, on the other hand, has up to 11 hydrogen-bonding sites, though all but one are capable of only being hydrogen bond acceptors. Perhaps due to the extra hydrogen bond accepting sites, 5X GlcN-MA can adsorb more water when UV cured than the 1.2X GlcN-MA, and thus allowing the 5X GlcN-MA to swell more when submerged in water.

4.2.6 Salt Effect on Hydrogel Rheology

Regardless of the additive, the addition of salt was found to lower the viscosity of the uncured hydrogel materials. However, the degree to which the salt lowered the viscosity varied between additive types, with 1.2X GlcN-MA being affected the most.

As discussed in the literature, GelMA is known to have a significant negative zeta potential due to its primary amines being capped with methacrylamide groups into secondary amines, lowering the effective dipole and reducing their capability to hydrogen bond [45]. Masking the negative functional groups with positively charged Ca^{2+} effectively neutralizes the zeta potential of the GelMA strands, lowering the electrostatic repulsion between GelMA, allowing the strands to be in a more relaxed, open conformation, flow around each other easier and lowering the material's viscosity [45].

It is thought that the observed results are a combination of two mechanisms, the extent of hydrogen bonding due to the type of additive, as discussed in section 4.2.2, and the masking effect salt has on the zeta potential and thus, electrostatic repulsion observed between molecules.

As noted previously, gelatin becomes negatively charged as the amines are functionalized, which is the same situation for 1.2X GlcN-MA, where its amine is functionalized, but the hydroxyls are left.

Therefore, it is possible that the 1.2X GlcN-MA has a non-zero zeta potential in these inks, while also increasing the extent of hydrogen bonding within the hydrogel system as described previously. If this is the case, the addition of $CaCl_2$ may passivate not only the negative zeta potential on GelMA, but also the charges 1.2X GlcN-MA, and with both being affected, there is a larger decrease in viscosity with the inclusion of salt for the 1.2X GlcN-MA/GelMA hydrogel compared to the control. However, since the 1.2X GlcN-MA would still lead to increased hydrogen bonding, the viscosity of its hydrogel is still higher than that of the control.

The 5X GlcN-MA, on the other hand, has all or nearly all of its hydroxyls and amines functionalized, which, while likely still expressing a non-zero zeta potential, the extent might be lessened when compared to the 1.2X or the GelMA alone. Thus, the addition of salt may largely be affecting the zeta potential of the GelMA overall, so a drop in viscosity is still seen for the 5X GlcN-MA/GelMA hydrogel, but the effect isn't nearly as large as observed for the 1.2X GlcN-MA/GelMA or control hydrogels. Additionally, the previously discussed "capping" of GelMA hydrogen bonding would still be in effect with the 5X GlcN-MA, and thus the material has an overall lower viscosity than the control hydrogel.

4.2.7 Effect of Salts on Curing Kinetics of GelMA/GlcN-MA Hydrogel Materials

As previously discussed, the intention of adding $CaCl_2$ was to lower the viscosity of the hydrogels to allow the inks to be printed on 3D printers, such as mSLA. However, with the previously discussed conformation changes expected to occur to the GelMA strands, the salt may have also affected the curing kinetics and depth of the material, so it was important to ensure that curing was sufficiently fast for 3D printing to still be viable.

As can be seen in Figure 14, like the hydrogels without salt, each of the tested hydrogels exhibit over 2 mm of curing with the smallest tested dosage of UV light, ~ 0.2 J/cm^2 or approximately 0.2 seconds of curing. For most 3D printing with layer heights on the order of hundreds of microns, this is sufficient for curing.

It was also noted in Figure 14 that the incorporation of salt appears to lead to slightly deeper curing when compared to the salt-free equivalent material, which is most notable at the higher tested UV dosage ranges, and was observed for similar materials reported from the laboratory [45]. However, the results for D_p and E_c obtained by fitting the data show less clear trends. If it is true that the addition of salt does improve curing kinetics, it may be due to salt loosening the conformation of GelMA, as previously discussed, allowing reactive sites to interact and react easier when exposed to photoinitiator and UV light.

The main conclusion from the cure depth results, however, is that the addition of salt does not negatively impact the cure depth of the tested materials and should not cause curing issues when printed on a 3D printer using 385 nm light.

4.2.8 Salt Effect on Hydrogel Mechanical Properties

Regarding Figure 15, it was noted that many of the explored mechanical properties significantly decreased with the inclusion of salt, including the complex modulus (storage and loss moduli), which is not what was observed previously in the laboratory on a similar material [45]. However, the effect of salt on hydrogel mechanical properties varies depending on the type of hydrogel, such as a 2-hydroxyethyl methacrylate-sulfobetaine copolymer exhibiting reduced Young's modulus in the presence of potassium thiocyanate, or a poly(hexafluorobutyl methacrylate-acrylamide) hydrogel which becomes tougher and stronger in the presence of sodium chloride salt [93, 94]. Additionally, there appears to be significant drops in many of the mechanical properties across the ink types with the inclusion of salt, though a literature comparison cannot be made for these properties.

There are a few potential reasons for the discrepancies. Firstly, due to lockdowns caused by the 2020 CoViD-19 pandemic, the salt-negative and salt-positive hydrogels were fabricated and tested in different seasons, the salt negative materials in the cooler, less humid winter and the salt-positive materials in the warmer, more humid summer. Due to the hydrogel's sensitivity to water content and hygroscopic nature, it is possible that the varying levels of humidity play a significant effect on the material's mechanical properties. Perhaps water adsorbed or absorbed from the air into the dried GelMA or fabricated hydrogel causes a significant change in the water content of the final hydrogel material between seasons or causes a conformation change in the dried protein that remains in the hydrogel material. Alternatively, as many polymers are known to have temperature dependencies on their mechanical properties, perhaps deviations in ambient temperature between winter and summer seasons results in differing mechanical properties. An alternative is that the data obtained is real and the tested inks are different enough from the materials previously produced in the lab to allow for the salt to cause a real effect in mechanical properties.

To test the potential issue of changes in the environmental testing conditions due to season, the control hydrogel was made with and without salt at the same time, resulting in Figure 16. Notably, many of the previously observed differences lost statistical significance with the updated tests, with exceptions being UCS, toughness and loss modulus, the former two decreasing with salt addition and the latter increasing. The work done previously in the lab had shown little difference in

complex modulus with the inclusion of salt but was also exhibited as the complex modulus instead of splitting between storage and loss modulus. Noting that the storage modulus for the updated mechanical testing was not statistically different, and is also over an order of magnitude larger than the loss modulus, it is very likely that little difference in complex modulus would be seen if given as the combined storage and loss modulus.

The more surprising results are the statistically significant lowering of UCS and toughness with the inclusion of salt. Given the toughness is affected by the UCS, likely the two properties have the same source of decreased performance. If the observed effect is real, it is possible that the presence of calcium masks some of the known negative zeta potential on highly-modified GelMA in such a way that the GelMA can be in a conformation that results in minimal loss of elastic modulus while creating a weak point in the network. As illustrated in Figure 21 below, with less electrostatic repulsion due to charges being masked, the GelMA is expected to be able to interweave more than when electrostatic repulsion is high and the GelMA forms a more rigid, straight conformation with little interweaving. Perhaps this more relaxed conformation allows for more microdefects, such as inhomogeneities, to form, allowing for stress concentration to build and thus the material fractures at lower stress.

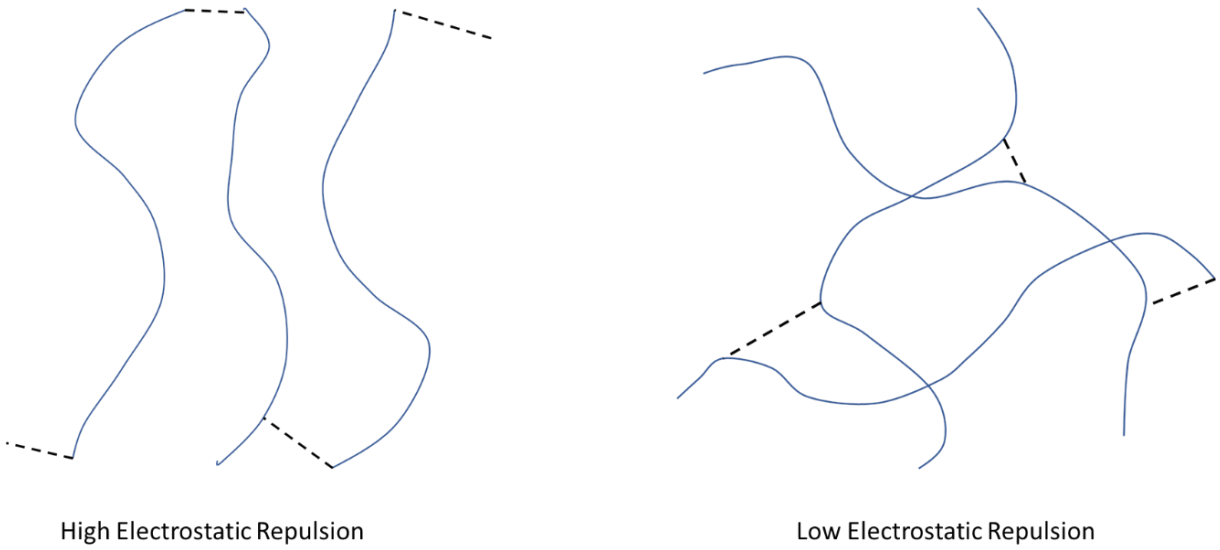

Figure 21 Cartoon representation (blue lines = GelMA. black dashes = covalent crosslinks) of anticipated GelMA structure in (left) mQ water, where the GelMA is highly charged and has high electrostatic repulsion, resulting in straight, stiff GelMA with little interweaving of strands and (right) GelMA in a salt solution, with charges masked, low electrostatic repulsion and significant overlap and interweaving of GelMA strands.

An alternative explanation is that UCS, being the maximum amount of force (over an applied area) that a material can bear before breaking, is highly sensitive to material defects, the presence of

which can lead to dramatically lower results. Though care was taken to avoid defects in samples and an elevated sample size was used to try and prevent defects being a significant issue, it is possible that enough defects, such as surface damage due to removal from the curing molds causing stress concentrations, crept in to cause the observed decreases in UCS and toughness [95].

These results suggest that some of the trends previously observed between inks made with and without salt were likely due to the environmental differences when testing, but the presence of salt may indeed significantly lower the strength and toughness of the hydrogel materials [96, 97].

4.2.9 Salt Effect on Cured Hydrogel Swelling

Referring back to Figure 17, it was found that for all material formulations, materials made with salt swelled significantly less than their salt-free counterparts. One potential reason for the improved swelling characteristics with salt is that the salt may interact with the charges and polar groups on GelMA favourably to form an overall tighter hydrogel matrix, or to make the matrix less attractive for water to adsorb to. When the salt is included, the Ca^{2+} is expected to interact with the free hydroxyls and carboxylic acids left on the GelMA, effectively shielding these groups and making the GelMA appear more neutrally charged. By neutralizing charges, it can be expected that electrostatic repulsion between GelMA strands would be reduced, and the uncured hydrogel may exhibit more interweaving between the strands.

With less interweaving between strands, it may be reasoned that there would be less resistance for the strands to expand upon water penetrating the matrix than if the GelMA strands are more tightly interweaved. This might allow a larger volume of water to enter the matrix, leading to the observed results with the salt-negative materials with expected more electrostatic repulsion and less entanglement showing increased levels of swelling.

Due to the positive correlation of additive concentration and degree of swelling, the Florey-Rehner theory of polymer swelling discussed earlier likely still applies to the composite materials. Though further improvements are necessary to obtain a reasonable amount of swelling with the GlcN-MA containing inks, the inclusion of salt significantly improves their swelling characteristics.

4.2.10 mSLA Printing of GelMA/GlcN-MA Hydrogel Materials

Due to its low viscosity, and cure depth showing sufficient curing the ink chosen for printing was the salt positive 1M 5X GlcN-MA/GelMA hydrogel. Notably, the mSLA printer makes use of 405 nm light to cure instead of 385 nm. However, while the photoinitiator used in the hydrogel inks, LAP, has peak absorbance at 385 nm, the absorbance spectra shows there should be some level of curing

capable with 405 nm light [98]. However, the curing efficiency would be significantly lower than if 385 nm light is used.

As shown in Figure 18, a small dogbone approximately 1.1 mm thick was printed on the mSLA printer using the 5X GlcN-MA/GelMA hydrogel material. With a layer height of 100 microns, this suggests 11 consecutive layers were printed to form this print. As a proof of concept, this gives strong evidence that the developed hydrogel materials can work as mSLA 3D printer inks, even when using a non-optimal wavelength as the curing light.

5. The Effects of Compositing GelMA/GlcN-MA Hydrogels with nHA

5.1 Results

5.1.1 Particle Settling Experiment

Gravimetric settling experiments were performed with the two additives to gain a qualitative understanding of the solvent-particle interactions, as displayed in Figure 22.

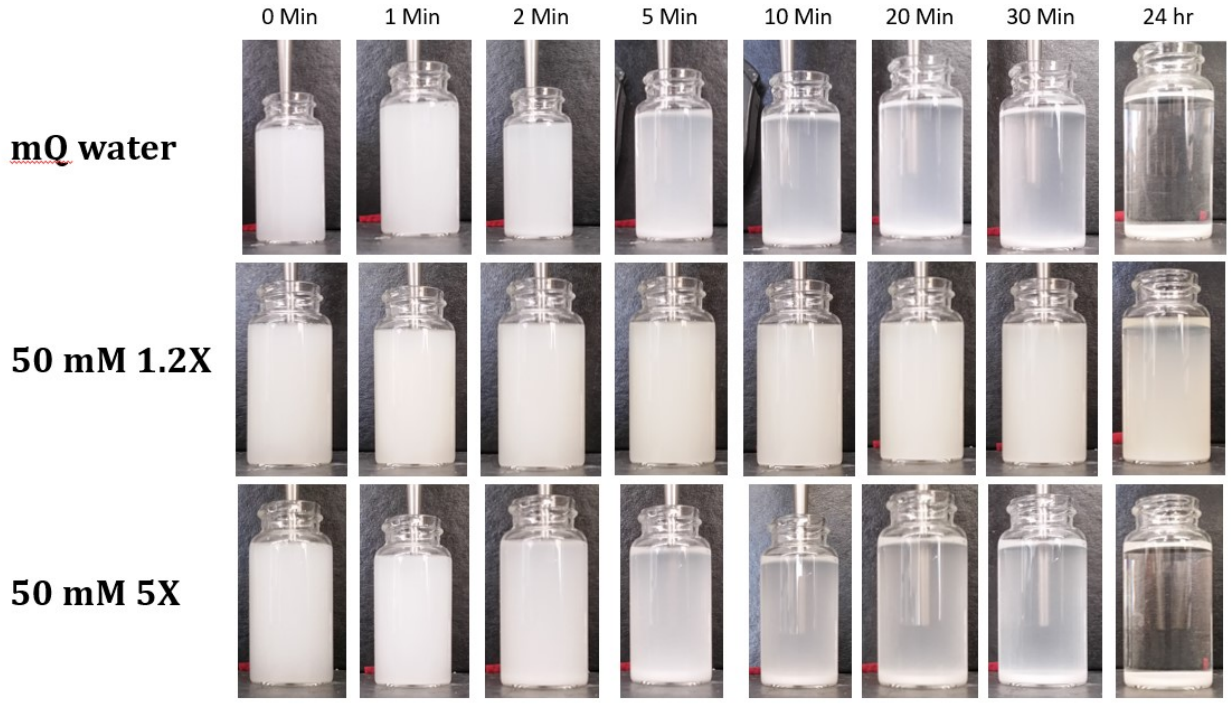

Figure 22 Gravimetric settling results of nHA nanoparticles dispersed in solutions of the developed additives over 24 hours.

The 1.2X GlcN-MA shows better particle-solution interaction over the other two solutions. For the control (mQ water) and 5X GlcN-MA solutions, settling begins to be apparent within the first 5 minutes after sonication, with a notable settled layer of nHA. Both solutions also show complete settling within 24 hours of sonication. Unlike the control and 5X GlcN-MA solutions, the 1.2X GlcN-MA solution shows no significant settling even 30 minutes after sonication, and 24 hours after sonication, there is still a significant amount of suspended particles.

5.1.2 Composite Material Rheology

The rheological profiles for composite materials with and without salt are provided in Figure 23.

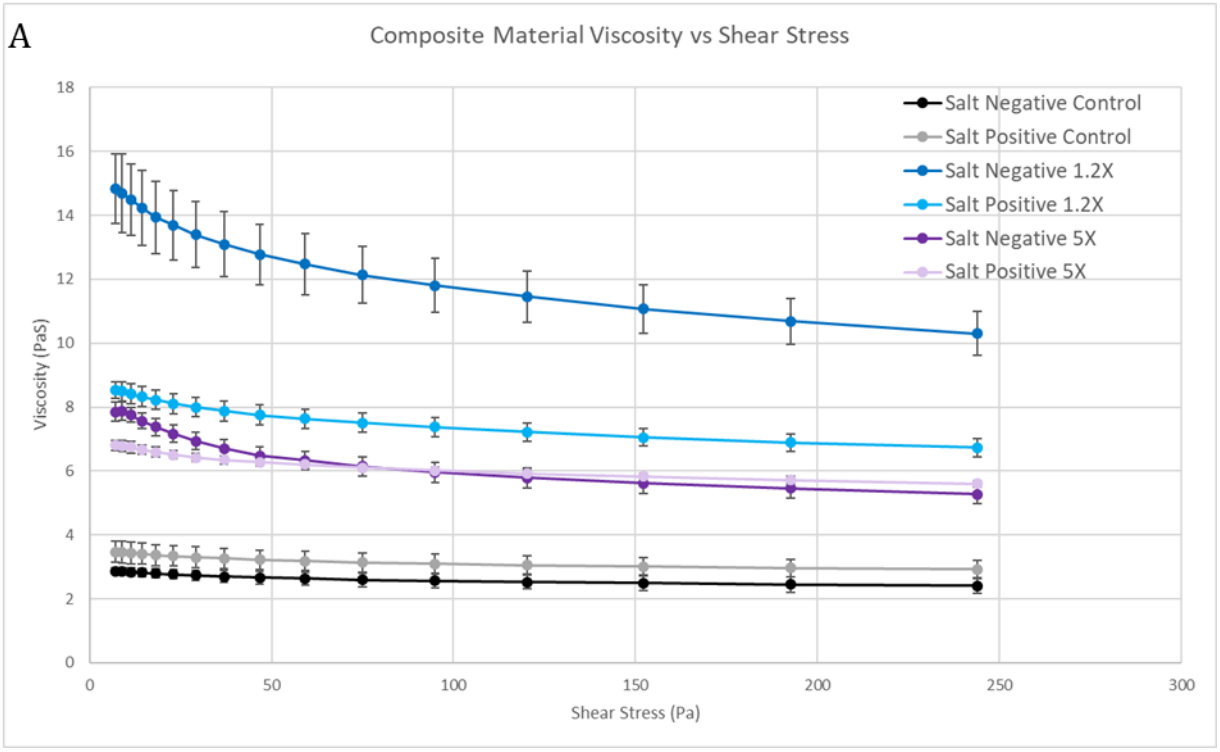

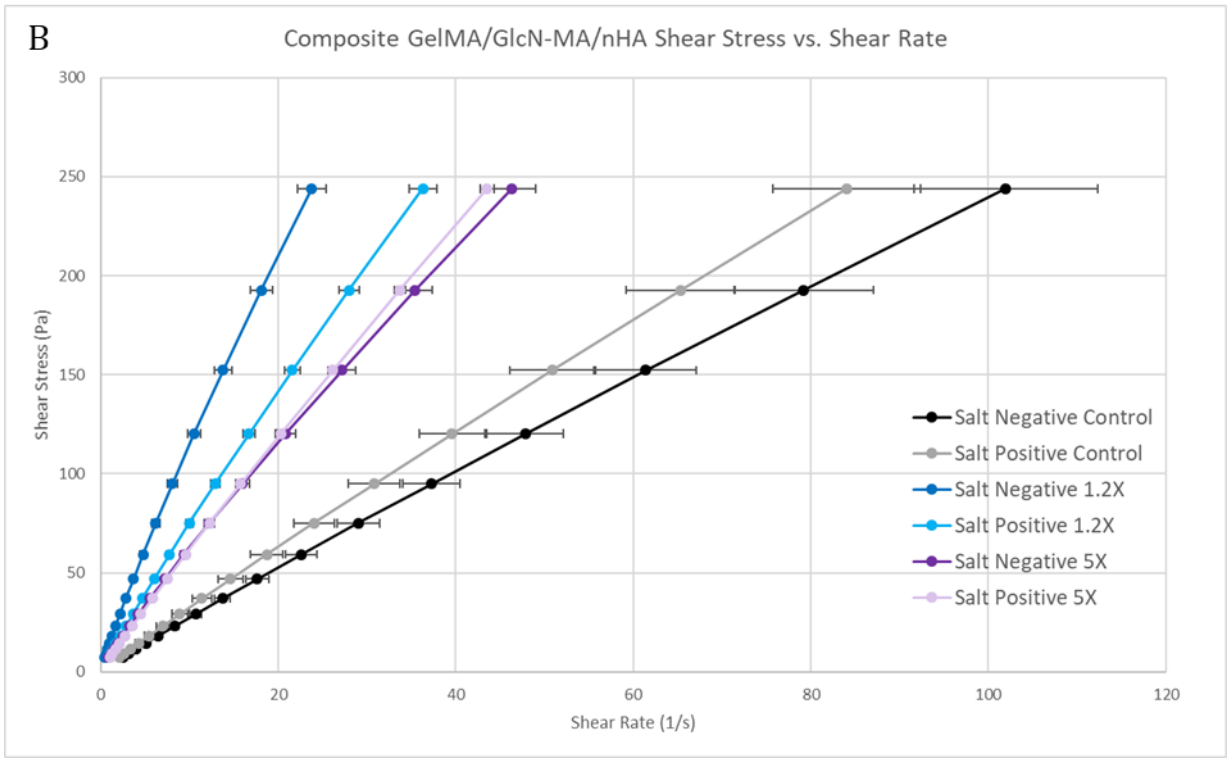

Figure 23 Rheological profiles of 10 vol% nHA, GelMA/GlcN-MA composite inks with and without CaCl2 salt, compared to nHA/GelMA-only composite inks, N=3 runs.

Looking first at the effect of GlcN-MA on the composite material's rheology, unlike the hydrogel materials, both forms of GlcN-MA explored in this work increase the uncured composite's viscosity over the control. At high shear, without salt the 1.2X GlcN-MA increases the material's viscosity by approximately 4.3 times over the control, and the 5X material increases the viscosity about 2.2-fold from the control (both $P<0.001$). With salt included the 1.2X increases the viscosity over the control by about 2.3 times, and the 5X is approximately 1.9 times more viscous than the salt-containing control (both $P<0.001$).

It can also be seen that the addition of salt does not significantly affect the viscosity of the control or 5X GlcN-MA composite inks at high shear ($P=0.212$ and $P=0.294$, respectively). However, the addition of salt does lower the high shear viscosity of 1.2X GlcN-MA containing composites, as the salt positive composite material is approximately 35% less viscous than its salt-free counterpart ($P<0.001$).

Another notable observation is that the composites containing salt do not appear to express any significant shear thinning behaviour nor a significant shear yield strength. However, without salt present, both the 1.2X and 5X GlcN-MA composite material express some shear thinning behaviours and possibly shear yield strength.

5.1.3 Composite Material Cure Depth

The results of composite curing kinetics with and without the presence of salt is displayed in Table 5 and Figure 24.

Table 5 Curing kinetics and coefficient of determination of the fit for composite materials.

Sample	Depth of Penetration (mm)	Critical Energy (mJ)	R^2
Salt-Negative Control	0.281	9.5	0.94
Salt-Negative 1M 1.2X	0.212	6.9	0.95
Salt-Negative 1M 5X	0.390	33.0	0.98
Salt-Positive Control	0.398	62.9	0.97
Salt-Positive 1M 1.2X	0.197	9.5	0.96
Salt-Positive 1M 5X	0.315	13.7	0.97

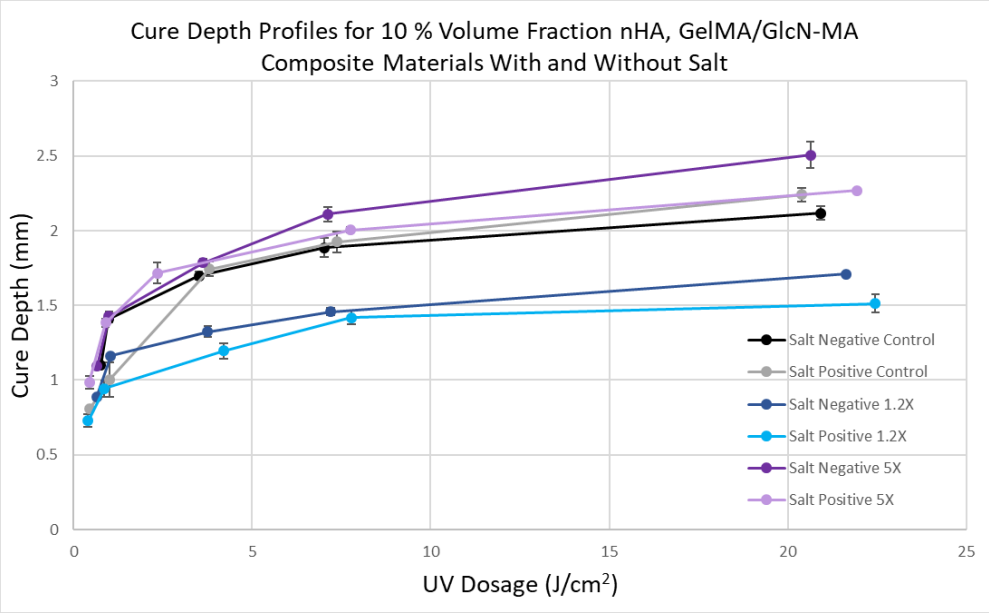

Figure 24 Cure depth profiles of GelMA/GlcN-MA/nHA composite materials, compared to nHA/GelMA-only composites, with and without salt, cured with 385 nm light. N=3

As can be seen in Figure 24, at the lowest tested dosage of ~0.6 J/cm², which correlates to 0.5 seconds of cure time, each of the materials was able to cure over 0.5 mm, and with a dosage of ~ 1 J/cm², each had cured at least 1 mm. The effect salt has on cure depth appears rather mixed for the composite material's curing profiles. The additive type appears to have an effect on the overall curing, however, as the 1.2X GlcN-MA composite materials appear to plateau at a smaller depth than the control and 5X GlcN-MA materials, regardless of salts presence. An important note, as seen in Table 5, is that the depth of penetration for all tested composite materials is on the order of hundreds of microns.

5.1.4 Composite Mechanical Testing

The compressive mechanical properties of these composite materials are shown in Figure 25.

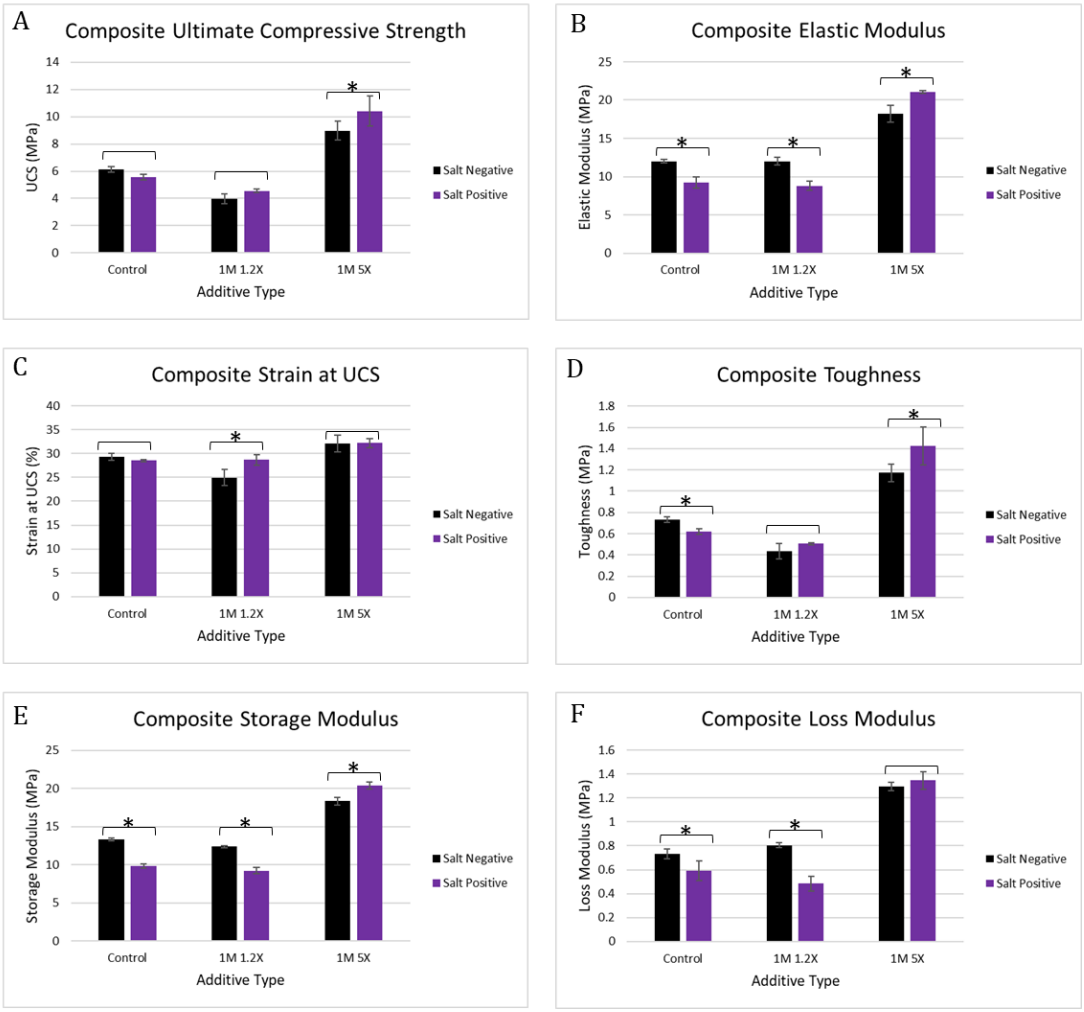

Figure 25 Comparison of compressive and dynamic mechanical properties of salt-negative and salt-positive GelMA/GlcN-MA/nHA composite inks with nHA/GelMA-only controls. "" representing a detectable effect due to salt presence. N≥5.*

For all explored mechanical properties, effects of the two factors, salt presence and additive type, as well as their interactions, are significant. The significance level of each factor and the interaction for the explored mechanical properties are summarized in Table 6.

Table 6 Significance of salt and additive factors for various mechanical properties of GelMA/GlcN-MA/nHA composite materials as determined by two-way ANOVA and a Holm-Sidak post-hoc test.

Mechanical Property	Salt Presence	Additive Type	Salt – Additive Interaction
UCS	P=0.023	P<0.001	P=0.002
Elastic Modulus	P<0.001	P<0.001	P<0.001
Strain at UCS	P=0.024	P<0.001	P<0.001
Toughness	P=0.027	P<0.001	P<0.001
Storage Modulus	P<0.001	P<0.001	P<0.001
Loss Modulus	P<0.001	P<0.001	P<0.001

When comparing the effects salt had on the composite material's UCS, the salt had minimal impact for the control and 1.2X GlcN-MA composite materials, but the UCS of 5X GlcN-MA composite material increased by ~16% with salt (P<0.001). Interestingly, the salt lowered the elastic moduli of the control (-23%) and 1.2X GlcN-MA (-27%) composites but improved the modulus for the 5X GlcN-MA (+16%) composite (all P<0.001). The strain at UCS was unaffected by the inclusion of salt, with the exception of the 1.2X GlcN-MA, which increased 15% (P<0.001). The salt lowers the control composite's toughness (-16%, P=0.044), while increasing 5X GlcN-MA's toughness (+22%, P<0.001), but has no significant affect on the 1.2X GlcN-MA composite material's toughness. Salt affects the complex moduli parameters in similar trends as the elastic modulus, with the storage and loss moduli lowering significantly for the control (-26% and -19%, respectively, both P<0.001) and 1.2X GlcN-MA (-25% and 40%, respectively, both P<0.001), but for the 5X GlcN-MA, the salt only had a significant effect on the storage modulus (+11%, P<0.001).

With regards to additive type, many trends previously found in the study, namely sections 4.1.4 and 4.1.8, were detected. Firstly, the 1.2X GlcN-MA appears to significantly lower the UCS of the material compared to the control, with a 35% drop (P<0.001) without salt and 18% drop (P=0.009) with salt. The 5X GlcN-MA increased UCS over the control 46% (P<0.001) without salt, 87% (P<0.001) with salt. Interestingly, the 1.2X GlcN-MA had no detectable effect on elastic modulus compared to the control, but the 5X GlcN-MA dramatically increased the modulus of the composite material, 52% (P<0.001) without salt and 128% (P<0.001) with salt. Without salt, the 1.2X GlcN-MA detectably to lowered the strain at UCS of the material by 15% (P<0.001) from the control, but there is no detectable difference between the control and 1.2X GlcN-MA with salt (P=0.872). The 5X GlcN-MA increases the strain at UCS slightly over the control, with a 10% increase without salt and a 13% increase with salt (both P<0.001). The 1.2X GlcN-MA material also appears to be less tough than the

control, with a 41% decrease (P<0.001) without salt and 18% decrease (P=0.043) with salt. The 5X GlcN-MA significantly increases the toughness over the control, however, with a 60% (P<0.001) and 130% (P<0.001) increase without and with salt, respectively. The additive type appears to affect the storage and loss moduli with and without salt as well compared to the control. The 1.2X lowers the storage modulus by ~7% (P=0.001) without salt, and 6% (P=0.007) with salt, compared to the controls. Without salt, the 1.2X GlcN-MA increases the loss modulus by ~10% (P=0.034) over the control, but with salt, it lowers the loss modulus by ~18% (P<0.001). The 5X GlcN-MA increases the storage modulus by 38% without salt, and 107% with salt (both P<0.001) over the control, and the loss modulus is increased 77% without salt and 128% with salt (both P<0.001). The effects of compositing with 10% VF nHA on salt positive hydrogel and composite mechanical properties are exhibited side-by-side in Figure 26.

Figure 26 Mechanical Property Comparison Between Salt Positive Hydrogels and Their Respective Composites, "" represents detectable difference between hydrogel and composite. N≥5.*

Firstly, all mechanical properties examined in this study show detectable differences between a given hydrogel and its respective composite. The UCS increased upon compositing, with the control, 1.2x and 5X materials increasing by 69%, 138%, and 27%, respectively. The moduli were also noted to increase for all materials when composited. Interestingly, only the 5X material showed a significant decrease in strain at UCS when composited, lowering by 23%. The changes to the control and 1.2X's strain at UCS was much smaller, however, with the control losing 2% and the 1.2X gaining 12% strain at UCS upon compositing. Finally, the toughness of all the materials were found to increase detectably upon compositing, with the 1.2X increasing the most with a 138% increase.

5.1.5 Composite Swelling

To understand the effects of nHA on the hydrogel's swelling, and the combined effect of salt and nHA, composites with and without salt were submerged in mQ water over a week. These results are exhibited in Figure 27.

Interestingly, the effect of compositing on swelling depended on the presence of salt, as can be observed in Figure 27A and 27B. Without salt, compositing significantly decreased the degree of swelling for all materials, with the control, 1.2X and 5X GlcN-MA materials decreasing by 30%, 42% and 42%, respectively. However, with salt present, the compositing had negligible impact on the control's swelling, as did the 1.2X GlcN-MA. The 5X material with salt did appear to decrease its swelling somewhat with compositing (-14% mass gain), but not nearly to the same degree as the same materials without salt.

As observed in Figure 27C, the same trends for additive type observed for the hydrogels are observed for the composite materials, with the control swelling the least and the 5X GlcN-MA swelling the most regardless of salt content. Comparing the composite materials for the effect of salt provides some interesting results. After 24 hours submerged in water, the control composite shows no significant difference in swelling when salt is present ($P=0.092$), but after a week submerged, the composite with salt swells ~43% more than without ($P=0.020$). The opposite effect is observed for the 5X material, which after 24 hours appears to swell ~7% less with salt present than without ($P=0.005$), but significance is lost after a week of swelling ($P=0.406$). The 1.2X GlcN-MA appears to consistently swell more with salt present than without, ~34% after 24 hours of swelling ($P<0.001$), and ~21% more after a week of swelling ($P=0.001$).

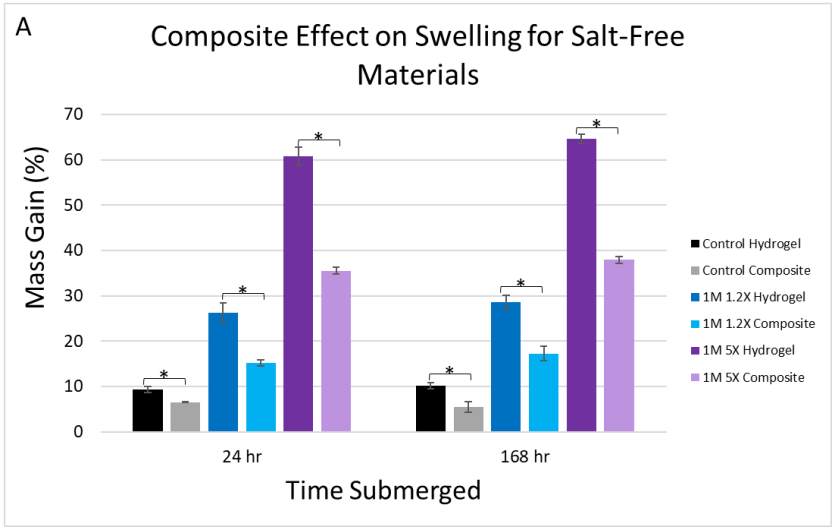

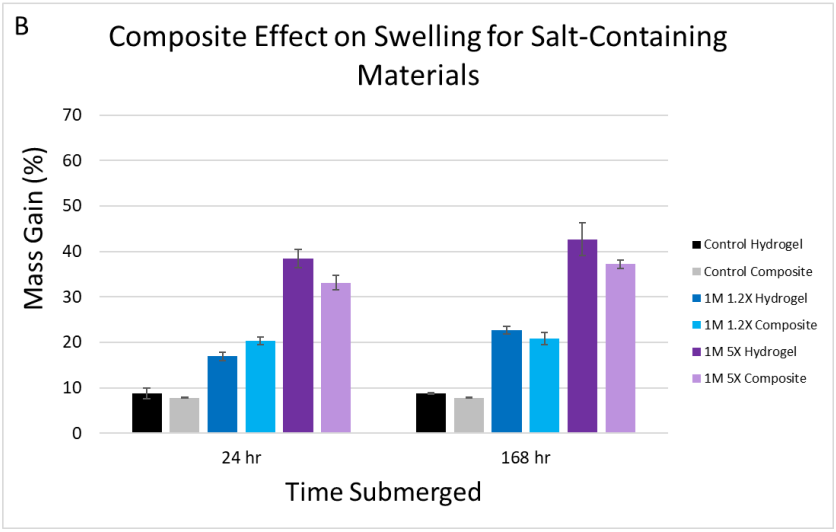

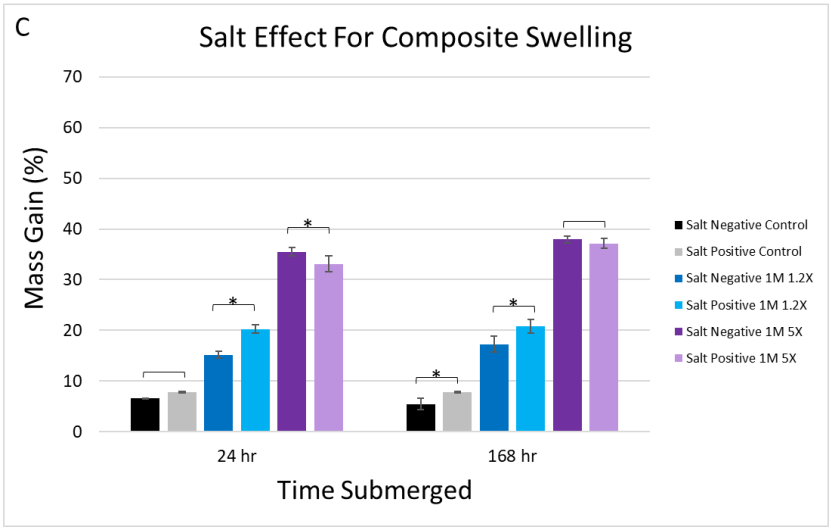

Figure 27 Summary of Swelling Effects of: (A) Compositing salt-free hydrogel with 10% VF nHA, (B) Compositing Salt-containing hydrogel with 10% VF nHA and (C) Salt Effect on Composite Materials. N=3.

5.1.6 mSLA Printing of Composite Inks

The result of attempting to print the 10 vol% nHA, salt-containing 5X GlcN-MA/GelMA composite material in an mSLA printer is given in Figure 28.

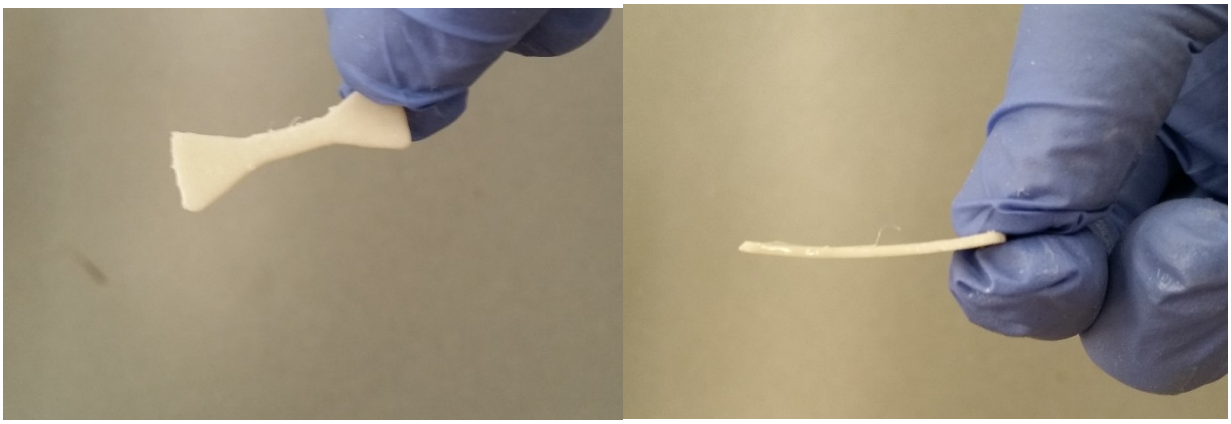

Figure 28 A dogbone of cured 1M 5X GlcN-MA/GelMA/nHA/CaCl2 composite material printed on a Phrozen mSLA 3D printer.

The above print was fabricated with a 100-micron layer height, and the print measured 1.3 mm in thickness. This suggests that the composite material was able to print 13 consecutive layers without issue on an mSLA 3D printer.

5.2 Discussion

5.2.1 Particle Settling

Referring back to Figure 22, the 5X GlcN-MA solution appears provided no additional benefit over the mQ water for maintaining a suspension of nHA. The 1.2X GlcN-MA solution, however, exhibited no notable settling within 30 minutes of suspending the particles, and there were still a significant amount of particles suspended 24 hours after the initial suspension. These results suggest that the 5X GlcN-MA solution should be no worse than mQ water for maintaining nHA dispersion, but the 1.2X GlcN-MA solution may provide a significantly more stable suspension with better particle dispersion.

It is known that the nHA used in this study is calcium-deficient and carbonated, possessing a negative zeta potential. Being calcium-deficient, it is reasonable to expect the particles to exhibit phosphates, particularly oxygen anions, on the surface. Interestingly, neither the mQ water nor the 5X GlcN-MA solution showed notable differences in particle settling. However, since the GlcN-MA solutions are mostly water, this stands to reason that the 5X is not providing any additional interaction over the water itself. It is possible, as previously discussed, that the general lack of protons available for hydrogen bonding donation on the 5X GlcN-MA may be the source of this, as if

hydrogen bonding between solvent and the phosphate oxygens is the main source of interaction, then the 5X GlcN-MA material would provide little benefit for interacting with the particles over water alone. The 1.2X GlcN-MA, on the other hand, has plentiful groups that can act as hydrogen bond donors, and was observed to have significantly more interaction with the nHA than water alone. Previously published research has shown that unmodified GlcN interacts with hydroxyapatite and similar materials through hydrogen bonding of GlcN's amines and hydroxyls with the ceramic/clay surface hydroxyls [73, 99]. While water may be able to provide some hydrogen bonding for suspending the particles, perhaps the additional donor groups on the 1.2X GlcN-MA improves the interaction further.

5.2.2 Composite Rheology

Regarding Figure 23, it was noted that for the composite materials, the addition of either GlcN-MA increased the viscosity over the control. This suggests that, unlike previously assumed in the work, there is some level of interaction between the nHA between both types of GlcN-MA. Regarding the gravimetric settling results of Figure 22, it was shown previously that the 1.2X GlcN-MA interacts to a significant degree with the nHA, allowing it to stay suspended much longer than was observed for mQ water or the tested 5X GlcN-MA. Perhaps, since the 5X GlcN-MA molecule has a secondary amine that can be a hydrogen bond donor, the 5X was exhibiting some interaction during the gravimetric settling experiment, but the analysis or testing parameters were not finely adjusted enough to see the effect. Relating the gravimetric settling results to the viscosity, the 1.2X, which suspended nHA particles much better than the other two solutions, also exhibited a much higher viscosity than the other two solutions.

Another notable rheological difference between the hydrogel and composite materials was the effect the addition of 100 mM $CaCl_2$ had. Unlike the hydrogel material which showed decreases in viscosity across all tested inks, only the 1.2X GlcN-MA composite ink showed any significant change in high-shear viscosity with the addition of salt, dropping the viscosity by ~35%. Given previous discussions on the salt's effect on viscosity due to neutralizing zeta potential, the results for the control and 5X are rather unexpected. A known phenomenon is that divalent salts, such as Ca^{2+}, can form ion bridges between molecules [100, 101]. For the control, perhaps without salt, the combination of electrostatic repulsion from the nHA and GelMA's negative zeta potential and hydrogen bonding between GelMA and nHA phosphates leads to the observed increase in viscosity. The addition of the Ca^{2+} ions may reduce the zeta potential effect as seen previously, but the added ions may also be forming ion bridges between the GelMA and nHA, counteracting the benefits of

neutralizing the system's zeta potential, leading to the observed lack of improvement for viscosity. A similar line of thinking might be applied to the 5X material for why minimal effect was seen when the salt is added to the solution. However, as previously discussed, the 1.2X GlcN-MA is thought to possibly exhibit a more notable zeta potential than the 5X, and perhaps due to the previously observed large effect of adding salt to the 1.2X GlcN-MA hydrogel, the benefits of neutralizing the zeta potential is greater for this system than the drawbacks of potential ion bridges.

The final key note made from Figure 23 is that both of the GlcN-MA containing composite materials without salt appear to exhibit both a shear-yield strength and shear-thinning behaviour, as their measured viscosity is higher at low shear than at high, and there is a notable plateau at the lowest shear stress data points. These two inks may be suitable for use with a DIW printer due to having the shear yielding property. However, with the addition of salt, the shear yielding behaviour appears to lessen or disappear, along with the shear-thinning behaviour. Thus, the salt-containing inks, as well as the salt-free control ink, may be suitable for mSLA printers, though ink viscosity may be a concern as most of these inks are above the 5 Pa·s viscosity limit.

5.2.3 Cure Depth and Kinetics of GelMA/GlcN-MA/nHA Composite Materials

The addition of nHA to the developed hydrogel inks was anticipated to affect many properties of the material, including properties critical for 3D printing effectively such as rheology and cure depth.

In terms of cure depth, all tested composite materials exhibited curing above 0.5 mm with the lowest tested UV dosage of ~0.6 J/cm^2, which correlated to 0.5 seconds of cure time. For the purposes of printing, a short exposure should be sufficient to fully cure a layer, as mSLA typically uses layer heights of 100 microns or less, and while DIW can change layer height depending on nozzle gauge, often layers are 400 microns or less [102].

Of note, however, is that the depth of penetration and critical energy is consistently lower for the composite materials than their hydrogel counterparts by approximately an order of magnitude. These results are not surprising, however, as the nHA is known to scatter incoming light, resulting in the UV curing light not penetrating nearly as deeply for the composite materials as it does for the hydrogels. This is attributed to Rayleigh scattering, due to the nanoparticles used being much smaller than the wavelength of the curing light (60 nm particles, 385 nm wavelength light), and the refractive index mismatch of nHA (1.63-1.64) and GelMA (1.387) [103, 104, 105].

Referring back to Table 4, it was noted that there might be a significant effect due to additive type and salt on the depth of penetration and critical energy for a given composite material. However,

due to only having one ink tested per sample type and the two parameters being derived from a fit, the ranges of depth of penetration and critical energy are not easily determinable and thus significance in the observed changes cannot be determined simply.

While significance between samples may be difficult to determine, the observed curing kinetics values for the composite materials are still positive results in the context of using these materials as 3D printer inks. The depth of penetration for the composite inks is on the order of hundreds of microns, and short exposure to UV light cures the material more than 500 microns regardless of additives, which either matches or exceeds the expected layer thickness of the anticipated 3D printers the inks would apply for. Therefore, in the context of 3D printing, none of the tested ink compositions are expected to cure insufficiently.

5.2.4 Mechanical Properties of GelMA/GlcN-MA/nHA Composite Materials

Regarding Figure 25, it was noted that for the composite material, there appears to be a significant effect of both salt and additive, as well as significant interaction between salt and additive across all explored mechanical properties. Overall, similar trends were observed for the effects of GlcN-MA addition between the hydrogel and their respective composites, with the 1.2X GlcN-MA providing lower or comparable results to the control for most tested properties, and the 5X material exhibiting improved mechanical properties over the control.

While each explored mechanical property appears to have at least one additive group where salt exhibits a significant, though usually quite minor, effect, salt's most prominent effect appears to be on the moduli of the composite materials. The elastic, storage and loss moduli are all lowered significantly with the inclusion of salt for the control and 1.2X GlcN-MA composite materials. However, the elastic and storage moduli increased significantly with the 5X GlcN-MA when salt is included. Perhaps with salt, the expected entanglement of the GelMA strands allows the 5X GlcN-MA to form a more interconnected crosslink network due to GelMA being able to be physically closer together without repulsion, providing the increased modulus with salt. Meanwhile, perhaps the salts in the composite systems affect the conformation of the GelMA in the control and 1.2X systems in such a way to make the materials less rigid, but due to not forming branched crosslinks, no additional interconnectedness forms unlike for the 5X.

The comparison between the salt positive hydrogel and its composites (as the sets were tested in the same season) are exhibited in Figure 26. Comparing between the hydrogel and its respective composite's mechanical properties, it is noted that for salt-containing inks, compositing raises the UCS, modulus and complex modulus to varying degrees for all tested compositions. The max strain

lowers for the 5X GlcN-MA but is nearly unaffected for the control and 1.2X GlcN-MA. With the above results, the toughness increased with compositing for all cases, but the 1.2X increased the most, approximately doubling its toughness as a composite.

Overall, the mechanical property results translating from hydrogel to composite material is not surprising. A simple way to approximate the properties of a composite is through the rule of mixtures, which predicts the resulting composite to have properties somewhere between the properties of the constituent materials by assuming each material contributes to the composite property proportional to its volume fraction [106]. Since the stiffening phase, nHA, has constant mechanical properties throughout the study, but the matrix of the composite has changing mechanical properties, the rule of mixtures would also predict that the resultant composites would have mechanical properties changing with the associated matrix. Thus, the increases in UCS and moduli are in line with what was expected. The max strain of the control and 1.2X GlcN-MA, however, is unexpected, as the addition of a ceramic was expected to drop the max strain compared to a hydrogel significantly, as seen for the 5X GlcN-MA material. It is possible that a significant decrease in max strain would be observed for an elevated VF of nHA, and that the tested composites didn't contain enough ceramic to significantly affect the max strain of the composite and 1.2X GlcN-MA materials.

5.2.5 Swelling Profiles for Composite Materials

The overall observed effects of salt, nHA compositing, and the combination of the two in terms of swelling characteristics is quite interesting and a challenge to parse. First, regarding Figure 27 as a whole, the previously discussed effect of molecular weigh of the crosslink appears to hold for all tested inks throughout the study. As the Flory-Rehner theory would predict, regardless of salt or nHA, the 5X GlcN-MA, with the largest molecular weight in its crosslink, swells the most and the control, with the smallest crosslink size, swells the least.

Figure 27A shows clearly that compositing any of the salt-free hydrogels with 10% VF nHA significantly decreases degree of swelling. The nHA nanoparticles are known to be hygroscopic, but won't dissolve in water. It is likely that the solid nanoparticles act as a physical barrier to impede the flow of water into the composite matrix and restrict the expansion of said matrix.

Interestingly, the effect of compositing is much less clear when the base hydrogel contains salt. It was previously shown and discussed that the presence of salt decreases the degree of swelling in the hydrogel material. This effect can be seen by comparing Figure 27A with Figure 27B, as the salt-positive hydrogel swells significantly less than the salt-free hydrogel. However, looking at the

Figure 27B, the addition of 10% VF nHA to salt-containing materials does not appear to affect the degree of swelling to a large degree nor consistently across additive types. This suggests that there is likely minimal to no interaction between the salt and the nHA in terms of swelling, that one of the effects predominates over the other, or that each matrix, depending on additive type, can only have its swelling restricted so far, and both methods of lowering swelling hit this maximum restriction. This trend can also be observed in Figure 27C, showing the effects salt has on the composite materials for swelling. Only the 1.2X GlcN-MA composite material showed any change in swelling with the inclusion of salt (increasing somewhat), but the degree of observed change is very small when comparing the effects of salt or compositing alone. Interestingly, noted in the salt-positive composite swelling stats as well, both the composite and additive sources of variation were found to be significant ($P=0.005$ and $P<0.001$ at 1 week), but the composite-additive interaction was not found to be significant ($P=0.078$).

5.2.6 mSLA Printing of GelMA/GlcN-MA/nHA Composite Materials

As with the hydrogel materials, being able to 3D print the composite shows further potential applications and manufacturing processes available for the developed materials. Due to its rheological profile and inclusion of one of the newly developed additives, the salt positive 1M 5X GlcN-MA/GelMA/nHA composite material was chosen for printing on an mSLA 3D printer for proof of concept. The viscosity of this ink, ~6 Pa·s, was known to be slightly above the recommended viscosity range of 0.5-5.0 Pa·s cited for mSLA printers [77]. Additionally, as noted previously, the mSLA printer available uses 405 nm light in its curing system, which, while not at the peak of the photoinitiator's efficiency, was shown to be sufficient to cure the hydrogel materials previously developed. However, the cure depth results for the composites show significantly less curing for much more exposure of 385 nm light.

Despite these potential challenges, Figure 28 shows the results of attempting to print a dogbone using a composite GlcN-MA/GelMA/nHA material. The print was found to be ~1.3 mm thick, which, at a layer height of 100 microns, showed successful consecutive printing of 13 layers. As a proof of concept, this result lends strong evidence that, at least for the 5X GlcN-MA containing materials, the composites can be used as mSLA 3D printer inks.

6. Limitations

There are some known limitations to the study that should be noted.

Firstly, 1-Octanol was used as an anti-foaming agent, acting as a surfactant to prevent air bubble defects in uncured inks, such that the cured samples would be as close to defect free as possible. While 1-Octanol succeeds as an anti-foaming agent, it is also known to be cytotoxic, and its current use in the inks could lead to poor biological response [107, 108]. A biocompatible surfactant to replace 1-Octanol should be sought.

As seen in the salt-positive hydrogel mechanical testing, the environment that the GelMA-based materials are made in, such as ambient humidity or temperature, may play a significant effect on some mechanical properties. The initial mass of swelling samples might also be affected by humidity. Thus, care should be taken in the planning stage of future works to ensure all relevant experiments occur within the same seasonal timeframe or in a highly controlled environment.

It is also known that ultrasonication of the uncured inks leads to the introduction of air bubbles and an excess of heat. As such, care was taken when compositing to ultrasonicate the least amount while still effectively dispersing the nHA. However, sonication must be done before ink use (for particle resuspension), increasing the chances for air bubble defects to be present in the cured composite samples, which would ultimately lower the average mechanical properties of the materials, and increase the variance in the obtained data.

Mechanical testing on both hydrogels and composite materials were performed at room temperature with freshly cured samples. While this gives good information on the performance of these materials for some applications, with the end-goal of using these materials for implants, the experimental set-up is not accurate.

Additionally, the range of additive concentrations is quite large, with the 1 M concentration having 20x the amount of additive as the lowest tested concentration. However, water and GelMA content was kept constant between inks, such that the 1 M concentration inks have significantly more solids content than the 50 mM concentration or GelMA-only control, which may be an additional factor when considering the observed mechanical properties.

For swelling, room-temperature mQ water was chosen as the swelling medium over salt-containing, physiological analogues such as simulated body fluid (SBF) or Dulbecco's phosphate buffer solution (DPBS). Understanding that salt may play a key role in swelling, as also shown in the data of this

study, mQ water was chosen as a likely worst-case scenario that would provide the most significant swelling results while avoiding potential confounding factors with uncontrolled salt addition. However, recognizing that the body contains many more solutes than mQ water, key influences may be lost by not testing the swelling in a more physiologically relevant medium.

Regarding the collection of curing kinetics data, while each dosage had multiple samples, only one set of inks was tested per material type, and as such deviation is not readily obtainable for the explored parameters in this experiment. Therefore, the differences between hydrogels and composites made with and without salt are difficult to truly test and should be considered with a healthy dose of skepticism of there being a real difference.

Finally, the wavelength of curing light used for cure depth and curing kinetics measurements was 385 nm, while the mSLA printer used for printing efficacy tests uses 405 nm light to cure. While the photoinitiator used in the study, LAP, can cure at both wavelengths, it is much more efficient at 385 nm as previously noted, and as such long cure times were required to print on the mSLA printer. Additionally, the specific model of mSLA available uses a relatively large print bed and as such requires a relatively large volume of ink to print properly, on the order of hundreds of mL. Unfortunately, the largest volume of ink currently fabricated approaches 40 mL, severely limiting the size of print that can be performed on the mSLA printer with the developed inks at this time.

7. Conclusion

The original hypothesis of this work was that by adding UV-curable, monosaccharide-derived additives that would resemble conventional polymers such as PS or PEEK when cured, these additives would improve the mechanical characteristics of a GelMA hydrogel matrix, and by extension, the mechanical properties of at GelMA/nHA composite material. It was also hypothesized that by adding divalent cations in the form of salts, the viscosity of the hydrogel materials would be lowered such that the materials would flow better, potentially allowing the material to be worked with and composited easier, as well as allowing both the hydrogel and composites to be printed.

Firstly, regarding the hypothesis based around mechanical properties, 5X GlcN-MA material exhibited some promising results, especially at the highest tested concentration. The 1M 5X GlcN-MA hydrogel showed overall improved mechanical properties when compared to the control materials as a hydrogel. Therefore, for the 5X GlcN-MA case, the hypothesis that UV-curable monosaccharides may improve a GelMA hydrogel material's compressive mechanical properties has been confirmed. Unfortunately, these mechanical improvements were not observed when adding 1.2X GlcN-MA. With little exception, the 1.2X GlcN-MA material showed equivalent or lower mechanical properties compared to the control at all tested concentrations. Additionally, as expected, the majority of the improvements or detriments observed for the hydrogel materials depending on additive type translated to the respective composite materials. As such, for the 5X GlcN-MA, the hypothesis that noted improvements to hydrogels from the additive would transfer to a composite material was also confirmed.

As hypothesized, it was found that the inclusion of $CaCl_2$ salt lowered the viscosity for all tested hydrogel material compositions compared to their salt-free counterparts. The magnitude of the effect varied depending on additive type, with the largest salt effect being seen with the 1.2X GlcN-MA containing material, and the 5X GlcN-MA material being least effected. However, the effects of salt on the composite material viscosity was mixed, as the control and 5X GlcN-MA/GelMA composite materials showed no significant difference in viscosity with salt included, but the 1.2X GlcN-MA/GelMA composite did show decreased viscosity with salt included.

It was also shown that, at least as a proof-of-concept, the 5X GlcN-MA/GelMA material was able to be printed on an mSLA 3D printer both as a hydrogel and a composite.

Some additional conclusions beyond the initial hypothesis can be made with the data collected during this work. Firstly, for the hydrogel materials, the 5X GlcN-MA additive appears to act as a

plasticizer, lowering the viscosity when added, while the 1.2X GlcN-MA additive acts as a thickening agent, increasing the viscosity. However, for the composite materials, both additives act as thickening agents, making the viscosity higher than the control.

It was noted that for both additives, the amount of water uptake increased with concentration of additive. The 5X GlcN-MA showed a stronger effect as well, with similar concentrations of additive leading to 5X GlcN-MA swelling significantly more than the 1.2X GlcN-MA. The addition of salt can help lower the degree of swelling for hydrogel materials quite dramatically, as can the addition of nHA nanoparticles. However, there is not a significant benefit of adding both salt and nHA with regards to swelling. The degree of swelling associated with the high-concentration materials may be the largest concern associated with the newly developed additives.

Ultimately, this work represents a potential path and step forward for the development of more robust biologically derived hydrogel and composite materials. The stiffness of the 1M 5X GlcN-MA hydrogel and composite materials are over an order of magnitude higher than the values cited for articular cartilage, and the UCS only a handful of MPa below the lowest cited value for articular cartilage, values much higher than those observed in the literature for GelMA-based materials as noted in Table 1. Much work still needs to be done for engineered GelMA hydrogel and composite materials to reach the properties of cortical bone.

8. Future Work

Should interest in this research lead to further exploration, there are a number of paths and future projects possible.

Firstly, the mechanical properties of novel GlcN-MA monomers hydrogels alone should be assessed if a solid, cured material is achievable. This may lead to the GlcN-MA material working as a pure material instead of just as an additive, and additionally, the results may aid in understanding the trends observed in this study.

Next, the volume fraction of nHA was quite low in the composites in this study. Judging from the viscosity of the inks when fabricated, significantly more nHA could be loaded into some of the hydrogels. If this were to be done, it would be expected that the viscosity of the uncured materials could be increased such that Direct Ink Writing could be used as the fabrication process, and the increased ceramic content would likely further stiffen and strengthen the material at the cost of the material's max strain. It is also possible that an increased volume fraction of nHA may decrease the amount of observed swelling, which would be especially important for the 5X GlcN-MA materials.

Throughout this study, the mechanical properties of freshly cured materials were assessed. Assessing the mechanical properties after the sample has been submerged in an aqueous environment at physiological temperature for an extended period of time would provide a step towards a more accurate assessment of how the material may behave in a body.

The mechanical properties in this work were obtained by studying the engineering stress and strain profiles of the materials. However, these materials show significant strain before failure and as polymeric materials, can be considered incompressible. Reanalysis of obtained data and future analysis of mechanical data of polymers should be done using the true stress and true strain of the materials, with surface area approximated using conservation of volume.

Since a body contains many solutes instead of just purely water, exploring the swelling characteristics of the developed materials in a more physiologically relevant medium, such as DPBS or SBF at 37^{o}C may prove important to gain insight on how the material may react if implanted. In this study, the degree of water uptake was compared to the freshly cured hydrogel's initial mass, the method chosen to match the anticipated end use of the material. However, it is recommended that in future work, the samples be desiccated or lyophilized after the swelling time points have been reached to obtain the solids mass of the samples, which would allow for the total water content of the hydrogel to be calculated. Additionally, to better match what is commonly displayed

in the literature, it is also recommended that an additional set of samples be made which are lyophilized first, then submerged in the swelling medium.

Much of the work performed focused on phenomena resulting from the addition of GlcN-MA additives, but little work was performed characterizing the material structure. To complement the ^{1}H NMR data, carbon NMR on unreacted GlcN and the two developed additives is recommended to provide further evidence towards the materials' chemical structures. The bond conversion degree, or curing efficiency, can be quantified via Fourier transform infrared spectroscopy, which could be used to ensure full conversion of the 1.2X GlcN-MA materials, and to potentially approximate the degree of interconnectedness for the 5X GlcN-MA crosslinks and potential networks. For better quantification of the sample composition, thermal gravimetric analysis (TGA) can be performed on the cured materials, and it is also recommended that dynamic scanning calorimetry be performed on both cured and uncured to explore potential changes in thermal stability, phase changes such as gelation or crystallization, or degree of crosslinking. If potential crystallinity is detected, x-ray diffraction analysis may also be performed for further analysis. Finally, it is recommended that scanning electron microscopy be performed at the fracture surfaces of the composite materials, as this will allow for direct imaging of nanoparticle aggregates.

It had also been noted that some of the material properties might be affected by seasonal changes, such as ambient humidity and temperature. A future project exploring the effects of humidity/absorbed water in GelMA powder vs. desiccated GelMA powder on hydrogel mechanical properties may aid in parsing potential environmental effects. Absorbed water content could be measured using TGA.

As many natural hydrogels, including gelatin, can physically gel, exploring the physical gelling characteristics of the GelMA/GlcN-MA based materials could prove very insightful. This would include determining a method to consistently induce gelation, such as through temperature change by placing uncured ink in a fridge or freezer. Additionally, exploring the effects of first physically gelling, then chemically curing the material has on its mechanical properties and matrix structure (crystallinity and polymer conformation) may prove fruitful.

Should the GlcN-MA be used for cell work, a more extensive purification process may be required to get good cell response. Currently two purification steps are taken, a toluene liquid-liquid extraction and an ethanol precipitation. Adding two more liquid-liquid extraction steps with toluene would help to ensure the final obtained material is free of unreacted additives and by-products.

Additionally, as previously mentioned, 1-octanol should be replaced with a more biocompatible surfactant before cell work should be attempted. A small study of potential biocompatible surfactants is recommended, ensuring efficacy of the anti-foaming properties while ideally not effecting mechanical properties of the material. Commercially available, advertised as biocompatible surfactants such as Tween 80, Triton X-100, or Pico-surf would be good starting points for exploring more biocompatible surfactants.

Finally, many of the observed rheological trends are expected to be reliant on electrostatic effects from non-zero zeta potentials. While previous research done in the lab has shown the zeta potential of highly-modified GelMA with and without salts, gaining insight into the zeta potential of the 1.2X and 5X GlcN-MA materials with and without salts, in their own solutions and with GelMA, would give further evidence to parse the main effects causing the observed rheological trends.

Bibliography

[1] M. Daniele, A. Adams, J. Naciri, S. North and F. Ligler, "Interpenetrating networks based on gelatin methacrylamide and PEG formed using concurrent thiol click chemistries for hydrogel tissue engineering scaffolds," *Biomaterials,* vol. 35, pp. 1845-1856, 2014.

[2] J. Perez, D. Kouroupis, D. Li, T. Best, L. Kaplan and D. Correa, "Tissue Engineering and Cell-Based Therapies for Fractures and Bone Defects," *Frontiers in Bioengineering and Biotechnology,* vol. 6:105, 2018.

[3] M. Wang, "Developing bioactive composite materials for tissue replacement," *Biomaterials,* vol. 24, pp. 2133-2151, 2003.

[4] R. Ravichandran, M. Islam, E. Alarcon, A. Samanta, S. Wang, P. Lundström, J. Hilborn, M. Griffith and J. Phopase, "Functionalized type-I collagen as a hydrogel building block for bio-orthogonal tissue engineering applications," *Journal of Materials Chemistry B,* vol. 4, no. 2, pp. 318-326, 2016.

[5] S. Levengood and M. Zhang, "Chitosan-based scaffolds for bone tissue engineering," *Journal of Materials Chemistry B,* vol. 2, pp. 3161-3184, 2014.

[6] D. Hutmacher, "Scaffolds in tissue engineering bone and cartilage," *Biomaterials,* vol. 21, pp. 2529-2543, 2000.

[7] S. Naahidi, M. Jafari, M. Logan, Y. Wang, Y. Yuan, H. Bae, B. Dixon and P. Chen, "Biocompatability of hydrogel-based scaffolds for tissue engineering applications," *Biotechnology Advances,* vol. 35, pp. 530-544, 2017.

[8] A. Costa and J. Mano, "Extremely strong and tough hydrogels as prospective candidates for tissue repair - A review," *European Polymer Journal,* vol. 72, pp. 344-364, 2015.

[9] T. Hoare and D. Kohane, "Hydrogels in drug delivery: Progress and challenges," *Polymer,* vol. 49, no. 8, pp. 1993-2007, 2008.

[10] W. Wang, Y. Zhang and W. Liu, "Bioinspired Fabrication of High Strength Hydrogels from non-Covalent Interactions," *Progress in Polymer Science,* vol. 71, pp. 1-25, 2017.

[11] K. Deligkaris, T. O. W. Tadele and A. van den Berg, "Hydrogel-based devices for biomedical applications," *Sensors and actuators. B: Chemical,* vol. 147, no. 2, pp. 765-774, 2010.

[12] M. Sun, X. Sun, Z. Wang, S. Guo, G. Yu and H. Yang, "Synthesis and Properties of Gelatin Methacryloyl (GelMA) Hydrogels and Their Recent Applications in Load-Bearing Tissue," *Polymers (Basil),* vol. 10:1290, no. 11, 2018.

[13] A. Hoffman, "Hydrogels for biomedical applications," *Advanced Drug Delivery Reviews,* vol. 64, pp. 18-23, 2012.

[14] W. Hennink and C. van Nustrum, "Novel Crosslinking Methods to Design Hydrogels," *Advanced Drug Delivery Reviews,* vol. 64, pp. 223-236, 2012.

[15] P. Eiselt, K. Y. Lee and D. J. Mooney, "Rigidity of Two-Component Hydrogels Prepared from Alginate and Poly(ethylene glycol)-Diamines," *Macromolucules,* vol. 32, no. 17, pp. 5561-5566, 1999.

[16] A. J. Kuijpers, P. B. van Wachem, M. J. van Luyn, G. H. Engbers, J. Krijgsveld, S. A. Zaat, J. Dankert and J. Feijen, "In vivo and in vitro release of lysozome from cross-linked gelatin hydrogels: a model system for the delivery of antibacterial proteins from prosthetic heart valves," *Journal of Controlled Release,* vol. 67, no. 2-3, pp. 323-336, 2000.

[17] P. Coimbra, M. Gil and M. Figueiredo, "Tailoring the properties of gelatin films for drug delivery applications: Influence of the chemical cross-linking method," *International Journal of Biological Macromolecules,* vol. 70, pp. 10-19, 2014.

[18] H. Goodarzi, K. Jadidi, S. Pourmotabed, E. Sharifi and H. Aghamollaei, "Preparation and in vitro characterization of cross-linked collagen-gelatin hydrogel using EDC/NHS for corneal tissue engineering applications," *International Journal of Biological Macromolecules,* vol. 126, pp. 620-632, 2019.

[19] S. Van Vlierberghe, "Crosslinking strategies for porous gelatin scaffolds," *Journal of Materials Science,* vol. 51, pp. 4349-4357, 2016.

[20] K. Sisson, C. Zhang, M. C. Farach-Carson, D. Bruce Chase and J. F. Rabolt, "Evaluation of cross-linking methods for electrospun gelatin on cell growth and viability," *Biomacromolecules,* vol. 10, no. 7, pp. 1675-1680, 2009.

[21] A. Bigi, G. Cojazzi, S. Panzavolta, K. Rubini and N. Roveri, "Mechanical and thermal properties of gelatin films at different degrees of glutaraldehyde crosslinking," *Biomaterials,* vol. 22, no. 8, pp. 763-768, 2001.

[22] J. P. Dreye, B. Delaey, A. Van de Voorde, A. Van Den Bulcke, B. De Reu and E. Schacht, "In vitro and in vivo biocompatibility of dextran dialdehyde cross-linked gelatin hydrogel films," *Biomaterials,* vol. 19, no. 18, pp. 1677-1687, 1998.

[23] D. P. Speer, M. Chvapil, C. D. Eskelson and J. Ulreigh, "Biological effects of residual glutaraldehyde in glutaraldehyde-tanned collagen biomaterials," *Journal of Biomedical Materials Research,* vol. 14, no. 6, pp. 753-764, 1980.

[24] M. J. M., S. Sawamura and R. Armstrong, "An examination of the biologic response to injectable, glutaraldehyde cross-linked collagen implants," *Journal of Biomedical Materials Research,* vol. 20, no. 1, pp. 93-107, 1986.

[25] M. Schuster, C. Turcek, G. Weigel, R. Saf, J. Stampel, F. Varga and R. Liska, "Gelatin-Based Photopolymers for Bone Replacement Materials," *Journal of Polymer Science: Part A: Polymer Chemistry,* vol. 47, pp. 7078-7089, 2009.

[26] W. van Dijk-Wolthuis, O. Franssen, H. Talsma, M. van Steenbergen, J. Kettenes-van den Bosch and W. Hennink, "Synthesis, Characterization, and Polymerization of Glycidyl Methacrylate Derivatized Dextran," *Macromolecules,* vol. 28, pp. 6317-6322, 1995.

[27] S. Möller, J. Weisser, S. Bischoff and M. Schnabelrauch, "Dextran and hyaluronan methacrylate based hydrogels as matrices for soft tissue reconstruction," *Biomolecular Engineering,* vol. 24, pp. 496-504, 2007.

[28] A. Van Den Bulcke, B. Bogdanov, N. De Rooze, E. Schacht, M. Cornelissen and H. Berghmans, "Structural and Rheological Properties of Methacrylamide Modified Gelatin Hydrogels," *Biomacromolecules,* vol. 1, pp. 31-38, 2000.

[29] C. Alcala-Orozco, I. Mutreja, X. Cui, D. Kumar, G. Hooper, K. Lim and T. Woodfield, "Design and characterization of multi-functional strontium-gelatin nanocomposite bioinks with improved print fidelity and osteogenic capacity," *Bioprinting,* vol. 18:e00073, 2020.

[30] J. Visser, F. Melchels, J. Jeon, E. van Bussel, L. Kimpton, H. Byrne, W. Dhert, P. Dalton, D. Hutmacher and J. Malda, "Reinforcement of hydrogels using three-dimensionally printed microfibres," *Nature Communications,* vol. 6:6933, 2015.

[31] M. Schnabelaruch, S. Vogt, Y. Larcher and I. Wilke, "Biodegradable polymer networks based on oligolactide macromers: synthesis, properties and biomedical applications," *Biomolecular Engineering,* vol. 19, pp. 295-298, 2002.

[32] Z. Wang, R. Abdulla, B. Parker, R. Samanipour, S. Ghosh and K. Kim, "A simple and high-resolution stereolithography-based 3D bioprinting system using visible light crosslinkable bioinks," *Biofabrication,* vol. 7:045009, no. 4, 2015.

[33] N. Monteiro, G. Thrivikraman, A. Athirasala, A. Tahayeri, C. França, J. Ferracane and L. Bertassoni, "Photopolymerization of cell-laden gelatin methacryloyl hydrogels using a dental curing light for regenerative dentistry," *Dental Materials,* vol. 34, no. 3, pp. 389-399, 2018.

[34] N. Annabi, D. Rana, E. Shirzaei Sani, R. Portillo-Lara, J. Gifford, M. M. Fares, S. Mithieux and A. Weiss, "Engineering a sprayable and elastic hydrogel adhesive with antimicrobial properties for wound healing," *Biomaterials,* vol. 139, pp. 229-243, 2017.

[35] D. Mondal and T. Willett, "Mechanical properties of nanocomposite biomaterials improved by extrusion during direct ink writing," *Journal of the Mechanical Behaviour of Biomedical Materials,* vol. 104:103653, 2020.

[36] E. Hoch, C. Schuh, T. Hirth, G. Tovar and K. Borchers, "Stiff gelatin hydrogels can be photo-chemically synthesized from low viscous gelatin solutions using molecularly functionalized gelatin with a high degree of methacrylation," *Journal of Materials Science: Materials in Medicine ,* vol. 23, pp. 2607-2617, 2012.

[37] Y. Wang, M. Ma, J. Wang, W. Zhang, W. Lu, Y. Gao, B. Zhang and Y. Guo, "Development of a Photo-Crosslinking, Biodegradable GelMA/PEGDA Hydrogel for Guided Bone Regeneration Materials," *Materials,* vol. 11:1345, 2018.

[38] C. Hutson, J. Nichol, H. Aubin, H. Bae, S. Yamanlar, S. Al-Haque, S. Koshy and A. Khademhosseini, "Synthesis and Characterization of Tunable Poly(Ethylene Glycol):Gelatin Methacrylate Composite Hydrogels," *Tissue Engineering Part A,* vol. 17, no. 14, pp. 1713-1723, 2011.

[39] C. Claaßen, M. Claaßen, V. Truffault, L. Sewald, G. Tovar, K. Borchers and A. Southan, "Quantification of Substitution of Gelatin Methacryloyl: Best Practice and CUrrent Pitfalls," *Biomacromolecules,* vol. 19, pp. 42-52, 2018.

[40] J. Van Hoorick, P. Gruber, M. Markovic, M. Tromayer, J. Van Erps, H. Thienpont, R. Liska, A. Ovsianikov, P. Dubruel and S. Van Vlierberghe, "Cross-linkable Gelatins with Superior Mechanical Properties Through Carboxylic Acid Modification: INcreasing the Two-Photon Polymerization Potential," *Biomacromolecules,* vol. 18, pp. 3260-3272, 2017.

[41] N. Celikkin, S. Mastrogiacomo, J. Jaroszewicz, X. F. Walboomers and W. Swieszkowski, "Gelating methacrylate scaffold for bone tissue engineering: The influence of polymer concentration," *Journal of Biomedical Materials Research Part A,* vol. 106, no. 1, pp. 201-209, 2018.

[42] J. Huang, L. Chen, Z. Gu and J. Wu, "Red Jujube-Incorporated Gelatin Methacryloyl (GelMA) Hydrogels and Anti-Oxidation and Immunoregulation Activity for Wound Healing," *Journal of Biomedical Nanotechnology,* vol. 15, no. 7, pp. 1357-1370, 2019.

[43] T. Lai, J. Yu and W. Tsai, "Gelatin Methacrylate/carboxybetaine methacrylate hydrogels with tunable crosslinking for controlled drug release," *Journal of Materials Chemistry B,* vol. 4, no. 13, pp. 2304-2313, 2016.

[44] K. Modaresifar, H. A. and H. Niknejad, "Design and fabrication of GelMA/chitosan nanoparticles composite hydrogel for angiogenic growth factor delivery," *Journal of Artificial Cells, Nanomedicine and Biotechnology,* vol. 46, no. 8, pp. 1799-1808, 2018.

[45] P. Comeau and T. Willett, "Printability of Methacrylated Gelatin upon Inclusion of a Chloride Salt and Hydroxyapatite Nano-Particles," *Micromolecular Materials and Engineering,* vol. 304:1900142, 2019.

[46] I. Pepelanova, K. Kruppa, T. Scheper and A. Lavrentieva, "Gelatin-Methacryloyl (GelMA) Hydrogels with Defined Degree of Functionalization as a Versatile Toolkit for 3D Cell Culture and Extrusion Bioprinting," *Bioengineering (Basel),* vol. 5:55, no. 3, 2018.

[47] X. Li, S. Chen, J. Li, X. Wang, J. Zhang, N. Kawazoe and G. Chen, "3D Culture of Chondrocytes in Gelatin Hydrogels with Different Stiffness," *Polymers,* vol. 8:269, no. 8, 2016.

[48] A. J. Kerin, M. R. Wisnom and M. A. Adams, "The compressive strength of articular cartilage," *Proceedings of the Institution of Mechanical Engineers, Part H: Journal of Engineering in Medicine,* vol. 212, no. 4, pp. 273-280, 1998.

[49] X. Chen, Y. Zhou, L. Wang, M. H. Santare, L. Q. Wan and X. L. Lu, "Determining Tension-Compression Nonlinear Mechanical Properties of Articular Cartilage from Indentation Testing," *Annals of Biomedical Engineering,* vol. 44, pp. 1148-1158, 2016.

[50] M. J. Mirzaali, J. J. Schwiedrzik, S. Thaiwichai, J. P. Best, J. Michler, P. K. Zysset and U. Wolfram, "Mechanical properties of cortical bone and their relationships with age, gender, composition, and microindentation properties in the elderly," *Bone,* vol. 93, pp. 196-211, 2016.

[51] D. T. Reilly and A. H. Burstein, "The elastic and ultimate properties of compact bone tissue," *Journal of Biomechanics,* vol. 8, no. 6, pp. 393-396, 1975.

[52] Q. Ou, K. Huang, C. Fu, C. Haung, Y. Fang, Z. Gu, J. Wu and Y. Wang, "Nanosilver-incorporated halloysite nanotubes/gelatin methacrylate hybrid hydrogel with osteoimmunomodulatory and antibacterial activity for bone regeneration," *Chemical Engineering Journal,* vol. 382:123019, 2020.

[53] Y. Zuo, X. Liu, D. Wei, J. Sun, W. Xiao, H. Zhao, L. Guo, Q. Wei, H. Fan and X. Zhang, "Photo-Cross-Linkable Methacrylated Gelatin and Hydroxyapatite Hybrid Hydrogel for Modularly Engineering Biomimetic Osteon," *Applied Materials and Interfaces,* vol. 7, no. 19, pp. 10386-10394, 2015.

[54] H. C. Bertram, M. Kristensen and H. J. Andersen, "Functionality of myofibrillar proteins as affected by pH, ionic strength and heat treatment - a low-field NMR study," *Meat Science,* vol. 68, pp. 249-256, 2004.

[55] C. Lakemond, H. de Jongh, M. Hessing, H. Gruppen and A. Voragen, "Soy Glycinin, Influence of pH and Ionic Strength on Solubility and Molecular Structure at Ambient Temperatures," *Journal of Agricultural and Food Chemistry,* vol. 48, no. 6, pp. 1985-1990, 2000.

[56] F. Hofmeister, "Zur lehre von der wirkung der salze," *Archiv for Experimentelle Pathologie und Pharmakologie,* vol. 24, p. 247, 1888.

[57] R. A. Curtis and L. Lue, "A molecular approach to bioseparations: Protein-protein and protein-salt interactions," *Chemical Engineering Science,* vol. 61, no. 3, pp. 907-923, 2006.

[58] K. D. Collins, "Ions from the Hofmeister series and osmolytes: effects on proteins in solution and in the crystallization process," *Methods,* vol. 34, no. 3, pp. 300-311, 2004.

[59] C. H. Schein, "Solubility as a Function of Protein Structure and Solvent Components," *Nature Biotechnology,* vol. 8, pp. 208-317, 1990.

[60] J. Liu, M. D. H. Nguyen, J. D. Andya and S. J. Shire, "Reversible Self-Association Increases the Viscosity of a Concentrated Monoclonal Antibody in Aqueous Solution," *Journal of Pharmaceutical Sciences,* vol. 94, no. 9, pp. 1928-1940, 2005.

[61] W. Du and A. M. Klibanov, "Hydrophobic salts markedly diminish viscosity of concentrated protein solutions," *Biotechnology and Bioengineering,* vol. 108, no. 3, pp. 632-636, 2010.

[62] A. Nakayama, A. Kakugo, J. Gong, Y. Osada, M. Takai, T. Erata and S. Kawano, "High Mechanical Strength Double-Network Hydrogel with Bacterial Cellulose," *Advanced Functional Materials,* vol. 14, no. 11, pp. 1124-1128, 2004.

[63] H. Suo, D. Zhang, J. Yin, J. Qian, Z. Wu and J. Fu, "Interpenetrating polymer network hydrogels composted of chitosan and photocrosslinkable gelatin with enhanced mechanical properties for tissue engineering," *Materials Science and Engineering C,* vol. 92, pp. 612-620, 2018.

[64] H. Suo and X. Zheng, "Using glucosamine to improve the properties of photocrosslinked gelatin scaffolds," *Journal of Biomaterials Applications,* vol. 29, no. 7, pp. 977-987, 2015.

[65] Y. Fu, K. Xu, X. Zheng, A. J. Giacomin, A. W. Mix and W. J. Kao, "3D cell entrapment in crosslinked thiolated gelatin-poly(ethylene glycol) diacrylate hydrogels," *Biomaterials,* vol. 33, pp. 48-58, 2012.

[66] J. Li, E. Weber, S. Guth-Gundel, M. Schuleit, A. Kuttler, C. Halleax, N. Accart, D. Arno, A. Basler, B. Tigani, K. Wuersch, M. Fornaro, M. Kneissel, A. Stafford and B. Freedman, "Tough Composite Hydrogels with High Loading and Local Release of Biological Drugs," *Advanced Healthcare Materials,* vol. 7:e1701393, 2018.

[67] K. Maji, S. Dasgupta, K. Pramanik and A. Bissoyi, "Preparation and Evaluation of Gelatin-Chitosan-Nanobioglass 3D Porous Scaffold for Bone Tissue Engineering," *International Journal of Biomaterials,* vol. 2016:9825659.

[68] J. P. Gong, "Why are double network hydrogels so tough?," *Soft Matter,* vol. 6, no. 12, pp. 2583-2590, 2010.

[69] "Nakajima T., Gong J.P. (2013) Double-Network Hydrogels: Soft and Tough IPN. In: Kobayashi S., Müllen K. (eds) Encyclopedia of Polymeric Nanomaterials. Springer, Berlin, Heidelberg. https://doi.org/10.1007/978-3-642-36199-9_67-1".

[70] P. Cass, W. Knower, E. Pereenia, N. Holmes and T. Hughes, "Preparation of hydrogels via ultrasonic polymerization," *Ultrasonics Sonochemistry,* vol. 17, no. 2, pp. 326-332, 2010.

[71] I. Ward and J. Sweeney, "Composites: A General Introduction," in *Mechanical Properties of Solid Polymers Third Edition*, West Sussex, John Wiley & Sons, 2013, p. 227.

[72] E. Sanchez, C. Zavaglia and M. Felisberti, "Unsaturated polyester resins: influence of the styrene concentration on the miscibility and mechanical properties," *Polymer,* vol. 41, pp. 765-769, 2000.

[73] H. Luo, W. Li, D. Ji, G. Zuo, G. Xiong, Y. Zhu, L. Li, M. Han, C. Wu and Y. Wan, "One-step exfoliation and surface modification of lamellar hydroxyapatite by intercalation of glucosamine," *Materials Chemistry and Physics,* vol. 173, pp. 262-267, 2016.

[74] T. Ngo, A. Kashani, G. Imbalzano, K. Nguyen and D. Hui, "Additive manufacturing (3D printing): A review of materials, methods, applications and challenges," *Composites Part B: Engineering,* vol. 143, pp. 172-196, 2018.

[75] A. Ribeiro, M. Blokzijl, R. Levato, C. Visser, M. Castilho, W. Hennink, T. Vermonden and J. Malda, "Assessing bioink shape fidelity to aid material development in 3D bioprinting," *Biofabrication,* vol. 10:014102, no. 1, 2018.

[76] E. Feilden, C. Ferraro, Q. Zhang, E. García-Tuñón, E. D'Elia, F. Giuliani, L. Vandeperre and E. Saiz, "3D Printing Bioinspired Ceramic Composites," *Scientific Reports,* vol. 7:13759, 2017.

[77] L. Strohmeier, H. Frommwald and S. Schlögl, "Digital light processing 3D printing of modified liquid isoprene rubber using thiol-click chemistry," *RSC Advances,* vol. 10, no. 40, pp. 23607-23614, 2020.

[78] L.-F. Wang, S.-S. Shen and S. Lu, "Synthesis and characterization of chondroitin sulfate-methacrylate hydrogels," *Carbohydrate Polymers,* vol. 52, no. 4, pp. 389-396, 2003.

[79] P. Comeau and T. Willett, "Impact of Side Chain Polarity on Non-Stoichiometric Nano-Hydroxyapatite Surface Functionalization with Amino Acids," *Scientific Reports,* vol. 8:12700, 2018.

[80] ThermoFisher Scientific, "Safety Data Sheet Methacrylouyl Chloride," 16 September 2020. [Online]. Available: https://www.fishersci.com/store/msds?partNumber=AAL1451114&productDescription=METHACRYLOYL+CLRIDE+MAY+.+25G&vendorId=VN00024248&countryCode=US&language=en. [Accessed 1 12 2020].

[81] ThermoFisher Scientific, "Safety Data Sheet Methacrylic Anhydride," 20 February 2020. [Online]. Available: https://www.fishersci.com/store/msds?partNumber=AAL1435718&productDescription=METHACRYLIC+ANHYDRID+94%25+S+50G&vendorId=VN00024248&countryCode=US&language=en. [Accessed 1 12 2020].

[82] Michigan State University, "Spectrosopy Tables," [Online]. Available: https://www2.chemistry.msu.edu/courses/cem251/SS13_HOVIG/Spectroscopy%20tables.pdf. [Accessed 1 12 2020].

[83] L. Starkey, "1H NMR Chemical Shifts," [Online]. Available: https://www.cpp.edu/~lsstarkey/courses/NMR/NMRshifts1H-general.pdf. [Accessed 1 12 2020].

[84] D. Bertuzzi, T. Becher, N. Capreti, J. Amorim, I. Jurberg, J. Megiatto and C. Ornelas, "General Protocol to Obtain D-Glucosamine from Biomass Residues: Shrimp Shells, Cicada Sloughs and Cockroaches," *Global Challenges,* vol. 2:1800046, no. 11, 2018.

[85] S. Michna, W. Wu and J. Lewis, "Concentrated hydroxyapatite inks for direct-write assembly of 3-D periodic scaffolds," *Biomaterials,* vol. 26, pp. 5632-5639, 2005.

[86] P. A. Comeau and T. L. Willett, "Triethyleneglycol dimethacrylate addition improves the 3D-printability and construct properties of a GelMA-nHA composite system towards tissue engineering applications," *Materials Science & Engineering C,* vol. 112:110937, 2020.

[87] P. Comeau and T. Willett, "An Alternative Approach to the Surface Methacrylation of Non-stoichiometric Hydroxyapatite Nanoparticles for Use in Bone-Inspired Composites," *Frontiers in Materials,* vol. 6:00263, 2019.

[88] S. Witharana, C. Hodges, D. Xu, X. Lai and Y. Ding, "Aggregation and settling in aqueous polydisperse alumina nanoparticle suspensions," *Journal of Nanoparticle Research,* vol. 14:851, 2012.

[89] TA Instruments, "Rheological Techniques for Yield Stress Analysis RH025," [Online]. Available: http://www.tainstruments.com/pdf/literature/RH025.pdf. [Accessed 30 11 2020].

[90] E. R.O., "Factors Affecting Glass Transition Temperature 6. Cross-Linking and Branching," in *Polymer Science and Technology*, Boca Raton, CRC Press, 2000, p. 107.

[91] Polymer Properties Database, "Flory-Rehner Theory of Polymer Network Swelling," Polymer Properties Database, [Online]. Available: http://polymerdatabase.com/polymer%20physics/Flory%20Rehner.html. [Accessed 20 11 2020].

[92] P. Flory, "Statistical Mechanics of Swelling of Network Structures," *The Journal of Chemical Physics,* vol. 18, no. 1, pp. 108-111, 1950.

[93] M. B. Huglin and J. M. Rego, "Influence of a Salt on the Properties of Hydrogels of 2-Hydroxyethyl Methacrylate with a Sulfobetaine Comonomer," *Macromolecules,* vol. 26, no. 12, pp. 3118-3126, 1993.

[94] B. Zhang, C. Wang, Y. Wang, T. Li, K. Zhai, F. Zhang, Y. Bai, Y. Tan, Y. Ma, K. Xu and P. Wang, "A facile method to synthesize strong salt-enhanced hydrogels based on reversible physical interaction," *Soft Matter,* vol. 16, no. 3, pp. 738-746, 2020.

[95] W. Soboyeho, "11.3 Notch Concenteration Factors," in *Mechanical Properties of Engineered Materials*, New York, Marcel Dekker, Ink, 2003, pp. 317-318.

[96] A. Gregorova, N. Saha, T. Kitano and P. Saha, "Hydrothermal effect and mechanical stress properties of carboxymethylcellulose based hydrogel food packaging," *Carbohydrate Polymers,* vol. 117, pp. 559-568, 2015.

[97] R. Ollier, C. Pérez and V. Alvarez, "Effect of relative humidity on the mechanical properties of micro and nanocomposites of polyvinyl alcohol," *Procedia Materials Science,* vol. 1, pp. 499-505, 2012.

[98] A. Nguyen, P. Goering, V. Reipa and R. Narayan, "Toxicity and photosensitizing assessment of gelatin methacryloyl-based hydrogels photoinitiated with lithium phenyl-2,4,6-trimethylbenzoylphosphinate in human primary renal proximal tubule epithelial cells," *Biointerphases,* vol. 14:021007, no. 2, 2019.

[99] X. Wang, B. Liu, X. Li and R. Sun, "Novel glucosamine hydrochloride-rectorite nanocomposites with antioxidant and anti-ultraviolet activity," *Nanotechnology,* vol. 23:495706, no. 49, 2012.

[100] K. Aldred, S. McPherson, C. Turnbough, R. Kerns and N. Osheroff, "Topoisomerase IV-quinolone interactions are mediated through a water-metal ion bridge: mechanistic basis of quinolone resistance," *Nucleic Acids Research,* vol. 41, no. 8, pp. 4628-4639, 2013.

[101] A. Sheikhi, S. Afewerki, R. Oklu, A. Gaharwar and A. Khademhosseini, "Effect of ionic strength on shear-thinning nanoclay-polymer composite hydrogels," *Biomaterials Science,* vol. 6, no. 8, pp. 2073-2083, 2018.

[102] P. Cain, "The impact of layer height on a 3D print," 3D Hubs, [Online]. Available: https://www.3dhubs.com/knowledge-base/impact-layer-height-3d-print/. [Accessed 2 12 2020].

[103] L. Dou, Y. Zhang and H. Sun, "Advances in Synthesis and Functional Modification of Nanohydroxyapaptite," *Journal of Nanomaterials,* vol. 2018:3106214.

[104] F. Fu, Z. Chen, Z. Zhao, H. Wang, L. Shang, Z. Gu and Y. Zhao, "Bio-inspired self-healing structural color hydrogel," *Proceedings of the National Academy of Science of the United States of America,* vol. 114, pp. 5900-5905, 2017.

[105] R. Eslami, R. Bagheri, Y. Hashemzadeh and M. Salehi, "Optical and mechanical properties of transparent acrylic based polyurethane nano Silica composite coatings," *Progress in Organic Coatings,* vol. 77, pp. 1184-1190, 2014.

[106] D. Kopeliovich, "Estimations of composite materials properties," Substances and Technologies, 02 June 2012. [Online]. Available: https://www.substech.com/dokuwiki/doku.php?id=estimations_of_composite_materials_properties. [Accessed 1 12 2020].

[107] S. C. McKarns, C. Hansch, W. S. Caldwell, W. T. Morgan, S. K. Moore and D. J. Doolittle, "Correlation between Hydrophobicity of Short-Chain Aliphatic Alcohols and Their Ability to Alter Plasma Membrane Integrity," *Fundamental and Applied Toxicology,* vol. 36, pp. 62-70, 1997.

[108] R. C. Baker and R. E. Kramer, "Cytotoxicity of short-chain alcohols," *Annual Review of Pharmacology and Toxicology,* vol. 39, no. 1, pp. 127-150, 1999.